UNIVERSITY OF UDINE

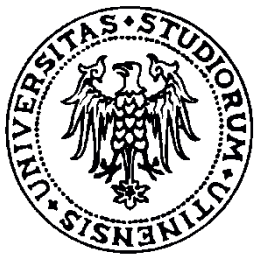

DEPARTMENT OF MEDICAL AND BIOLOGICAL SCIENCES

PhD Programme in Biomedical Sciences and Biotechnology

XXIX Cycle

PhD THESIS

MITOCHONDRIAL OXIDATIVE PHOSPHORYLATION PLASTICITY/ADAPTATION TRIGGERED BY DISTURBANCES AND STRESSES AND TARGETED BY THERAPIES

PhD Student:

Alessia Buso

Supervisors:

Prof.ssa Irene Mavelli

Prof. Bruno Grassi

Co-Supervisor:

Dott.ssa Marina Comelli

Academic Year 2015-16

A mio padre

Siamo cresciuti e ognuno di noi
prenderà il proprio cammino.
Cosa c'è di più semplice?

Alessia Gazzola

ABSTRACT

Mitochondrion is an important organelle for cells survival. In fact, it is responsible for many processes such as cellular metabolism, i.e. oxidative phosphorylation for ATP production, energy homeostasis and regulation of apoptosis and autophagy. Mitochondrion, due to this role, needs to be "plastic" in order to respond and adapt quickly to any perturbation and change of conditions in the different tissues of the human body. The induction of mitochondria biogenesis is required to meet different energetic demands under stress conditions. Thus, mitochondrial plasticity is the mechanism that controls modification in conditions of cellular stress or in response to environmental stimuli like exercise, caloric restriction, cold exposure, oxidative stress, cell division and renewal, and differentiation. Recently, mitochondrial modulation has become also a topic of interest as a therapeutic target. The master regulator gene of mitochondrial biogenesis is PGC1α that, through nuclear transcription factors and subsequent metabolic sensors and other signalling proteins, is capable to modulate mitochondrial abundance, activity and oxidative phosphorylation as a consequence of energy homeostasis unbalance. Mitochondrial plasticity during the last few years was extensively studied in skeletal muscle models, due to its fast adaptation in exercise and rest condition, but also in cancer cachexia, ageing and heart disease. Also in cancer, mitochondrial adaptations have become a fundamental topic, in particular to understand the underling pathogenic mechanism of disease progression, to identify prognostic factors and to design adjuvant therapies targeting mitochondria.

In this frame, this PhD Thesis investigates the role and adaptations of mitochondria in different pathophysiological models of skeletal muscle and brain tumors.

The expression of some key proteins of the signalling pathways involved in mitochondrial biogenesis regulation, such as PGC1α, LKB1-AMPK an energy sensing axis, Sirt3 a regulator of mitochondrial enzymes functionality, are investigated together with the OXPHOS complexes, HSP60, CS and TOM20 as mitochondrial mass markers.

The first model is aimed at testing the expression levels of the protein panel in skeletal muscle biopsies from a cohort of 16 elderly and 7 young people subjected to immobility (bed-rest) causing hypotrophy and subsequent rehabilitation via exercise training. Based on quantitative immunoblot data, there is a down-regulation of PGC1α, Sirt3 and OXPHOS complexes II, III and IV occurring during bed-rest with a subsequent up-regulation after rehabilitation in both groups. AMPK and LKB1 do not change during bed-rest and rehabilitation in elderly and young subjects suggesting that there is not energetic impairment.

According to the down-regulation of OXPHOS biogenesis during bed-rest there is the up-regulation of GAPDH evocative of a metabolic shift during hypotrophy from oxidative phosphorylation towards glycolysis, which is reversed by exercise training. OXPHOS complex V is down-regulated in both groups during bed-rest, but after rehabilitation the complex expression does not increase, maybe due to an imbalance between protein biogenesis and degradation. It is tempting to speculate that exercise could regulate complex V activity, as a compensatory response, through deacetylation mediated by Sirt3, which is up-regulated after rehabilitation. CS and TOM20 present the same pattern: in elderly subjects there is a down-regulation during immobility that is counteracted by exercise training, whereas young subjects present a similar pattern but differences do not reach statistical significance. In conclusion, immobility is effective in down-regulation of mitochondria-related protein expression and training protocol counteracts this effect. The pattern is similar in both elderly and young subjects, with some differences for PGC1α, and Sirt3 appearing less responsive to rehabilitation in elderly.

Training is a fundamental tool to recover from immobility periods but also to maintain muscle tonicity as a non-pharmacologic therapeutic treatment for chronic heart failure patients (CHF). In the second model is studied the effect of aerobic exercise training (2 months) on mitochondrial respiration in skeletal muscle of CHF transgenic (Tgαq*44) mice, focusing also on the impact of CHF on skeletal muscle of sedentary mice. Oxidative phosphorylation and electron transport system capacity of biopsies from soleus muscle is assayed by high-resolution respirometry. Sedentary CHF mice exhibit in comparison to wild type an impaired complex I – State 3 respiration and ADP-stimulated respiration sustained by Complex I+II, in contrast to rotenone insensitive electron transport system respiration that is unchanged. This suggests an inactivation of complex I rather than an impairment of OXPHOS biogenesis in soleus muscle, also confirmed by unchanged value of PGC1α expression. Exercise training improves exercise performance, but it does not affect mitochondrial respiration. Factors "upstream" of mitochondria are likely mainly responsible for the functional improvement.

The third model focuses on the study of ATP synthase Inhibitory Factor 1 as prognostic marker in low-grade astrocytomas (LGA). 19 pairs of surgical specimens of LGA are evaluated for the tumor border zone in which IF1 abundance is significantly lower than in the tumoral zone. Immunohistochemistry analyses of 68 specimens by Tissue-MicroArrays prove a weak association of IF1 with NF-kB p65-subunit and consolidated radiologic indexes of tumor infiltration and resection. Kaplan–Meier estimation of patients overall survival indicates that IF1 may serve as a prognostic marker. Intriguingly, IF1 expression significantly

increases in lesions with suspected first signs of anaplastic transformation (LGA*) as showed, in accordance, by immunofluorescence (12 specimens), immunohistochemistry (11) and immunoblot (9) analyses. Finally, immunoblot analyses provide a picture of mitochondrial and glycolytic markers, suggesting no improvement of glycolysis and little changes in mitochondrial mass. On the contrary, OXPHOS complexes show a significant upregulation in LGA*. IF1 expression levels could be proposed as a biomarker of OS in LGA, rare tumors with a good prognosis, which could nonetheless evolve in anaplastic lesions and are still without an adjuvant therapy.

TABLE OF CONTENTS

1. INTRODUCTION

1.1 Mitochondrion

Mitochondrion is a double membrane organelle, present in the cytoplasm of most eukaryotic cells, which main function is to produce metabolic energy as ATP in order that the cell can function (Mitchell, 1961). Beside this function, mitochondria are important regulators of calcium homeostasis, apoptosis and proper cell viability (Berg et al., 2008). Mitochondrion, due to its characteristics of endosymbiotic organelle, possesses its own DNA (mtDNA) that codifies for 22 transfer RNAs, 2 subunits of ribosomal RNA and 13 mitochondrial proteins all vital for the correct functioning of the organelle, even though the majority of mitochondrial proteins are encoded by nuclear DNA (Calvo and Mootha, 2010). Mitochondria present a highly conserved structure, even though they have a great variability in number and morphology in different tissues. Their structure consists in two membranes, one in contact with the cytoplasm (outer mitochondrial membrane – OMM) and one inner (IMM), that is folded in the classical cristae conformation and delimits different compartments which accomplish specific metabolic processes (Frey et al., 2002). OMM separates the organelle from the cytoplasm and other cellular components and represents a physical barrier preventing the release of mitochondrial proteins involved in apoptosis, such as cytochrome *c*. Through porins like the Voltage-Dependent Anion Channel (VDAC), OMM is permeable to small molecules and ions such as ATP, ADP, malate and pyruvate, and is involved in communications between enzymes of different metabolic pathways, Ca^{2+} regulation and apoptosis. IMM, whose permeability to solutes is controlled by highly specific transporters (e.g. ATP/ADP, citrate and pyruvate transporters) and tightly regulated channels, is impermeable to most polar molecules and ions, including protons. It is the site of coupling between substrate oxidation and ATP synthesis in the process of oxidative phosphorylation (OXPHOS). IMM organization in cristae results in expansion of the allocation space for OXPHOS complexes to optimize ATP production and reflects different ATP requests of different tissues (Kuhlbrandt, 2015).

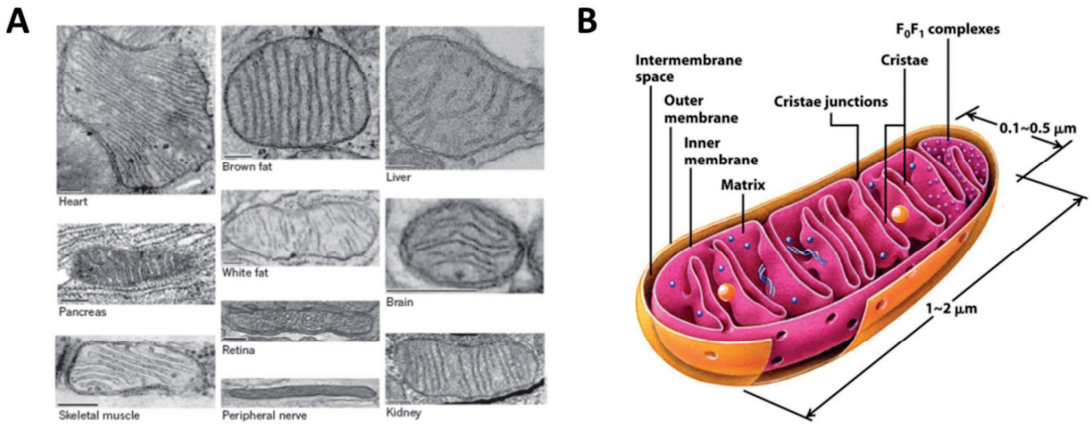

Fig. 1. Mitochondrial Structure. (A) Mitochondrial ultrastructure in different tissues. (B) Cartoon of mitochondrial structure. Modified from (Vafai and Mootha, 2012)

Cristae are also very fluid structures, that could encounter fusion or fission phenomena, in order to better fulfil the energy demands of the cell in different conditions and respond also to autophagy or apoptosis.

1.1.1. Mitochondria, the Powerhouse of the cell: ATP synthase and its inhibitor IF1

Mitochondrion is always referred as the powerhouse of the cell because of its role in the production of ATP through the oxidative phosphorylation as the last step of oxidative catabolism of carbohydrates, lipids and aminoacids. This process, which takes place in the inner mitochondrial membrane, occurs only when there is the cooperation between the respiratory chain and ATP synthase (also known as OXPHOS complex V). Mitochondria operate a sequence of energy conversion processes through which the exergonic flow of electrons along the respiratory complexes supports the endergonic pumping of protons from the matrix to the intermembrane space. The resulting proton motive force drives the rotation of the Fo sector of ATP synthase leading to the synthesis of ATP in the F1 sector (Mitchell & Moyle, 1967).

The respiratory chain is composed by four protein complexes: three protonic pumps, namely NADH-Q oxidoreductase or complex I, Q-Cytochrome c oxidoreductase or complex III and Cytochrome c oxidase or complex IV, and one direct connection to the Krebs cycle (Succinate-Q reductase or complex II) (Fig. 2).

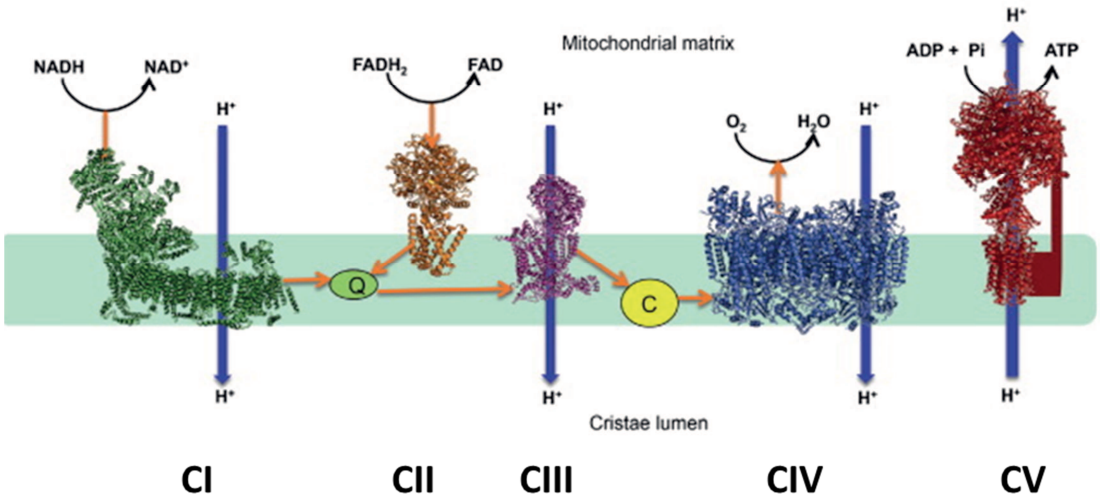

Fig 2. The respiratory chain and ATP synthase. The transfer of electrons (orange arrows) and proton pumping activity of respiratory complexes (blue arrows) are indicated. Images of the crystallographic structure of the complexes are taken with PyMOL Molecular Graphics System. Complex I (green) (PDB: 4QU8), complex II (orange) (PDB: 1ZOY), complex III (purple) (PDB: 1BE3) and complex IV (blue) (PDB: 1OCC). The ATP synthase F1-domain and c-ring (red) in monomeric form (PDB: 2XND). Q: coenzyme Q (green sphere). C: cytochrome c (yellow sphere). Crystallographic structures were taken from PDB (Protein DataBase). Modified from (García-Bermúdez & Cuezva, 2016)

Complex I is a large enzyme of ~ 900 KDa and is formed by 46 subunits. It has a characteristic L-shape, where the horizontal arm is located in the membrane and the vertical one protrudes in the matrix. Complex I is the entry point of nicotinamide adenine dinucleotide (NADH) electrons into the respiratory chain. NADH bounds to the complex and transfers its two electron to the prosthetic group of flavin mononucleotide (FMN), which is thus reduced to $FMNH_2$. Then, electrons are transferred to Fe-S centres. The transfer of two electrons from NADH to coenzyme Q through complex I makes possible the pumping of four hydrogen ions outside mitochondrial matrix. In this way coenzyme Q acquires two protons from the matrix and is reduced to ubiquinol, leaving complex I and moving to the hydrophobic zone of the membrane (Kuhlbrandt, 2015 – Lenaz et al., 2006).

Complex II is both a part of Krebs cycle and ETC. Electrons of reduced flavin adenine dinucleotide ($FADH_2$), formed during Krebs cycle, are first transferred to Fe-S centres and then to coenzyme Q to enter in the ETC (Oyedotun et al., 2004). Complex II does not transport protons and consequently oxidation of $FADH_2$ produces less ATP with respect to NADH.

Complex III catalyses the flow of two electrons from QH_2 to oxidize cytochrome c and at the same time pumps two protons outside the mitochondrial matrix. Complex III has two types of cytochromes, namely *b* and c_1, which use heme as a prosthetic group (two for *b* and one for c_1). Together with the cytochromes, complex III has a 2Fe-2S centre (Rieske centre), where the iron ions are coordinated by two histidines instead of two cysteines, in order to

maximize the reduction potential and easily accept the electrons from QH_2 (Kramer et al., 2004). Complex III translocates four protons into the intermembrane space by oxidation of coenzyme Q and reduction of cytochrome c, a mobile electron- carrier between complex III and IV.

Complex IV, a transmembrane protein complex appearing as a Y-shaped dimer, consists in 13 subunits and has a molecular weight of 200 KDa. It catalyses the transfer of electrons from cytochrome c to oxygen molecules, which are the final acceptors and converted to water (Kuhlbrandt, 2015).

Finally, all the protons, pumped from the matrix to the intermembrane space, generate the proton motive force that leads to the synthesis of ATP through Complex V. ATP synthase is a complex enzyme of large dimension, whose structure (Fig. 3A) was resolved and studied extensively during the 80s by Sir John Walker. The whole complex has a molecular mass that varies between 540 and 585 KDa depending on the source. Complex V is composed by two different domains: F_O domain, in the IMM, and F_1 domain, directed towards the matrix. F_O domain contains the proton channel formed by subunits a, b, c8-10, d, e, f, g, CF6, A6L. F_1 domain, the catalytic portion of the enzyme, is composed by α3, β3, γ, δ and ε subunits. Numerous atomic structures have revealed that F_1 comprises 3 copies of each of the nucleotide-binding subunits α and β, which alternate around the central α-helical coiled coil of the γ subunit (Walker et al., 1982 – Walker et al., 1991 – Wittig & Schägger, 2008). The α and β subunits constitute the majority of the all complex and are disposed in alternate conformation in an exameric ring. α and β subunits are similar but only the β subunit has catalytic nucleotide-binding sites and catalyses the ATP synthesis/hydrolysis reaction (Gibbons et al., 2000 – Boyer, 1993). The two domains are connected in a central (subunits γ, δ, ε) and a peripheral (subunits b, d, F_6, and oligomycin sensitivity conferring protein OSCP) structure, known as rotor and stator.

ATP synthesis is catalysed by a reversible reaction in which are involved ADP and P_i. The enzyme reaction depending on cell condition could produce or hydrolyse ATP (Fig 3B).

In 1975, Boyer proposed the mechanism of bond modification for ATP synthesis. This mechanism affirms that β subunit can catalyse every steps that lead to ATP synthesis/hydrolysis, which coincide to the different conformations of the same subunit. These conformations are known as β_E empty site, β_{TP} tight binding site, β_{DP} loose binding site and β_{HC} half-closed (representing the post-hydrolysis, pre-product release state) (Menz et al., 2001). The different conformations are the result of β and γ subunits interaction, with the latter rotating of 120° at every step of ATP synthesis or hydrolysis. Thus, ATP is synthetized and

released with just one γ subunit rotation. ATP synthase, in conditions of low electrochemical gradient, is capable also to hydrolyse ATP and transport protons in the intermembrane space (Fig 3B) (Boyer, 1993).

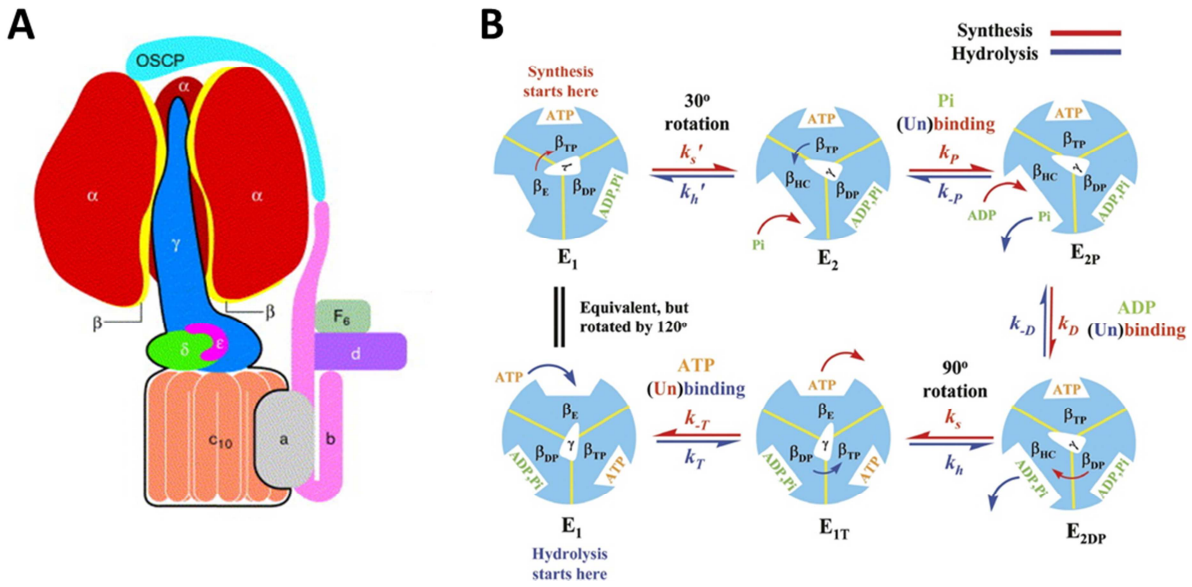

Fig 3. ATP synthase structure and rotational catalysis mechanism for ATP synthesis and hydrolysis. (A) ATP synthase structure and its subunits. (B) Rotational catalysis mechanism. The figure shows a 120° rotation cycle for the molecule, which corresponds to the synthesis or hydrolysis of one ATP. The catalytic binding sites are labelled according to their structural descriptions (β_E, β_{TP}, β_{DP}, and β_{HC}) and indicated by various shapes similar to those used in the literature. ATP is orange and ADP/Pi is green. The sequence of events for ATP synthesis is shown by red arrows, whereas blue arrows indicate the sequence for ATP hydrolysis. Figure modified from (Stock et al., 2000) and (Gao et al., 2005).

The function of this important enzyme is finely regulated by several different mechanisms like post-translational modification, ligand association and gene expression regulation. By far the most important physiological regulatory factor is the ATP Synthase Inhibitory Factor 1 (IF1). During the last few years, IF1 has been extensively studied by several laboratories to elucidate its pathophysiological role in different tissues and illnesses. IF1 is a nuclear-encoded small thermostable protein of ~12 KDa (Pullman and Monroy, 1963). Human IF1 gene on chromosome 1, by unknown regulatory mechanisms, could give at least 3 codifying transcripts whose biologic function is still unidentified. The first isoform is the one normally detected and studied. The full-length isoform has 106 aminoacids and a molecular weight of 12.2 KDa. At the N-terminal of the protein, there is a mitochondrial targeting sequence of 25 aminoacids that is cut off in the mitochondrial matrix. The other two isoforms, which differ from the canonical isoform because of modifications on the C-terminal, are of 71 (7.9 KDa) and 60 aminoacids (6.6 KDa) (MitoMiner Database, 2016).

IF1 is classically described as an inhibitor of the futile hydrolase activity of ATP synthase by binding the interface of the F_1 αβ subunits at β_{DP} and preventing the rotation of the F_OF_1 complex (Green & Grover, 2000 – Gledhill & Walker, 2006 – Cabezon et al., 2000) (Fig. 4A).

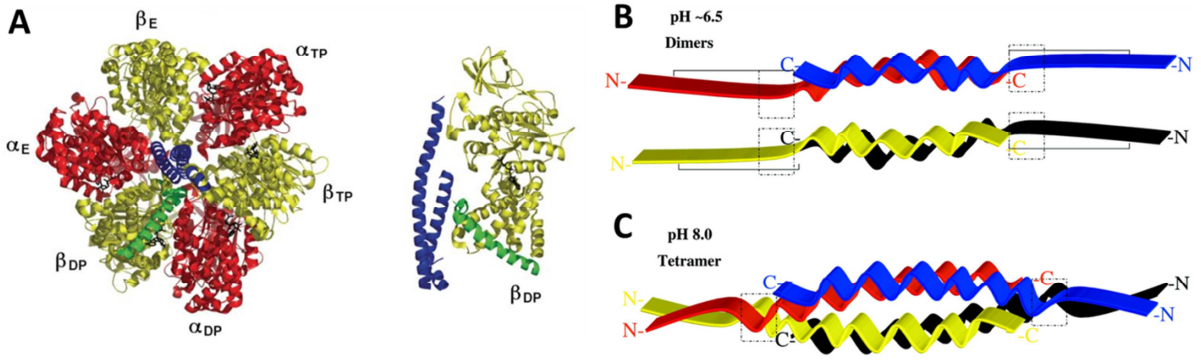

Fig 4. Inhibitory sites in F1-ATPase from X-ray crystallography and Model of the interconversion between active dimeric and inactive tetrameric states in a pH-dependent manner. (A) View of the F1-ATPase inhibited by IF1 along the central axis (left panel) from the membrane towards the catalytic sites. Side view (right panel) showing the interacting β-subunit and the γ-subunit. The α-, β- and γ-subunits are shown in red, yellow and blue respectively. The inhibitors are shown in green and nucleotides are coloured black. Images were produced with the program PyMOL (DeLano Scientific, San Carlos, CA, U.S.A.). (B) Two IF1 molecules dimerize by forming an antiparallel α-helical coiled-coil structure in the C-terminal region. (C) at pH 8.0, two dimers associate forming a tetramer. The interaction between the two dimers involves residues in the region from ~35 to 47. These residues are placed indashed boxes. At pH 8.0, the inhibitory regions including residues 9–22 and also residues 23–47 which are involved in binding to F1 are masked in the tetramer. Modified from (Gledhill & Walker, 2006 – Cabezon et al., 2000).

IF1 discover and activity were reported in 1963 by Pullman and Monroy in isolated bovine mitochondria. Several studies have shown that its activity as inhibitor of the hydrolytic activity of ATP synthase is maximal at low pH (pH 6.7), in absence of mitochondrial membrane potential and in condition of ischemia/reperfusion in the tissues (Power et al., 1983 – Lippe et al., 1988 a – Lippe et al., 1988 b). IF1 to be active and to exploit its inhibitory activity, as shown in bovine, must be assembled as a dimer through the C-terminal region of two monomers creating an antiparallel coiled-coil, a conformation favoured by low pH. Conversely, at high pH IF1 forms tetramers, but this is an inactive conformation in which the inhibitory sequence is masked (Cabezon et al., 2000) (Fig 4B and C). Strong evidence has been provided that IF1, when overexpressed, also inhibits the synthase activity in the *in vivo* context. As an example, the overexpression of active IF1 in mouse neurons causes the inhibition of the mitochondrial ATP production and triggers a mild reactive oxygen species (ROS) signal that promotes a metabolic reprogramming toward an enhanced aerobic glycolysis (Formentini et al., 2014).

The expression of IF1 in the diverse human tissues can diverge significantly, with high levels in tissues with high-energy demand, like in heart and brain, but negligible ones in others like colon, breast and lung (Sánchez-Aragò et al., 2013 – Sánchez-Cenizo et al., 2010). In addition, in many types of cancers IF1 is highly expressed in contrast to non-tumoral cells (Santacatterina et al., 2016 – Sánchez-Aragò et al., 2013 – Bravo et al., 2004). This particular feature seems to contribute to the induction of the aerobic glycolytic phenotype (Warburg effect), common to most of the cancers. Conversely, when IF1 is silenced, the activity of OXPHOS is enhanced and glycolysis reduced (Sánchez-Cenizo et al., 2010 – Formentini et al., 2012). Several studies reported that an higher expression of IF1 correlates with a worse prognosis (lung, ovaries, oesophagus, liver, gastric and brain cancers) (Sánchez-Aragó et al., 2013 – Song et al., 2014 – Wu et al., 2015 – Gao et al., 2016), but in other studies a better prognosis was associated with higher IF1 expression (breast and colon cancers) (Sánchez-Aragó et al., 2013). The reason of this discrepancy is still without a clear answer, and the regulation of IF1 expression/activity and its relevance in induction of the high-proliferating phenotype in cancer have to be definitively elucidated.

1.1.2. Mitochondrial biogenesis and metabolic adaptations under pathophysiological conditions

Mitochondrion, due to its role in energy homeostasis and cellular metabolism, needs to quickly respond to any perturbation and change of conditions. The biogenesis of mitochondria is a process leading to higher abundance of mitochondrial membranes and DNA (mtDNA) in conditions of cellular stress or in response to environmental stimuli, like exercise (Nisoli and Carruba, 2006), caloric restriction (Civitarese et al., 2007; Lopez-Lluch et al., 2006), cold exposure, oxidative stress, cell division and renewal, and differentiation, in order to meet cell's different energetic demands (Ventura-Clapier et al., 2008 – Hock and Kralli, 2009).

Mitochondrial biogenesis is regulated by several nuclear factors such as nuclear respiratory factors 1 and 2 (NRF1 and NRF2) and mitochondrial transcription factor A (TFAM), which control the expression of nuclear encoded factors involved in mitochondrial transcription, protein import and assembly, OXPHOS genes and mitochondrial translation factors (Wenz, 2013). Other transcriptional factors involved in the process are oestrogen related receptor α (ERRα), the cAMP response element (CREB) and ying yang 1 transcription factor (YY1) (Scarpulla, 2011). Upstream of these factors there is the master regulator gene of mitochondrial biogenesis: the peroxisome proliferator-activated receptor gamma, coactivator 1 alpha (PPARGC1A, also known as PGC1α). PGC1α is capable to induce mitochondrial

biogenesis and oxidative phosphorylation through the activation of these factors and it can be rapidly induced in energy stress conditions (Ventura-Clapier et al., 2008).

In stress conditions the expression and/or activity of PGC1α have been shown to be regulated by thyroid hormone (TH), nitric oxide synthase (NOS/cGMP), p38 mitogen-activated protein kinase (p38MAPK), sirtuines (Sirts), calcineurin, calcium-calmodulin-activated kinases (CaMKs), adenosine-monophosphate-activated kinase (AMPK), cyclin-dependent kinases (CDKs), and β-adrenergic stimulation (β/cAMP), through post-translational modifications such as (de)-acetylation, phosphorylation, SUMOylation, ubiquitination and O-linked β-N-acetyl glucosamination and methylation (Ventura-Clapier et al., 2008 – Canto & Auwerx, 2009 – Housley et al., 2009 – Rytinki & Palvimo, 2009).

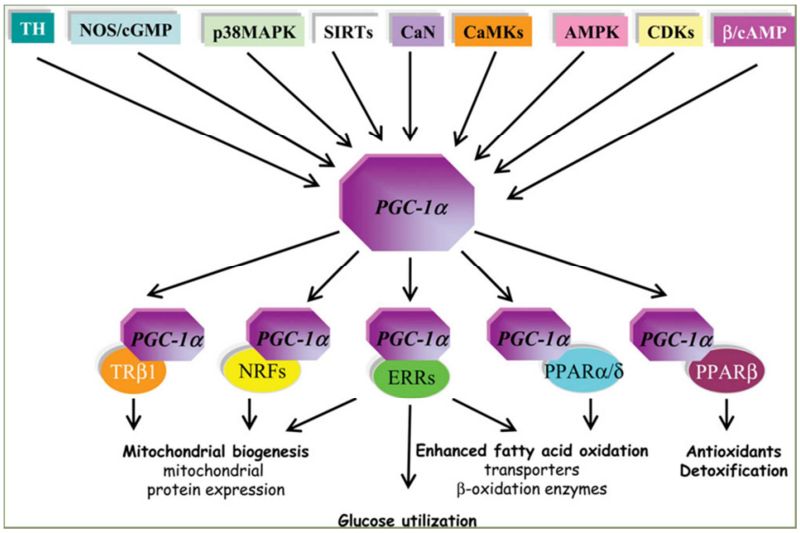

Fig 5. PGC1α regulatory cascade. TH, NOS/cGMP, p38MAPK, SIRTs, calcineurin, CaMKs, AMPK, CDKs, and β/cAMP regulate expression and/or activity of PGC1α. PGC1α then co-activates transcription factors such as NRFs, ERRs and PPARs, known to regulate different aspects of energy metabolism including mitochondrial biogenesis, fatty acid oxidation, and antioxidant. (Ventura-Clapier et al., 2008)

PGC1α, after its activation can regulate, through the nuclear factor like NRFs, ERRs and PPARs, different aspects of energy metabolism including mitochondrial biogenesis, fatty acid oxidation, and antioxidant response. Moreover, PGC1α can induce also its own expression via YY1 (Ventura-Clapier et al., 2008).

Mitochondrial biogenesis can be promoted by different physiological conditions (cold exposure and caloric restriction) and physical activities (exercise training) but also during pathological conditions and in some cases in cancer.

During caloric restriction, restricted nutrient supply, and exercise mitochondrial biogenesis is promoted by the energy unbalance that results in an increase of AMP/ATP and NAD^+/NADH ratios. Thus, both AMPK and Sirt1 are activated and in turn activate PGC1α

through phosphorylation and deacetylation (Wenz, 2013). In such conditions, AMPK phosphorylates also mTOR, inhibiting it. The inhibition of mTOR activity leads to an increased OXPHOS proteins expression and fatty acid oxidation (Duvel et al., 2010). The opposed effect is present with an excess of nutrients.

Mitochondrial biogenesis is connected also to hypoxia sensing through hypoxia-inducible factor 1α (HIF-1α). It was demonstrated that PGC1α is capable to stabilize HIF-1α under normoxic conditions. This process seems to involve intracellular hypoxia as a result of increased oxygen consumption after mitochondrial biogenesis in skeletal muscle (Wenz, 2013 – O'Hagan et al., 2009).

As far as cancer, in particular aggressive cancers PGC1α was found upregulated in cancer stem cells (CSC) along with oxidative phosphorylation and antioxidant defences favouring the metastatization of the neoplasia. Moreover, antioxidants and functional mitochondria are of great importance for cancer cell viability both in the hypoxic and in the border zones of the neoplastic mass, mainly to sustain the biosynthetic pathways, and the deriving ATP production is needed for survival when the cancer cells are detaching from their basement membrane (Jose et al., 2011 – Koppenol et al., 2011 – LeBleu et al., 2014).

Mitochondrial biogenesis is definitely a fundamental process in physiological and pathological conditions in order to respond to different stimuli that need particular metabolic adaptation.

1.1.3. Signalling pathways involved in adaptation responses

Metabolic adaptations are finely regulated and in particular the balance between oxidative phosphorylation and glycolysis, the two main metabolic sources of energy in the cell.

In the last few years, LKB1-AMPK-PGC1α-Sirt3 signalling pathway was vastly characterised due to its role in regulating mitochondrial biogenesis and cell metabolism in adaptation responses. In this pathway silent mating-type information regulation 2 homolog sirtuin (Sirt3) functions as a downstream target of PGC1α, which is directly regulated by AMPK, and may act as an activator of LKB1-AMPK axis.

The protein deacetylase Sirt3 is a NAD^+-dependent protein deacetylase and the most well characterized and studied among the mitochondrial sirtuins, that has been shown to regulate almost every major aspects of mitochondrial biology and, not surprisingly, is reported to contribute to a number of mitochondria related diseases and cancer (George and Ahmad, 2016). Intriguingly, PGC1α, a master regulator of mitochondrial biogenesis and

structural/functional integrity (Scarpulla, 2002), and Sirt3 appear to form a positive feedback loop to promote mitochondrial function. In fact, mitochondrial Sirt3, besides functioning as a downstream target of PGC1α, which increases its expression at the mRNA and protein level and improves its activity (Rato et al., 2014), is also reported to impact PGC1α, directly and/or by modulating activities of upstream mitochondrial regulators, such as TFAM, AMPK, p53 or other key regulators (Chen et al., 2014). The normal functioning of the PGC1α-Sirt3 axis has been reported as essential for the regulation of mitochondrial metabolism, biogenesis and oxidative stress (Giralt & Villaroya, 2012 – George and Ahmad, 2016 – Brenmoehl & Hoeflich, 2013). Furthermore, Sirt3 regulates OXPHOS complexes I, III and V acetylation status and activities, along with enzymes of Krebs cycle, fatty acid oxidation (Nogueiras et al., 2012) and glycolysis through the destabilization of HIF-1α resulting in a metabolic switch towards a more oxidative phenotype (Finley et al., 2011). Interestingly, Sirt3 was appointed as mitochondrial tumor suppressor (Zhu et al., 2014 – Finley et al., 2011). In accordance, in three breast cancer cell lines with different invasive potential it was demonstrated that less invasive is the cancer, more active is Sirt3, more deacetylated are two Lys in the C-term of complex V - β subunit and more active is ATP synthase, suggesting a role of Sirt3 in the metabolic shift towards glycolysis during cancer progression (Rahman et al., 2014). Other ATP synthase subunits are Sirt3 target proteins as a means of direct regulation of the complex activity (Bao et al., 2010 – Vassilopoulos et al., 2014). In particular, Sirt3 deacetylates Lys 139 of Oligomycin Sensitivity Conferral Protein (OSCP) in response to nutrient- and exercise-induced stress in mouse skeletal muscle (Vassilopoulos et al., 2014).

Sirt3 may also regulate LKB1-AMPK axis, which acts as a sensor of cellular energy status, thereby regulating the mitochondrial synthesis of ATP (Giralt and Villaroya, 2012). In fact, the liver kinase B1 (LKB1) tumour suppressor, a key upstream activator of AMPK, has been found to be deacetylated (and thereby activated) by Sirt3 in the heart, with the activated $LKB1^{Ser428}$, activating in turn $AMPK^{Thr172}$, thus augmenting the activity of LKB1-AMPK pathway and leading to high levels of ATP (Pillai et al., 2010). Activated AMPK affects PGC1α transcriptional activation and increases the activity of PGC-1α at least through two mechanisms. Firstly, PGC1α within the nucleus is phosphorylated and activated by AMPK directly (Jäger et al., 2007), and can then co-activate its own promoter to stimulate its expression (Brenmoehl and Hoeflich, 2013). Finally, AMPK increases the levels of cellular NAD+, thereby stimulating Sirt1 to deacetylate and activate PGC1α within both the cytosol and nucleus (Cantò et al., 2009).

AMPK-PGC1α-Sirt3 axis is also linked to other signalling pathways related to tumour suppressor p53. Indeed, AMPK in the nucleus has been reported to serve to phosphorylate p53 (Imamura et al., 2001) together with some other transcription factors and coactivators. Moreover, p53 ablation was shown to result in reduction of PGC1α content and mitochondrial respiration (Bartlett et al., 2014). Upon muscle contraction, p53, phosphorylated on serine 15, translocates to the mitochondria where it forms a complex with TFAM to control complex IV activity (Bartlett et al., 2014). Furthermore, Sirt3 has been shown to target and deacetylate the lysine residues of not only key mitochondrial proteins of oxidative and energetic metabolism, but also numerous other proteins as well. In this context, a link between Sirt3 and p53 has been shown in certain cancers, and the opposite effects elicited by Sirt3 overexpression on p53 protein stability and activity have led to hypothesize that Sirt3 can have oncogenic or tumour-suppressive functions based on cancer types and both known and possibly yet unidentified downstream targets (George and Ahmad, 2016).

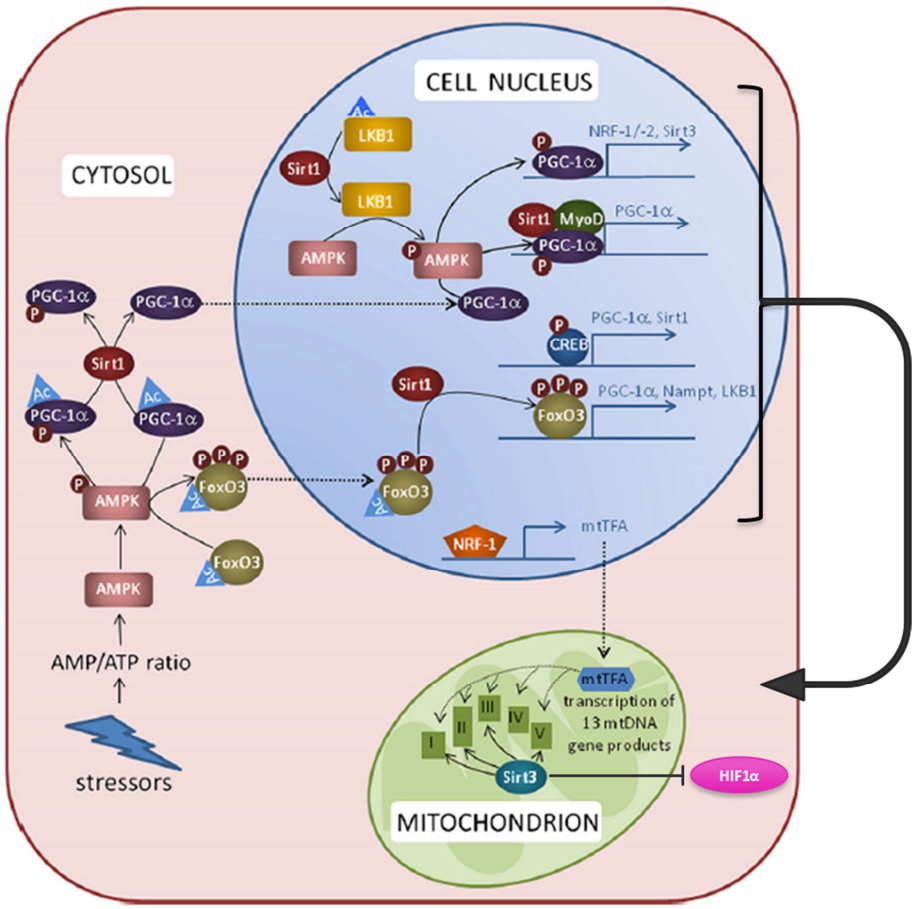

Fig 6. Pathways involved in the control of mitochondrial biogenesis and metabolic regulation. The conditional increase of AMP levels induces activation of AMPK. In the nucleus Sirt1 deacetylates FoxO3, which induces transcription of LKB1, PGC1α and Nampt. Nampt will increase NAD+ levels required for Sirt1-dependent deacetylation and thus activation of LKB1 or PGC1α. Deacetylated PGC1α is translocated to the nucleus. Nuclear and cytosolic PGC1α is phosphorylated and thus activated by AMPK. In complexes with Sirt1 and MyoD, phosphorylated nuclear PGC1α can induce its own gene expression. PGC1α also enhances expression of NRF-1 and -2, that in turn upregulate the expression of OXPHOS complexes. NRF-1 also induced expression of TFAM, which is imported into mitochondrial sub-compartments. Within the mitochondrial matrix, TFAM binds to mtDNA and initiates the expression of mtDNA gene products encoding different subunits of OXPHOS complexes. Mitochondrial Sirt3 deacetylates subunits of OXPHOS proteins and leads to their activation, promoting oxidative phosphorylation and enhancing ATP levels. Furthermore, Sirt3 inhibits HIF-1α activity downregulating glycolysis. Modified from (Brenmoehl & Hoeflich, 2013).

1.2 Two different models of mitochondrial plasticity/regulation: Skeletal Muscle & Brain tumors

Skeletal muscle and brain are very different tissues but have similar characteristics to rely heavily on oxidative phosphorylation and mitochondrial metabolic pathways. Such different tissues, and different pathophysiological conditions, consent to study extensively and in detail all the adaptations of mitochondrion.

Brain cells are very heterogeneous due to different histotypes and metabolic features. Furthermore, they have a high metabolic demand in particular of oxygen and glucose compared to the human whole body

Skeletal muscle represents 40-50% of total body mass making it the largest organ of human body (Ehrenborg & Krook, 2009). Thus, skeletal muscle has the ability to influence the metabolism of the whole body. It has different functions such as regulation of electrolytes, nutrients, pH and protein storage (Ehrenborg & Krook, 2009 and references therein). Skeletal muscle metabolism is very variable, for example, it can consume large quantities of ATP during contraction and also be under hormonal control, i.e. insulin, for glucose utilization (DeFronzo, 1988). Besides, skeletal muscle is a very plastic tissue that can quickly respond to periods of immobility or training and, in order to maintain the tissue homeostasis, mitochondria also need to adapt to these changes. In particular, during exercise training and fasting the activation of PGC1α leads to an increase in mitochondrial mass along with several mitochondrial enzymes and glucose transporters (GLUT4) (Woods et al., 2003). On the contrary, during muscle disuse, mitochondria change in shape and number through fusion and fission processes, and function due to mitochondrial membrane remodelling, thereby downregulating major enzymes such as OXPHOS complexes and decreasing oxidative phosphorylation (Power et al., 2012).

Likewise, there is growing evidence that mitochondrial plasticity is a characteristic of human brain tumor cells. For years, it was common believed that tumor cells prefer to rely on glycolysis, an inefficient way to produce ATP, because of mitochondrial damage (Warburg, 1956). Despite this, nowadays, it is known that cancer cells rely also on oxidative phosphorylation and mitochondria to produce ATP and proliferate. Because of the heterogeneity of the tumoral mass, cancer cells must adapt to the environment in which they are, i.e. the peripheral and hypoxic zones. In fact, cells present in one of these zones should adapt to the diverse flux of nutrient and the oxygen availability. Recently it was proposed a turnover between glycolysis and oxidative phosphorylation as a consequence of “waves” of

genic reprogramming (Smolkova et al., 2010). This mechanism can explain the metabolic heterogeneity in the tumoral mass where coexists hypoxic and oxygenated areas leading to distinct groups of cells with different metabolic characteristics as seen in glioma, a tumor of glial cells in the central nervous system (CNS) (Scrideli et al., 2008 – Marie et al., 2008). At first, due to oncogenes alteration, there is an increase in glycolytic flux and a suppressed mitochondrial biogenesis. Then, because of a high proliferation rate with little quantities of nutrients, there is an upregulation of glutamminolysis followed by revitalization of mitochondria, through PGC1α, in order to sustain cancer proliferation and invasion (Smolkova et al., 2010 – LeBleu et al., 2014).

The project of this thesis is based on the knowledge idea that skeletal muscle and brain tumors represent good models to investigate mitochondrial adaptation to different stimuli.

1.2.1. Mitochondria as intervention target

Mitochondria due to its plasticity and importance in cell metabolism has become an intervention target for many muscle pathologies of the muscle and cancer. Moreover, mitochondria exert biochemical functions that determine cell death or survival, being in a strategic power position over other cell organelles. In particular for muscle, mitochondrion is a very critical organelle due to its function as energy source. During ageing, mitochondrial function tends to decrease also due to low levels of physical activity that can induce muscle wasting. In order to revert this process it was reported that strategies increasing an increase in the levels of PGC1α could preserve muscle mass and functionality due to an enhanced mitochondrial biogenesis (Cannavino et al., 2015). Also some molecules, such as resveratrol, are used as new pharmacological approach to ameliorate aerobic capacity by improving insulin resistance (often impaired in mitochondrial dysfunction), biogenesis activation and genes related to ETC (Lagouge et al., 2006).

Mitochondrion, because of its central role in energy metabolism, has a pivotal role in cancer treatment. Metabolic dysfunction are very frequent in cancer cells. Nowadays, it is known that cancer cells metabolism is very heterogeneous and more complicated than what was thought fifteen years ago. A neoplastic cell can use aerobic glycolysis to proliferate or oxidative phosphorylation in order to infiltrate or metastasize, so targeting mitochondrial metabolism has become a more and more challenging strategy. Form a different point of view, in these last few years research groups have focused their attention on the role of mitochondria in apoptotic process in order to provide new cancer cures. One option is to increase the

apoptotic stimuli in cancer cells (Fulda, 2010 – Hagland et al., 2007). For example the suppression of pyruvate dehydrogenase kinase and lactate dehydrogenase activities using dichloroacetate, results in a shift from glycolysis to glucose oxidation and in mitochondria decreases membrane potential, increases production of ROS and activates K+ channel Kv1.5 inducing apoptosis in neoplastic cells, but not in normal ones (Bonnet et al., 2007).

Just from these few examples in different tissues like skeletal muscle and brain, it is possible to comprehend the major well-documented potential of targeting mitochondria in interventions for different pathophysiological conditions.

1.3 Skeletal Muscle

1.3.1. Mitochondrial adaptations in skeletal muscle during immobility/microgravity (Bed-Rest model) and ageing

Skeletal muscle, as stated in the precedent paragraph, is a tissue that can rapidly adapt to training, nutrient and hormone homeostasis. Disuse is a major feature that can shape muscle molecular and systemic structure and function and is a very common condition that can be caused by many situations, such as a cast leg/arm, absence of gravity as during space flights, or ageing. The molecular pathways and phenomena that occur during a period of disuse/immobility are not completely characterized and understood yet. In order to study these changes in skeletal muscle are often used bed rest studies. This approach simulates a reduced level of physical activity as well as microgravity. Bed rest conditions lead to skeletal muscle hypotrophy and/or atrophy that consent to evaluate systemic and molecular changes experienced.

At a systemic level muscle mass loss and impairment of oxidative function are very frequent in subjects that have experienced immobility or microgravity (Short et al., 2005 - Bergouignan et al., 2009 – Bergouignan et al., 2011 – Salvadego et al., 2011 – Wall et al., 2014 – Dirks et al., 2014). The process seems to be led, at a molecular level, by protein degradation (Sandri, 2008) and/or reduction of OXPHOS function elicited by hyperacetylation (Menzies and Auwerx, 2013). However, there is still a major debate to understand which mechanisms are involved in muscle atrophy. In fact, complete details of the signalling events that regulate the muscle wasting process remain obscure. In this scenario, it is known that disuse muscle atrophy is associated with mitochondrial damage and energy stress due to an impaired capacity to produce ATP (Romanello and Sandri, 2010 – Min et al., 2011).

In the light of these findings, during the last few years, a new interest has arisen around the role played by skeletal muscle mitochondria function and biogenesis in the mechanisms involved in immobility (Carter et al., 2015). Numerous studies reported mitochondrial mass and metabolism downregulation during immobility but it is still a matter of discussion whether these changes are a consequence or a prerequisite of atrophy. During disuse was reported a fragmentation in the mitochondrial reticulum that undergone a remodelling, through autophagy, resulting in enlarged swelling mitochondria (Romanello et al., 2010 – Wiggs et al., 2015). This promotes an imbalance between mitochondrial fission (mitochondrial membranes separation) and fusion events (mitochondrial membranes merger). Furthermore, it was

described an increase of proteins related to fission such as Fission1 protein and downregulation of Mitofusin 1 and 2, involved in fusion, (Romanello et al., 2010 – Chen et al., 2010) resulting in an altered mitochondrial structure. Fusion is an essential process in skeletal muscle excitation-contraction, due to its function to increase oxidative capacity, and during energy demand conditions, where fusion protects mitochondria against mitophagy (Eisner et al., 2014 – Romanello & Sandri, 2016). The mitochondrial remodelling during fission is reported to be associated to a decrease in OXPHOS function and to an increase in ROS production. This upregulation of ROS during immobility seems to be caused not only by fission, but also by imbalance of calcium homeostasis and increase of fatty acid hydroperoxides that can control mitochondrial function and mitochondrial matrix-direct superoxide production (Powers et al., 2012 and references therein). The augmented ROS production during atrophy can also led to the release of pro-apoptotic factors such as cytochrome c, which in turn can activate caspase-3 and protein breakdown. Interestingly, ROS upregulation leads to oxidized proteins, which are more prone to proteolysis because they can be directly degradated by the proteasome without being ubiquitinated (Grune et al., 2003). In addition, protein degradation seems to be related to a decrease in PGC1α protein level with a consequent activation of Forkhead box O3 (FOXO3A) and nuclear factor kappa-light-chain-enhancer of activated B cells (NF-kB) (Brault et al., 2010). In particular FOXO family, controlled by Akt pathway, induces protein degradation, of also fusion proteins like Mitofusin 2, and upregulation of ubiquitin ligases Atrogin-1 and E3 ubiquitin-protein ligase TRIM63 (MuRF1) along with several other autophagy related genes. Moreover, FOXO3A, along with the induction of MuRF1 and Atrogin-1, induces the ubiquitine proteasome and autophagy-lysosome systems for protein degradation (Sandri, 2013). The first degrades mainly myofibrillar proteins, whereas the latter removes damaged organelles, protein aggregates and unfolded and toxic proteins (Romanello & Sandri, 2016). Besides protein breakdown, also a decrease in protein synthesis seems to be related to atrophy. This might be determined as a consequence of decrease ATP production that could also result in energy stress (Romanello et al., 2010).

The same processes are present in skeletal muscle also during ageing. It is known that after the fourth decade of life muscle mass and strength start to decline due also to low levels of physical activity, along with mitochondrial function (Peterson et al., 2012). In particular, advancing with age, skeletal fibers experienced an increase of ROS levels, apoptosis and protein damage/degradation, decrease in antioxidant system and autophagy and changes in

mitochondrial structure and function as it occurs in atrophy following immobility (Peterson et al., 2012 and references therein).

Despite everything, there are many unanswered question about the processes occurring in muscle wasting during ageing, along with discordant reports. In fact, there are several reports about mitochondrial biogenesis and ageing focusing on PCG1α that account for decreased or unchanged levels of protein and mRNA (Romanello & Sandri, 2016 – Peterson et al., 2012). Unclear is also the role in ageing of alteration in OXPHOS and energy production gene transcripts. Moreover, it was reported that key genes associated to the deterioration of muscle in elderly people are involved in inflammation, apoptosis, and regulating mRNA splicing, not in OXPHOS (Giresi et al., 2005 – Peterson et al., 2012). Notably, reports on the increase in ROS levels during ageing as in immobility confirmed an increase in oxydated mitochondrial proteins thereby affecting mitochondrial proteostasis (Ross et al., 2015).

In conclusion, these are three main independent and/or interdependent mitochondrial pathways that can induce skeletal muscle function impairment during atrophy and age related sarcopenia (Fig 7). Nevertheless there are still unanswered question over the induction of muscle atrophy and its connection to mitochondria.

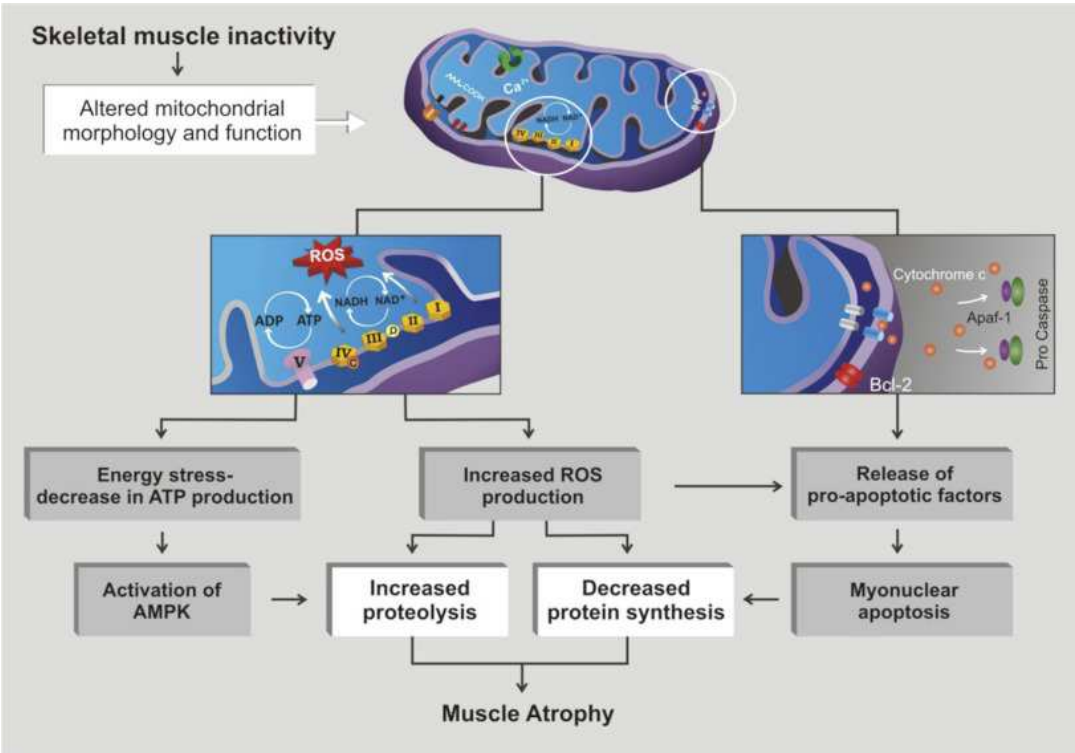

Fig 7. Mitochondrial pathways related to skeletal muscle atrophy (Powers et al., 2012)**.**

1.3.2. Skeletal Muscle and mitochondria performance in Chronic Heart Failure

Chronic heart failure (CHF) is a progressive syndrome in which the heart is unable to adequately perfuse body tissues. It is mainly caused by coronary heart disease, hypertension, diabetes, cardiomyopathy and congenital heart defects (Hirai et al., 2015). This clinical syndrome is a major health concern for national health systems since more than 50% of patients die within 5 years after diagnosis (Czarnowska et al., 2016 – Go et al., 2013). CHF has a great impact on skeletal muscle where the patients experience fatigue and dyspnoea during exercise training. In fact, in CHF patients exercise intolerance represents one of the clinical hallmarks (Poole et al. 2012, Hirai et al. 2015), significantly affecting the patients' quality of life and has a strong prognostic value (Myers et al. 2002, Hirai et al. 2015).

An impairment of skeletal muscle oxidative metabolism, with functional consequences involving other organs and systems, seems to play a key role in the pathogenesis of exercise intolerance in CHF patients (Poole et al. 2012). The role of skeletal muscle is even more pronounced in patients with CHF and preserved ejection fraction (Haykowski et al. 2015).

Several works reported in skeletal muscle, during heart failure, a shift of muscle fiber distribution towards glycolytic ones (Type II) along with increase in glycolysis, fiber atrophy and reduction in lipolysis and oxidative enzymes (Schaufelberger et al., 1995 – Szentesi et al., 2005 – Opasich et al., 1996 – Simonini et al., 1996). In particular, decreased mitochondrial volume and cristae surface density were reported, suggesting a compromised oxidative capacity that, along with altered skeletal muscle metabolism, was the major cause of exercise intolerance in CHF patients (Drexler et al., 1992). Many other enzymes like citrate synthase, creatin kinase, succinate dehydrogenase and lactate dehydrogenase were decreased in the pathology confirming an impaired metabolism (Mettauer et al., 2001 – Drexler et al., 1992 – Mancini et al., 1992).

These changes can be linked to a reduced activity by Krebs cycle and consequently to decreased ATP levels, suggesting an energy depletion in skeletal muscle of CHF patients (Drexler et al., 1992). In association with these changes, defects of oxidative phosphorylation rates through OXPHOS complex I and decreased amount of I/III_2 supercomplex were found (Rosca & Hoppel, 2013). In accordance to this, also OXPHOS I, II and III complexes were found decreased in gastrocnemius muscle mitochondria of CHF patients (Rosca et al., 2009).

A useful animal model to investigate these aspects at functional, cellular and molecular levels is represented by the Tgαq*44 mice, a transgenic mouse model of CHF resulting from a cardiac-specific overexpression of a constitutively active Gαq protein (Mende et al. 2001).

Gαq protein is coupled to a protein kinase C-mediated cascade and in cardiac muscle is a transducer of neurohumoral signals (Takeishi et al., 1999 – Bowling et al., 1999). Thus, Gαq protein activation contributes to the development of changes in myocardial proteins leading to cardiac hypertrophy and ultimately to heart failure (de Jonge et al., 2008 – Huang et al., 2001 – Edes et al., 2008). Through the overexpression of Gαq protein, Tgαq*44 mice mimics the phenotype of human dilated cardiomyopathy both at functional and morphological levels (Mende et al, 2001). Moreover the Tgαq*44 mice model is characterized by a delayed progression from cardiac hypertrophy to overt CHF, differently from most animal models of CHF where the transition to uncompensated CHF is rather rapid (Czarnowska et al. 2016). Indeed, although the activation of hypertrophic genes is evident in Tgαq*44 mice starting from ~4 months of age, cardiac function may be preserved up to ~10 months of age, and cardiac decompensation usually occurs at ~12-14 months of age, exiting in the animals' death starting from ~14 months of age (Czarnowska et al. 2016). This delayed progression is of particular interest, since in humans the progression from cardiac hypertrophy and asymptomatic diastolic dysfunction to overt CHF often occurs over several years (Braunwald 2013). Besides this aspect, Tgαq*44 mice model consents to study the mitochondrial changes during the transition phase of the pathology in order to clear whether mitochondrial dysfunction precedes or it's a consequence of the development of disease. In this mice model were observed, in the last stages of the disease, an impairment in cardiomyocytes mitochondria, such as alteration of mitochondrial structure, reduced cristae structure, downregulation of Fe-S centres, COX, citrate synthase and Q pool (Elas et al., 2008 – Mende et al., 2001). These characteristics fully matched the already characterized mitochondrial abnormalities in CHF cardiomyocytes such as impaired ATP production, switch to glucose metabolisms, increase in ROS levels and cytochrome c release (Elas et al., 2008 – Huss & Kelly, 2005).

In Tgαq*44 mice model is still missing a report on skeletal muscle adaptations following the transition phase from the compensate to the uncompensated CHF.

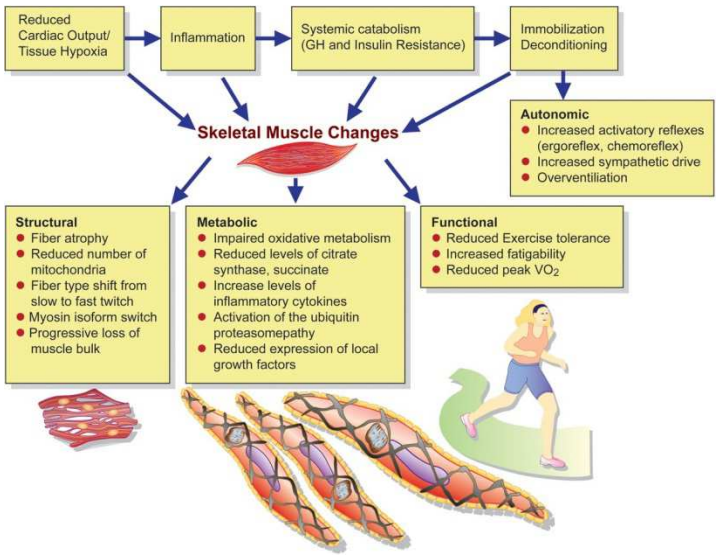

Fig 8. Skeletal muscle changes and specific intrinsic muscle derangements in heart failure
(Piepoli & Stewart Coats, 2013)

1.3.3. Exercise as therapeutic intervention

It is common knowledge that exercise has many benefits to the whole body and is one of the most prescribed therapy in health and diseased people. Exercise is used as prevention in many pathologic conditions such as pulmonary, cardiovascular, muscle, bone, joint diseases, cancer and depression (Vina et al., 2012).

In muscles, that have experienced a period of immobility and consequently present atrophy, exercise induces a switch from type II fast-twitch fibers (glycolytic fibers) to type I slow- twitch fibers (oxidative fibers) due to an increase in mitochondrial biogenesis. This increase in mitochondria content leads to an amelioration of oxidative function and aerobic capacity along with an increase in fatty acid oxidation (Mootha et al., 2003). In addition, antioxidant defences are increased with exercise, maintaining low levels of ROS (Vina et al., 2012). Exercise training, as cell homeostasis perturbation, is capable to activate processes of mitochondrial biogenesis due to increased PGC1α levels, fusion events and selective mitophagy through the pathway described in paragraph 1.1.3 and 2.1.1 (Fig 9). With the right recovery protocol of exercise training a patient who have been subjected periods of immobility and/or absence of gravity can recover his muscle mass and function.

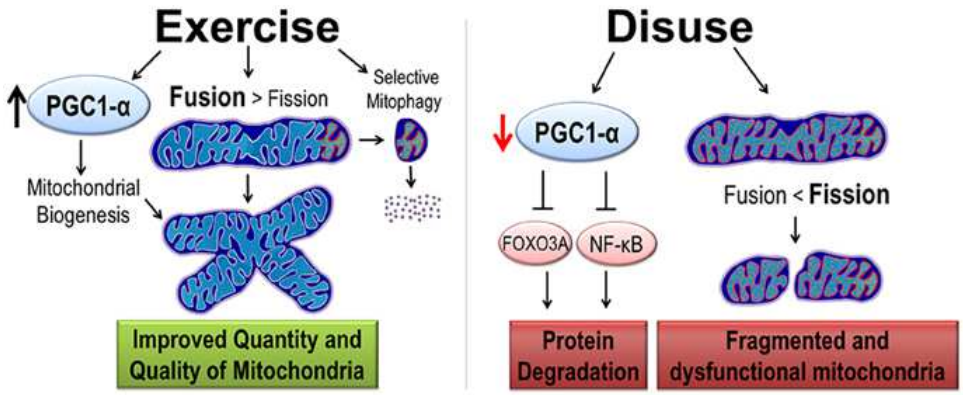

Fig 9. Exercise and disuse effects on mitochondrial quality and quantity. (Wiggs, 2015)

Exercise is beneficial also during ageing. In fact, as referred above, skeletal muscle around the fourth decade of life tends to decline in mass and strength. Such decline, that can only accelerate with ageing (Hughes et al., 2001) leads, advancing with age, to a decreased physical activity that can be deleterious for skeletal muscle and cardiovascular function (Brower, 2009). Physical activity in these subjects can help to recover their muscle function and it was demonstrated that differences in mitochondrial function, protein abundance and/or mRNA levels between young and elderly people are no longer present if the latter practise some physical activity (Brierly et al., 1996 – Abadi et al., 2009).

Exercise is known to be a therapeutic intervention also in patients affected by heart failure due to their intolerance to physical activity. Endurance training, in particular, in CHF patients proved to increase the blood flow across muscle tissues, mitochondrial volume and oxidative enzymes activities, diffusion and delivery of oxygen, nitric oxide (as vasodilator to augment blood flow to the body periphery) and vascular stiffness, along with a decrease in pro-inflammatory cytokines, ROS production, apoptosis and muscle atrophy (Poole et al., 2012 and references therein). All these events during training ended in an amelioration of maximum oxygen uptake ($V'O_{2max}$), lactate threshold and decreased cost of exercise, finally resulting in exercise tolerance and in an improvement of patients quality of life (Poole et al., 2012 and references therein).

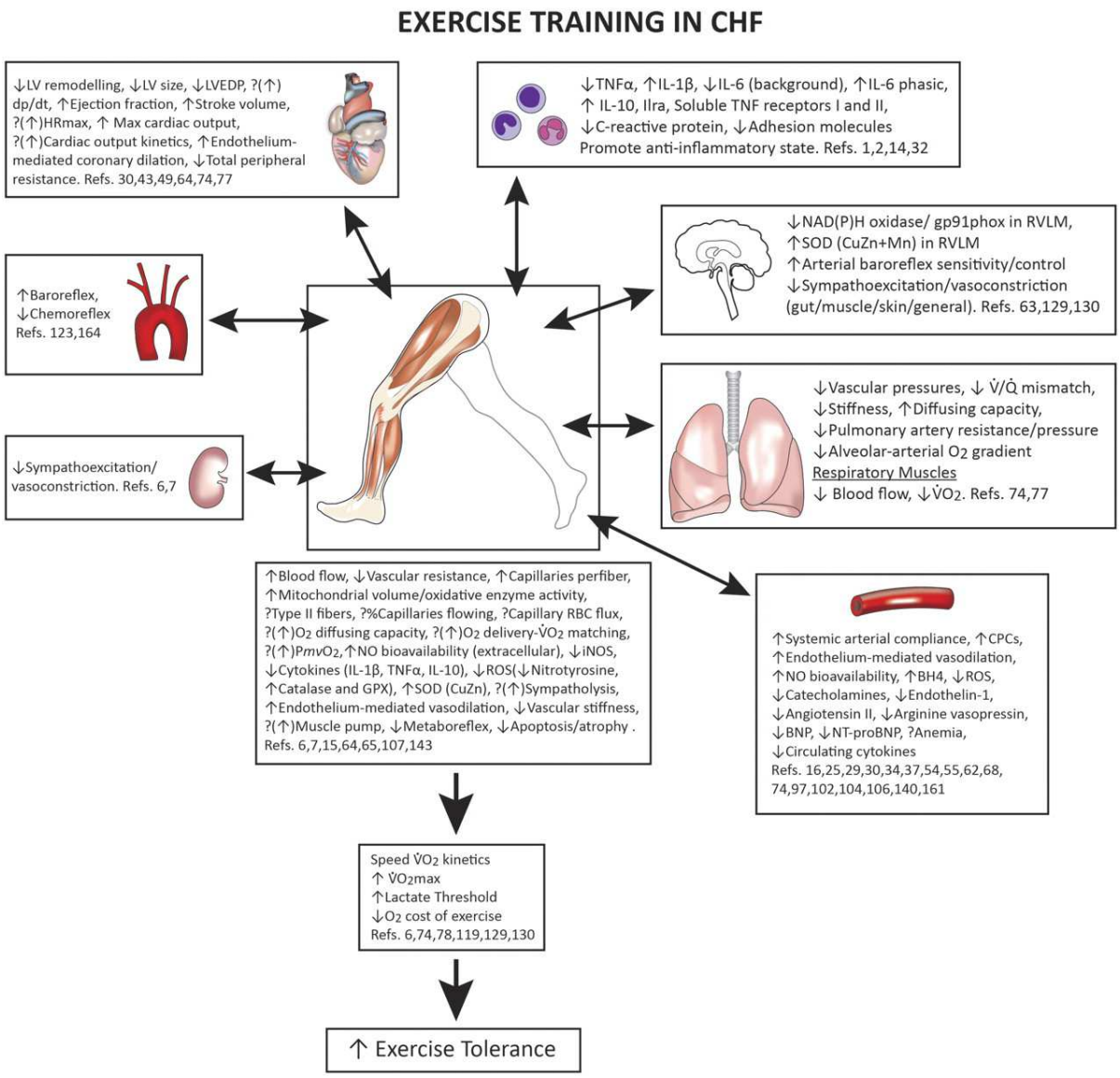

Fig 10. Endurance exercise training opposes many of the dysfunctional elements of CHF and facilitates improved skeletal muscle gas exchange and exercise tolerance. (Poole et al., 2012)

1.4 Glioma

Gliomas represent the most common type of intracranial neoplasia, comprehend almost 60% of all primary tumors of CNS and originate from glial cells. Glia, the supporting structure of CNS, has several important functions such as to supply oxygen and nutrients to neurons, remove waste products and produce the myelin, which coats nervous fibers permitting the transduction of electrical impulse. Gliomas have an incidence of 5 cases every 100'000 people/year. Social, sanitary and economic costs from diagnosis to patients managements are very high (Ordys et al., 2010).

There are several types of gliomas that could be classified by the different histological type of the glial cells from which the tumor has developed: diffuse astrocytomas (fibrillary astrocytoma, protoplasmic astrocytoma and gemistocytic astrocytoma) and glioblastoma multiforme from astrocytes, oligodendrogliomas from oligodendrocytes and oligoastrocytomas from oligoastrocytes.

Gliomas are further classified by histopathologic analysis in which is determined the grading of the neoplasia, from I to IV according to the World Health Organization (WHO) guidelines based on atypical cells quantity, mitosis, endothelial proliferation and necrosis (Grier & Batchelor, 2006). In particular, tumors without any of these features are regarded as grade I, on the contrary if they have only one, usually atypical cells quantity, are regarded as grade II. If the tumor has more than two of the characteristics reported above, are considered malignant and referred as grade III or IV. Along with this analysis, there were recently introduced new genetic parameters in order to choose the best clinical approach for every case (Luis et al., 2016).

From WHO grading it is possible to distinguish two different groups: low-grade (LGG – I-II grade) and high-grade gliomas (HGG – III-IV grade). LGG are well differentiated, benign and have a good outcome, but they can also recur and progress into anaplastic forms. On the contrary, HGG are undifferentiated or anaplastic tumors and have a poor prognosis.

1.4.1. Low Grade Astrocytomas

Astrocytic tumors represents 10.2% of primary neoplasia in CNS and are the most represented type among all gliomas (30%) with an high tendency of low-grade lesions for recurrence and progression into malignant forms if not completely resected by surgery (CBTRUS, 2011). Clinical outcome of these tumors depends on age of diagnosis, genetic markers and extent of the surgical resection.

Astrocytomas preferentially develop in young adults, around the third and fourth decade of life. The survival rates in these patients at 1, 5, and 10 years are 91.6%, 58.5%, and 40.7%, respectively (CBTRUS, 2011). Usually the prognosis is good when the diagnosis is fast. Nevertheless, even if they are slow-growing tumors the recurrence (10 years) is very high and researchers are now focusing on new diagnostic and therapeutic methods in order to better personalize the therapeutic intervention to reduce the recurrence of pathology.

In many young patients cases low-grade astrocytomas are just the first step in the tumor progression towards secondary glioblastomas. For this reason is essential, and very difficult to date, to identify molecular characteristics which can distinguish low-grade from high-grade astrocytomas and primary from secondary glioblastomas (Louis et al., 2007 – Ino et al., 2000 – Bethke et al., 2008).

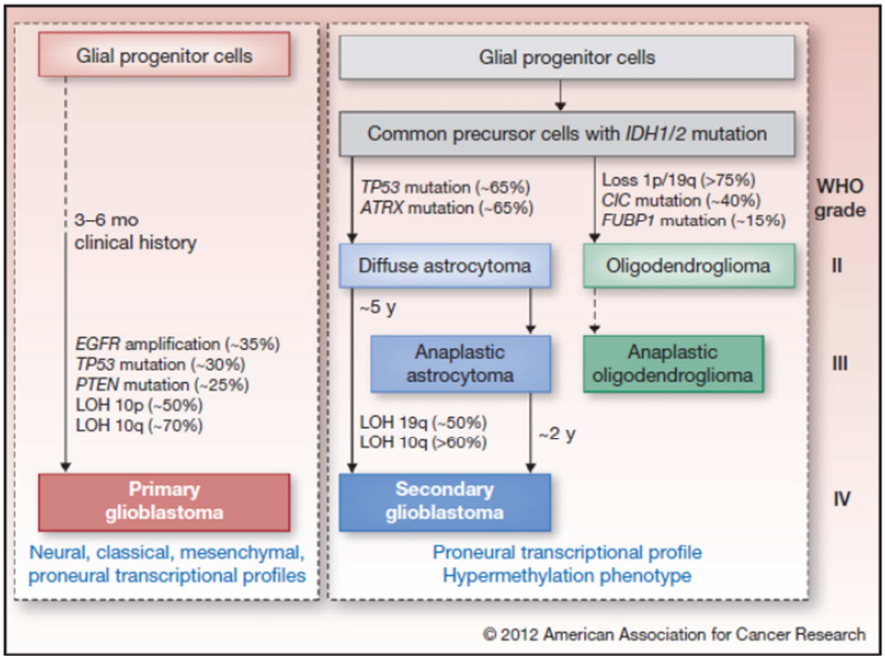

Fig 11. Molecular characteristics and genetic pathway that lead the progression to glioblastomas.
(*Ohgaki et al., 2013*)

In low-grade astrocytomas (LGA) are observed mainly chromosomic alteration on chromosome 7 in particular with trisomies or polysomies (Schröck et al., 1999 – Wessels et al., 2002). Nevertheless, deletion of 1p36 and 19q13.3 chromosome regions are reported in 18% and 38% of the cases, respectively. Instead, codeletions of these regions are observed just in 11% of the patients (Smith et al., 1999). 60% to 80% of LGAs present an allelic loss of chromosome 17p on which there is TP53 genic locus that codifies for p53 protein (Rees &

Wen, 2010). Even in the cases where the locus is retained TP53 gene presents mutation, making it the major genic mutation in these tumors.

Many metabolic enzymes are mutated or involved in gliomas biology. In particular, mutations of the isoforms 1 and 2 (IDH1 and IDH2) of isocitrate dehydrogenase, an enzyme of Krebs cycle, are the most present in both low-grade astrocytomas and secondary glioblastomas. In fact, 80% of all astrocytomas show IDH1 mutation and the other 20% IDH2 mutation (Yan et al., 2009). The most prevalent modification is a mutated arginine in position 132 on IDH1 that results in overproduction of 2-hydroxyglutarate metabolite (Balss et al., 2008). There are many hypothesis around IDH1/2 mutations and some authors say that they are oncogenic, whereas others say they represent a protective mechanism against tumor cells metabolic reprogramming.

Although during the last few years researchers were able to classify molecular abnormalities and genomic mutations, still there is not any definitive biomarker that is caplable to identify a low-grade lesion that could be able to progress into a secondary glioblastoma. Nevertheless, there were recently proposed many biomarkers, such as the phosphorylated eukaryotic translation initiation factor 4E (p-eIF4E), MAP kinase-interacting kinases (p-Mnk1) and p70S6 kinase (p-p70S6K), as factors involved in promoting cellular proliferation, malignant transformation and metastasis in LGA (Fan et al., 2016).

1.4.2. Glioblastomas or High Grade Astrocytomas

High-grade gliomas are very aggressive being III-IV grade tumors that could evolve *de novo* or as evolution from low-grade lesions. HGG comprehend tumors that originate from the three different histotypes of the glial cells. The most frequent is glioblastoma (WHO IV grade astrocytoma). It represents half of all gliomas and it is the most malignant (18 month prognosis) and common neoplasia of the CNS in adults (55-87 yo) (Ordys et al., 2010 – Daga et al., 2011). Every year in Europe the incidence is 2-3 new cases every 100’000 people meanwhile in Italy there are 7’000 new cases every year. This neoplasia can be treated with surgery in association to chemotherapy and radiotherapy.

Glioblastomas are divided into two groups: primary and secondary (Fig 11) (Agnihotri et al., 2013). Primary glioblastoma is the most frequent one, affects usually elderly patients and develops *de novo*. Genetically it is characterized by amplifications and mutations of epidermal growth factor receptor gene (EGFR), mutations of phosphatase and tensin homolog gene (PTEN), overexpression of Mouse Double Minute 2 gene (MDM2), deletion of p16 and

complete loss of chromosome 10. Secondary glioblastoma is more sporadic, affects people in their 40s and is a progression of low-grade lesions. Genetically is characterized by mutations of p53 and Retinoblastoma gene (Rb), overexpression of platelet-derived growth factor A and platelet-derived growth factor receptor alpha (PDGFA/PDGFRα); loss of heterozygosity of chromosome 19q, mutations of IDH1.

Males are usually more affected than females and the clinical history of these patients is of 6 months for primary glioblastomas and 17 months for secondary glioblastomas (Daga et al., 2011).

Based on analyses on DNA, mRNA and miRNA, glioblastomas could be further classified as (Verhaak et al., 2010):

- Classical: amplification and mutation of EGFR gene, PTEN and CDKN2A deletion and overexpression of Nestin;
- Mesenchymal: mutation and inactivation of neurofibromin 1 (NF1), p53 and PTEN, overexpression of MET, CD44, chitinase 3-like 1 (CHI3L1);
- Proneural: has a similar expression profile to neurons in the first phases of development and shows mutation of IDH1/2, p53, amplifications of PDGFRA, cyclin-dependent kinase 6 e 4, MET and PTEN inactivation;
- Neural: has similar characteristics of healthy nervous tissue and presents human epidermal growth factor receptor 2 (HER2) overexpression (Sameer et al., 2013).

Aside from molecular characteristics, it is known that in glioblastoma cells, the most significant reprogramming occurs in the metabolic machinery. Thus, metabolism is now an area of intense research to identify novel therapeutic targets and biomarkers. In fact, IF1 (see paragraph 1.1.1) was recently found to be a prognostic factor in gliomas and in particular to be overexpressed in glioblastomas promoting infiltration and proliferation of the tumoral mass (Wu et al., 2015). In this perspective mitochondrial has gained new interest in the molecular oncology field.

1.4.3. The role of mitochondria in gliomas

Tumor metabolism is highly heterogeneous and also gliomas present this characteristic along with an abnormal energy production driven by aerobic glycolysis. In particular, astrocyte cells from which originate astrocytomas usually rely on glycolysis and are the most involved cells in the metabolic shift towards aerobic glycolysis during physiological neural activity. Moreover, different intercellular signals released by active neurons, e.g. glutamate,

K^+, NH^{4+}, are known to stimulate aerobic lactate production by astrocytes to support neurons metabolism and demands. Astrocyte does not use only glycolysis but also oxidative phosphorylation in order to produce ATP for self-energy demands (Kim et al., 2015).

This kind of heterogeneity reflects not only on healthy cells but also on cancer cells. In this perspective mitochondria as gained new interest in this field of study.

An implication in the early stages of cancer by mitochondria is shown by the amplification of mtDNA. This modification is present in the early stages of low-grade gliomas in contrast with modifications of nuclear DNA that are present in the subsequent stages of the pathology (Liang et al., 2011).

Mitochondrial proteins were found to be mutated in astrocytomas such as IDH1 and 2, as already mentioned in paragraph 1.4.1. For these two enzymes it was hypothesized a different tumor progression mechanism aside from Warburg effect. In this hypothesis, the tumor produces acidic molecules in order to suppress neighbour cells and promotes itself (Scott et al., 2011).

According to Warburg metabolic phenotype, major ATP source of glioblastoma cells is frequently reported to be via aerobic glycolysis, although Krebs cycle is still active (Wolf et al., 2010; Feichtinger et al., 2014). In contrast, some studies report that gliomas cells may rely on both glycolysis and mitochondrial oxidation for glucose catabolism (Margareto et al., 2007, Griguer et al., 2005; Kim et al., 2015), thereby documenting a certain degree of oxidative activity as in astrocytes (Azarias et al., 2011). Indeed, a significant number of genes involved in the OXPHOS process are reported to be overexpressed in glioblastomas if compared to the low-grade astrocytomas (Margareto et al., 2007). Moreover, the activation of the OXPHOS pathways reported in some glioma cell lines under low glucose condition may imply that such cells must hold functional OXPHOS activity, being able to switch from to oxidative metabolism in response to specific environmental conditions (Griguer et al., 2005). Furthermore, an “oxidative phenotype” where ATP is produced by OXPHOS from fatty acids oxidation, or glutamine oxidation, has been reported for glioblastomas in a recent review, as well as for some other cancer types (Obre and Rossignol 2015).

Based on these reports it easy to recognize a major role for mitochondria in cancer metabolism and in particular in gliomas, and that this field of research could be very promising in finding new prognostic factors and treatments that involve mitochondrial metabolism.

2. AIM

The aim of the project of this PhD Thesis was to provide a contribution to define if up- and down- regulation of mitochondria biogenesis and activity are required in humans to meet different energetic demands under pathophysiological conditions such as aging and cancer. A purpose was to support in this way the potential of targeting mitochondria in therapeutic interventions, as well as to identify possible prognostic biomarkers. To this aim, two models were investigated, namely skeletal muscle under stress conditions and brain tumors. Skeletal muscle and brain are very different tissues but have similar metabolic characteristics, i.e. a high metabolic demand in particular of oxygen and glucose, relying heavily on oxidative phosphorylation and mitochondrial oxidative pathways, but also on glycolysis due to skeletal muscle metabolic plasticity and heterogeneity of brain cells histotypes and metabolic features. The idea was that investigating different pathophysiological conditions of such tissues could allow the extensive study of mitochondria adaptation and the related signalling, which may be triggered by disturbances and stresses and targeted by therapies. Indeed, such topic has recently come to prominence in many pathophysiological conditions due to its central role in pathogenic mechanisms and as a therapeutic target.

The focus was on the study of mitochondrial OXPHOS complexes, together with the GAPDH, as glycolytic marker, HSP60, CS and TOM20 as mitochondrial mass markers. The expression levels of some key proteins of the pathways involved in biogenesis regulation were concomitantly analysed, i.e. LKB1-AMPK an energy-sensing axis, PGC1α the regulator of mitochondrial biogenesis, Sirt3 as controller of mitochondrial enzymes functionality, IF1 a natural inhibitor of OXPHOS complex V. The study was divided into three different sections, each one representing a different *ex vivo* model.

Mitochondrial adaptations were firstly studied in human skeletal muscle after bed-rest with subsequent rehabilitation protocol in both young and elderly subjects. The goal was to identify not only the mitochondrial modifications that occur during immobility and exercise, but also different responses due to ageing.

The effect of exercise training on mitochondrial functionality was further evaluated in a chronic heart failure mice model (Tgαq*44), during the transition from the compensated to uncompensated phase of the disease. The goal was to identify mitochondrial dysfunctions caused by heart failure in skeletal muscle, if any, and if it was possible to revert them with exercise training.

Finally, mitochondrial modifications, in terms of protein expression of OXPHOS complexes, mitochondrial markers and ATP synthase inhibitory factor IF1, were investigated in human low-grade astrocytomas and in their progression. The main aim was to identify possible prognostic factors that could discriminate low-grade lesions at high or low risk to recur. Beside this, we focused on mitochondrial proteins modifications in low-grade astrocytomas with suspected initial anaplastic evolution with respect to canonical low-grade astrocytomas.

3. MATHERIALS & METHODS

3.1. Study Models

3.1.1. Bed Rest Study: Participants and Study Design

Twenty-three healthy men, of which 7 young (Y; aged 18-30 years) and 16 elderly subjects (E; aged 55-65 years) were recruited for the study. All participants underwent medical examination and routine blood and urine analysis. Basic anthropometric parameters of the two groups were: age (years) → 23.1 ± 2.9 (mean ± SD) for Y and 59.6 ± 3.4 for E; stature (m) → 1.77 ± 0.07 for Y and 1.73 ± 0.05 for E; body mass (kg) → 74.8 ± 8.8 for Y and 79.9 ± 12.3 for E; body mass index (kg/m^2) 24.0 ± 2.4 for Y and 26.6 ± 4.4 for E (Pišot et al., 2016). Exclusion criteria were: smoking; regular alcohol consumption; ferromagnetic implants; history of deep vein thrombosis; acute or chronic skeletal, neuromuscular, metabolic and cardiovascular disease conditions; pulmonary embolism. Participants were informed of the purpose, procedures and potential risk of the study before signing the informed consent. The study was performed in accordance with the ethical standards of the 1964 Declaration of Helsinki and was approved by the National Ethical Committee of the Slovenian Ministry of Health on April 17, 2012 under the acronym: IR-aging 1200.

The study was conducted in controlled medical environment of the Orthopaedic Hospital of Valdoltra, Slovenia. The participants were housed in standard air-conditioned hospital rooms and were under constant surveillance with 24-hour medical care. For 14 days, the participants performed all daily activities in bed and received standard hospital meals three times a day. All participants followed an individually controlled eucaloric diet during BR period. Dietary energy requirements were designed for each subject multiplying resting energy expenditure by factors 1.2 and 1.4 in BR and ambulatory period, respectively (Biolo et al., 2008). The macronutrient food content set at 60% of carbohydrates, 25% fat, and 15% of proteins. Energy balance was checked weekly by fat mass assessment. After the bed-rest, participants underwent a rehabilitation protocol (R+14) that consisted of 2- week supervised multimodal exercise program with 3 sessions per week. In each session, 6 participants performed 12-minute warm-up, 15-20 minutes of balance and strength training, and 20-30 minutes of endurance training.

Three different biopsies were taken from *vastus lateralis* muscle of each subject: one before starting bed rest for baseline data collection (BCD), one after the bed rest period (BR14) and the last after the rehabilitation protocol (R+14).

For Citrate Synthase (CS) activity measurements were used samples from the young group of control described in [Salvadego et al., 2016], due to similar anthropometric characteristics such as age (24.1 ± 1.7 years); body mass (73.4 ± 12.1 kg); stature (1.79 ± 0.07 m); body mass index (22.7 ± 3.1 kg/m^2).

3.1.2. Effects of Exercise in Healthy and Tgαq*44 Transgenic CHF Mice Study: Animals Characteristics and Exercise Protocol

For this study were used 26 adult female FVB wild-type (WT) and 30 homozygous Tgαq*44 (TG) mice, aged 10 months at the start of the study (body mass 30.2 ± 2.9 g, range 23.5-36.7 g in WT, 28.8 ± 3.0 g, range 22.5-36.3 g in Tg, no significant differences between groups). Tgαq*44 mice were maintained in the FVB background. Impaired cardiac function of Tgαq*44 mice used was verified in parallel experiments by MRI. Mice were divided into four groups: 15 sedentary (S) and 9 trained (T) WT mice and 15 S and 14 T TG mice. Tgαq*44 were previously characterized by (Mende et al., 2001). The animals utilized in the present study were bred at the Institute of Experimental and Clinical Medicine of the Polish Academy of Sciences in Warsaw (Poland). Prior to the experiments, the animals were transported to the animal house of the Faculty of Pharmacy, Medical College, Jagiellonian University in Kraków (Poland). Mice were housed one per cage (floor area of 355 x 235 x 190 mm) and maintained at 22-24°C under a 12 h light cycle with ad libitum access to water and rodent chow.

The training groups were placed in cages equipped with a running wheel allowing to perform voluntary running activity. Voluntary wheel running activity of each mouse was recorded continuously using the Running Wheel System (Columbus Instruments Inc., Ohio, USA). The system was programmed to record all running episodes that lasted more than 10 seconds. Moreover, the mice were monitored by a digital camera placed in the animal house, allowing the supervising person to check the mice behaviour at a given time without disturbing its normal life. Based on the number of revolutions of the wheel and its radius, the covered distance and the running velocity of the animals were calculated. The data were stored in a computer and were downloaded on a weekly basis. The individual data of covered distance and velocity of running were expressed as a mean ± SD value per 24 h, and were further averaged for the entire period of training (56 days).

All experimental protocols were conducted according to the Guidelines for Animal Care and Treatment of the European Union, and were approved by the Local Bioethics Committee in Kraków (approvals No. 914/2012 and 27/2014).

3.1.3. ATPase-Inhibitory Factor 1 (IF1) as Prognostic Factor in LGA Study: Study Design and Sample Characteristics

The samples used for this study were obtained by the Institute of Anatomic Pathology of the "Santa Maria della Misericordia" University Hospital. The independent ethic committee of the University of Udine has approved the research. Written informed consents were obtained from patients and all clinical investigations have been conducted according to the principles expressed in the Declaration of Helsinki. Patients underwent surgical resection of the tumor at the Neurosurgery Department of the University Udine Hospital.

For immunohistochemical analyses, formalin fixed and paraffin embedded (FFPE) tissues obtained from 13 WHO grade II astrocytomas (6 grade II – LGA – and 7 grade II with a suspected anaplastic evolution – LGA* –) and 14 WHO grade IV astrocytomas (glioblastomas) were employed.

For immunofluorescence analyses, surgical specimens obtained from 12 WHO grade II astrocytomas (7 LGA and 5 LGA*) and 9 WHO grade IV astrocytomas (glioblastomas) were employed. For western blot analyses, snap-frozen tissue samples obtained from 4 LGA and 5 LGA* specimens, were used. 68 WHO grade II astrocytomas were analysed by IHC in Tissue MicroArray. 19 pairs of these specimens were also used to evaluate tumoral and border zones.

Extensive surgical resection was done at diagnosis and radio- and/or chemotherapy was administered in case of tumor progression or malignant transformation.

3.2 Biopsies and Samples Collection

3.2.1. Human Muscle Biopsies

Samples were obtained from the mid-region of the left *vastus lateralis* muscle. Biopsy was done after anaesthesia of the skin, subcutaneous fat tissue, and muscle fascia with 2 ml of lidocaine (2%). A small incision was then made to penetrate skin and fascia, and the tissue sample was harvested with a purpose-built rongeur (Zepf Instruments, Tuttlingen, Germany). The samples were frozen in cryopreservation solution (BIOPS solution pH 7.1: imidazole 20mM, MES 50mM, DTT 0.5mM, EGTA- calcium buffer 10mM – free Ca^{2+} concentration

100nmol/L, $MgCl_2$ 6.56mM, ATP 5.77mM, phosphocreatine 15mM; DMSO 30% and BSA 10mg/mL) in fluid nitrogen, kept at -80°C (Kuznetsov et al., 2003) and divided into several pieces for different analyses in different laboratories. When possible, remaining of the samples, conserved in another cryo-vial, were used for the assessment of CS activity. For the baseline of the young group the samples collected and described in [Salvadego et al., 2016] were used, considering them compatible with the characteristics of the young group of this study.

3.2.2. Mouse Muscle Collection

At the end of the study, 2-8 hours after the last running activity, the mice were sacrificed by spinal cord displacement after stunning. No anaesthetics were used in order to avoid effects on mitochondrial function. The *soleus* muscles from the right leg were removed and immediately placed in ice-cold BIOPS solution (see above) and subsequently used for high-resolution Respirometry (HRR) measurements (see below). After HRR the muscle bundles were retrieved, frozen in liquid nitrogen and stored at -80°C for subsequent determination of citrate synthase activity (see below).

3.2.3. Glioma Samples Collection

The analysed low- and high- grade astrocytomas samples were provided by the Institute of Anatomic Pathology of the "Santa Maria della Misericordia" University Hospital. The biopsies, excised after surgery, were kept at -80°C until IHC, IF and immunoblot analyses.

3.3 Determination of Protein Concentration: Lowry Method

In this Thesis to determine protein concentration it was used the Lowry Method (Lowry O. H. et al., 1951). This assay is simple to perform and very sensitive in a range between 0.01-1 mg/mL.

The original samples is diluted (1:10 v/v) in mQ water because the absorbance values need to be in the linearity interval of the assay. Some aliquots at scalar quantities of the sample are prepared. mQ water is added to reach a final volume of 200 µl. The eppendorfs are vortexed. Then is added 1 mL of solution A (50 part of 2% Na_2CO_3 in NaOH 0.1 N and 1 part of $CuSO_4$ tetra-hydrate 0.5% in Na-K tartrate 1%), prepared fresh every day, and the samples are

incubated at RT for 10 minutes. After this are added 50 µl of solution B (Folin-Ciocalteau reactive diluted 1:2 in H_2O mQ) and again vortexed. After 30 minutes of incubation, the samples' optical density could be read at 750 nm. The protein concentration is determined taking into account the calibration slope made using a BSA standard.

3.4 Western Blotting analyses

Protein expression levels in muscle and glioma samples were analysed by immunoblotting technique. Firstly, samples were processed by different homogenization protocols, then samples protein extract were separated by electrophoresis, blotted on a membrane and revealed by chemiluminescence method. Data were finally evaluated by densitometric analysis.

3.4.1. Sample Preparation

3.4.1.1. Tissue Homogenates

Just thawed biopsy samples were rapidly washed in PBS solution, dried, weighted and placed in a cooled glass-Teflon Potter-Elvehjem (Wheaton, USA), in a (1:4 w/v) suspension for muscles with homogenization buffer (Sucrose 0.32 M and PBS 5 mM (PBS 1X: NaCl 137mM, KCl 2.7mM, Na_2HPO_4 pH 7.4 10mM, KH_2PO_4 pH 7.4 2mM)), P8340 – Sigma protease inhibitors (1:50 v/v) and phosphatase inhibitors (sodium fluoride 10 mM and sodium orthovanadate 1mM) (Mavelli et al., 1978). Muscle samples were homogenized with 40 motor driven strokes at 500 rpm (ForLab AT120, Carlo Erba, Italy). Further 1:1 v/v dilution of the residual homogenates was made with RIPA buffer (Tris/HCl pH 8.0 50mM, NaCl 150mM, SDS 0.1% (w/v), Nonidet P40 1% (v/v), Sodium deoxycholate 0.5% (w/v), EDTA 0.4mM) 2X, followed by other 40 motor driven strokes, to obtain a better membrane protein solubilisation (modified from Nakashima et al., 2006). Then homogenates were incubated for 30 minutes. All processes were carried out on ice-bath. Homogenates were centrifuged at 10000xg for 10 minutes and the extracts (supernatants) were used for quantitative immunoblot after protein determination.

The same procedure was followed for glioma samples except for the initial dilution (1:2 w/v) and the number of hand-made strokes (20).

Extracts of H9c2 cell line (ATCC® CRL-1446™) were used as an internal standard (IS) for quantitative immunoblot of muscle homogenates.

3.4.1.2. Whole Cell Extracts

In order to prepare whole cell extracts from H9c2 cell line, $3*10^6$ cells/ml were obtained by resuspension of cellular pellet in 1 mL RIPA buffer 1X (see above) containing protease (P8340 - Sigma) and phosphatase (NaF 10 mM and Na_3VO_4 1 mM) inhibitors. After 30 minutes of incubation at 4°C, the sample was centrifuged at 14000xg for 15 min at 4°C and the supernatant was used for quantitative immunoblot.

3.4.2. Electrophoresis and Immunoblotting

Samples' proteins were separated by denaturing SDS-PAGE using 8-16% gradient polyacrylamide precast gels (Thermo Scientific, USA) according to Laemmli method (Laemmli, 1970). Samples homogenates were denaturated with sample buffer 5X (Tris/HCl 0.5 M pH 8.6 0.15M, Glycerol 50%, SDS 10%, β-mercaptoethanol 18.5% and Bromophenol Blue 0.015%) and heated for 5 min at 95°C. Analyses of protein expression levels were carried out by immunoblotting. For quantification purposes, at discretion, two different methods were used.

The first one consists on loading a maximum of 13 samples taken randomly on each gel together with molecular weight markers (BioRad Laboratories, USA), and the internal standard (IS) (H9c2 cell extracts for muscle samples and a commercial HeLa whole cell extract by SantaCruz Biotechnlogies – SCBT – for glioma samples) to analyse the results from different gels. 20 μg of proteins were loaded for each sample and 40 μg for IS.

The second one consists:

- for muscle samples to load on the same gel, for each patient, the three conditions investigated (BCD, BR 14, R+14) in scalar amounts (5, 10, 15, 20 μg). In this way it was possible to analyse together, with no experimental variation, the three condition for every subject;
- for glioma samples to load on the same gel, three different samples in scalar amounts (5, 15, 30 μg) along with the IS, namely HeLa whole cell extract, also in scalar amounts (12.5, 25, 37.5 μg). This method guarantees to verify the loading error, the detection limit and the non-saturating conditions for all the investigated antibodies.

Electrophoresis was ran at constant voltage of 185V for approximate 45-60 minutes in Running buffer 1X (Tris 25mM, Glycine 250mM, SDS 0.1%). After proteins separation on

gel, they were transferred (90 minutes at constant 250 mA) to a polyvinylidene fluoride (PVDF) (first method) or nitrocellulose (second method) membrane by wet western blot technique in Trans Blott Buffer (pH 8.1 – 8.3 containing Tris 25mM, Glycine 192mM, ethanol 20%). Then, membrane was cut, according to the molecular weight markers (BioRad Laboratories), for single protein identification. Different membranes were used because only PVDF ones can be stained with Coomassie Blue in order to correct the loading (see below). Membranes were blocked with a blocking solution (TBS, Tween-20 0.1% and BSA 2.5%) for 1 hour at RT and then incubated overnight with the proper antibody at 4°C. The membranes were probed with different antibodies specific for OXPHOS complexes (1:5000 dilution) (Ab Cocktail from AbCam against: mitochondrial NADH dehydrogenase [ubiquinone] 1 beta sub-complex subunit 8 – NDUFB8 for complex I; succinate dehydrogenase [ubiquinone] iron-sulfur subunit – SDHB for complex II; Cytochrome b-c1 complex subunit 2 – UQCRC2 for complex III; CV subunit α for complex V; cytochrome c oxidase subunit 2 – COXII for complex IV); cytochrome c oxidase subunit 4 – COXIV for complex IV (1:10000) (AbCam), AMPK and p-AMPK^{Thr172} (1:500 both) (SCBT), GAPDH (1:10000) (SCBT), Citrate synthase (1:10000) (AbCam), PGC1α (1:5000) (AbCam), SIRT3 (1:1000) (Cell Signalling Technologies – CST), LKB1 and p-LKB1 (1:1000 both) (Phosphoplus Duet CST), TOM20 (1:7000) (SCBT), IF1 (1:1000) (SCBT), ATP synthase subunit β (1:1000) (AbCam) and HSP60 (1:10000) (SCBT). The day after, the membranes were washed with TBS-T solution (TBS and Tween-20 0.1%) for three times and incubated in the presence of the secondary antibody (rabbit-anti-mouse or goat-anti-rabbit, Thermo Fisher Scientific) conjugated with horseradish peroxidase (HRP) for 2 hours at 4°C. The protein bands were revealed by SuperSignal West Dura (Pierce, Rockford, IL, USA) substrates (1:1 dilution of peroxide and luminol solutions). The newly compound is oxidized by HRP conjugated on the secondary antibody, becoming chemiluminescent. The bands, during revelation with SuperSignal West Dura, were recorded every minute, for a maximum of 10, by QuantityOne software of ChemiDoc (BioRad Laboratories, Berkeley, CA, USA).

PVDF membranes, after bands detection, were washed twice in mQ water and then stained with a blue Coomassie solution (Coomassie Blue R250 0.1%, Methanol 50%) for 15 minutes. Membraines were destained for subsequent lane densitometric analysis with a solution containing acetic acid (10% v/v) and methanol (40% v/v), according to [Sanchez et al., 1992].

Each sample was tested at least in triplicate.

3.4.3. Densitometric analysis

The protein bands were visualized and acquired by an enhanced chemiluminescence method using ChemiDoc and quantified, according to the used Western Blot analysis approach, with ImageQuant TL (GE Healthcare, Little Chalfont, UK) or QuantityOne software (BioRad Laboratories) as the volume given by the band pixel's intensity for the area of a single pixel per mm2. In addition, the Coomassie stained lanes were quantified by ImageQuant TL software as for the bands.

With the first method described in 3.4.2, the densitometric band values, determined by ImageQuant TL, were then normalized for the total lane density (pixel intensity) of the Coomassie-stained PVDF membrane in order to correct any loading error and to compare different experiments as in [Sanchez et al., 1992]. The obtained values, for each patient's proteins, were further normalized with the one of the IS, which consent to compare results of different experiments.

To analyse together the three conditions investigated in muscle (BCD, BR 14, R+14) or three different glioma samples along with IS, in which each sample was loaded on the same gel in scalar amounts, with the second method, QuantityOne software was used. For each protein the different densitometric values of the immunoreactive bands (volume INT * mm2) gave a slope as a function of the quantities (μg of protein) loaded on to the gel. Through the use of MS Excel Office 2007 software we were able to determine the linear regression along with the coefficient of determination R^2, where R^2 values near to 1 proved the linearity of all the graphs obtained. For each glioma sample the slope, which was proved the linearity and R^2 value near 1, was normalized by the slope obtained from IS loaded on the same gel in order to compare different experiment and different samples.

3.5 High Resolution Respirometry Analyses

3.5.1. Skeletal Muscle Samples

High-resolution respirometer Oxygraph-2k (Oroboros, Innsbruck, Austria) was used to evaluate the oxygen consumption *ex vivo* of *soleus* skeletal muscles in physiological condition of healthy and CHF mice, both divided into two groups: sedentary and trained.

In brief, the entire muscle was separated with sharp-ended needles, leaving only small areas of contact between fibers, and incubated in 5 mL of BIOPS solution (see above for composition) in an ice-bath containing 50 μg/mL saponin for 30 min with continuous stirring. This procedure permeabilizes the plasma membrane in order to consent the entrance into the

fibers of the substrates during the experiment. After rinsing in respiration medium (MiR05 – pH 7.1, EGTA0.5mM, MES 60mM, $MgCl_2 \bullet 6H_2O$ 3mM, Taurine 20mM, KH_2PO_4 10mM, HEPES 20mM, Sucrose 110mM and BSA 1 g/mL), the muscle bundles were measured for wet weight and immediately transferred into the respirometer containing 3 mL of air-saturated respiration medium (MiR05 plus 280 U/mL catalase) at 37°C (Gnaiger & Pesta, 2012).

A substrate-uncoupler-inhibitor-titration protocol was applied (Pesta & Gnaiger 2012, Salvadego et al. 2016). Non-phosphorylating resting mitochondrial respiration was measured in the presence of malate (4 mM), glutamate (10 mM) and in absence of adenylates, so that O_2 consumption was mainly driven by the back leakage of protons through the inner mitochondrial membrane (Complex I, State 2 leak respiration). Saturating ADP (2.5 mM) was added to measure the Complex I respiration in phosphorylating condition (Complex I, State 3 respiration) (Pesta & Gnaiger, 2012 – Lanza & Sreekumaran Nair, 2009). Succinate (10 mM) was added to support convergent electron flow into the Q-junction through complexes I and II. Maximal ADP-stimulated mitochondrial respiration (i.e. oxidative phosphorylation capacity P) was then determined after addition of further 2.5 mM ADP to avoid limiting effects. The addition of cytochrome c (10 μM) permits to evaluate the intactness of the outer mitochondrial membrane. To evaluate the electron transport system (ETS) maximal respiration (i.e. ETS capacity E), the membrane potential was dropped by adding scalar concentrations of carbonylcyanide-p-trifluoromethoxyphenylhydrazone (FCCP) (0.6 – 1.2 μM), a membrane protonophore, in order to uncouple the ETS from the phosphorylating system (PS), consisting in Complex V, ADP/ATP translocator and Pi transporter. Then, the addition of rotenone (10 μM), an inhibitor of Complex I, allowed the evaluation of ETS respiration sustain by only Complex II, measured as residual rotenone-insensitive respiration.

Data were recorded digitally using DatLab4 software (Oroboros) and oxygen flux was calculated as the negative time derivate of oxygen concentration, cO2(t). Prior to every assay air calibration and background correction was performed as manufacturer protocol. During the experiments O_2 concentration was maintained between 300 – 400 μM (average O_2 partial pressure ~250 mmHg) to avoid oxygen limitation of respiration. Intermittent reoxygenation steps were performed during experiments by adding a 200 mM H_2O_2 solution into the medium containing catalase (Pesta & Gnaiger, 2012).

3.6 Citrate Synthase Activity Assay

Each still frozen sample, after conservation in a cryopreservation solution (see above), was dissected in tiny pieces on a petri dish. The thawed specimen was quickly washed, dried and weighted before a motor driven homogenization in a pre-cooled 1mL glass-glass potter (Wheaton, USA). The specimen was suspended 1:20 w/v in a homogenization buffer containing sucrose (250mM), Tris (20mM), KCl (40mM) and EGTA (2mM) with 1:50 v/v protease (P8340 - Sigma), phosphatase (NaF 10 mM and Na_3VO_4 1 mM) and deacetylase (Trichostatin A 40 µM, EX-527 1 mM and Nicotinamide 400 mM) inhibitors. The specimen was then homogenised in an ice-bath with 20 strokes at 500 rpm. The obtained homogenate was centrifuged at 600 xg for 10 minutes in order to discard cellular debries. The supernatant was tested for protein concentration with Lowry method. 10µg of protein extracts were added to each well of a 96-well-microplate along with 100 µl of 200 mM Tris-Triton X-100 (0,2% v/v), 20 µl of 1 mM 5,5'-dithiobis-2-nitrobenzoate (DNTB) freshly prepared, 6 µl of 10 mM acetyl-coenzyme A (Acetyl Co-A) and mQ water to a final volume of 190µl. A background ΔAbs, to detect any endogenous activity by acetylase enzymes, was recorded for 90 seconds with 10 seconds interval at 412 nm by the spectrophotometer EnSpire 2300 Multilabel Reader (Perkin Elmer). This ΔAbs was subtracted from the one given after the addition of 10µl of 10mM oxalacetic acid that started the reaction. All assays were performed at 25°C in triplicate on both fresh and frozen homogenates. Activity was expressed as mUnit (nanomoles/min) per mg of protein or Unit per tissue wet weight mg. This protocol was modified from (Srere, 1969 – Spinazzi et al., 2012).

3.7 Analysis of myosin heavy chain (MHC) isoforms content

MHC isoforms content was determined by an electrophoretic approach previously described in detail (Brocca et al. 2010). Briefly, about 6 µg of each muscle sample were dissolved in a lysis buffer (Tris-HCl 20mM, Triton X100 1%, glycerol 10%, NaCl 150 mM, EDTA 5mM, NaF 100mM, NaPPi 2mM, protease inhibitor cocktail from Sigma and PMSF 1 mM. The lysates were loaded onto 8% polyacrylamide SDS-PAGE gels. Electrophoresis was run for 2h at 200 V and then for 24 h at 250 V; the gels were stained with Coomassie Blue. Densitometric analysis of MHC bands was performed to assess the relative proportion of MHC isoforms (Pellegrino et al. 2003).

3.8 Immunohistochemistry and Immunofluorescence

Immunohistochemistry (IHC) and immunofluorescence (IF) analyses were performed by the Pathology Department of the University Hospital of Udine. Tumors were histologically reviewed by two expert neuropathologist according to the World Health Organization classification of tumors of the central nervous system (Louis et al., 2016). 4μm-thick formalin-fixed paraffin-embedded slides were used for immunohistochemistry and immofluorescence analyses. p65/NFkB (Abcam) was stained using an automated immunostainer (Autostainer Link 48, Dako), after heat induced epitope retrieval using EnVision™ FLEX citrate buffer, pH 6.1, in PT Link (Dako). Primary antibody, after incubation for 30 minutes at room temperature, were detected using EnVision™ FLEX system (Dako). p65/NF-kB was qualitatively evaluated as negative or positive. For IF1 (SCBT), ATP synthase subunit β (Abcam) and anti-mitochondria (Thermo-Scientific) staining, slides were unmasked by using EnVision™ FLEX citrate buffer, pH 9.0, in PT Link (Dako). Primary antibodies were incubated overnight at 4°C, 1 and 2 hours at 37°C, respectively, and detected either by EnVision™ FLEX system (Dako) or by using Alexa dyes (1:800, Invitrogen). Slides stained by immunohistochemistry were acquired by Leica DMD 108 equipped with a 20X (numerical aperture: 0.40) and a 40x (numerical aperture: 0.65) dry objective. Confocal images were acquired by Leica TCS-Sp2 (Leica Microsystems). Adobe Photoshop software was utilized to compose, overlay the images and to adjust contrast (Adobe).

The quantification of the expression of mitochondria marker, anti-mitochondria, ATP synthase subunit β and IF1 (both for immunohistochemical and immunofluorescence staining) was performed by using Image J program (ImageJ 1.44v, NIH), calculating the integrated optical density of pictures acquired keeping constant the acquisition parameters.

3.9 Tissue MicroArray

Tissue MicroArray (TMAs) have been constructed incorporating formalin-fixed paraffin embedded (FFPE) tumor blocks obtained from the archives of the Department of Pathology of “Santa Maria della Misericordia” University Hospital. TMA were constructed by using GALILEO CK4500 instrument. 3 cores of 1 mm were collected from each tumor block or alternatively 2 cores from the tumor zone and 1 from the tumor border zone of the block. TMA were stained by immunohistochemistry for IF1, NF-kB p65 subunit and mitochondria as previously described. TMA slides were scanned with the digital scanner Aperio CS2 (Leica

Biosystems) at a magnification of 40X. Expression of IF1, NF-kB p65 and mitochondria marker was analysed by ImageJ program (ImageJ 1.44v, NIH) evaluating the optical density per unit area of each tumoral sample core and calculating, for each patient, the mean value. When the border zone was present, we compared the optical density of the border zone with the average intensity of the two tumor cores.

3.10 Statistical Analyses

Collected data were analysed with different statistical methods, according to data subdivision, number of groups and clinical intervention on the studied group.

3.10.1. Shapiro-Wilk Test

This test was used to verify the normal distribution of a population, in particular for small groups. Normal distribution (W) assumes values between 0 and 1. In order to verify if a population is normally distributed p must be ≥ 0.05.

3.10.2. Student *t*-test and Mann-Whitney Test

Student *t*-test was used in order to verify when two datasets, normally distributed, differ significantly from each other. *t*-test for independent data was used in case of independent datasets, equally distributed, and obtained by each compared population.

In the case of non-gaussian groups were applied Mann-Whithney non-parametric test. p was considered significant when ≤ 0.05 for both tests.

3.10.3. ANOVA Test and Kruskal-Wallis Test

ANOVA test was used to analyse three or more gaussian population through the variances' analysis. Before performing this test, it was verified if the populations were normally distributed with Shapiro-Wilk test and if the variances were homogeneous with Barlett test (variances are homogeneous with $p \geq 0.05$).

If populations were not normally distributed, Kruskall-Wallis test, the non-parametric counterpart of ANOVA test was used.

When $p \leq 0.05$ there was at least two groups that differ significantly from each other. To identify which were these groups, Bonferroni correction or Tukey correction were used.

3.10.4. Linear Mixed Models for Longitudinal Data

Linear Mixed Models for Longitudinal Data was used to explore the variation of different protein expression levels between different groups and throughout different conditions. Before this statistical analysis, the continuous variables were summarized as mean ± standard deviation, data were tested for normal distribution using Shapiro-Wilk test and the equality of variance was assessed using Levene test. Comparisons between groups for each condition and among conditions within each group were achieved using paired t-test and Bonferroni correction for multiple comparisons was applied. Differences were considered statistically significant when $p \leq 0.05$

3.10.5. Kaplan-Meier Estimator and Log-Rank Test

Overall survival in the model investigated in this thesis was assessed by Log-Rank Test. This non-parametric test consents to compare two different conditions in relation to time. In association with this test is frequently used the Kaplan-Meier estimator, also a non-parametric test, in order to confirm the previous result. Both test consider significantly different the investigated population if $p < 0.05$.

3.10.6. Pearson and Spearman Correlation

The Pearson correlation coefficient (r) is an index of the linear dependence of two variables, X and Y, giving a value between -1 and +1, where -1 indicates a negative correlation, 0 no linear correlation and +1 a direct correlation. Usually the interpretation of the strength of the correlation between the investigated variables is given by the value of r:

- $0 < r < 0.2$ there is no correlation;
- $0.2 < r < 0.5$ there is a weak correlation;
- $0.5 < r < 0.8$ there is a good correlation;
- $0.8 < r < 1$ there is a strong correlation.

Pearson correlation is used when the investigated population have a normal distribution. When this aspect is not satisfied it is used the Spearman correlation.

3.11 Gene Expression Analysis from Public Databases

Datasets were downloaded manually from public repositories, ArrayExpress (Parkinson et al., 2007) and GEO (Barrett et al., 2011); the data were all related with Bed Rest

or atrophy due to disuse. The raw files were downloaded when available. All the CEL files were processed together by using standard tools available within the affy package in R (Gautier et al., 2004). An UniGene ID centred Chip Description file (CDF) was used in order to have only one intensity value per gene. CDF was downloaded from the Molecular and Behavioural Neuroscience Institute Microarray Lab (http://brainarray.mbni.med.umich.edu/Brainarray/Database/CustomCDF/genomic_curated_CDF.asp) (Dai et al., 2005). All annotation information were downloaded from the same website. The normalization step was done with the standard RMA algorithm (Irizarry et al., 2003). For the differentially expressed genes determination, standard t-test was performed and the genes were selected based on fold change > +1.5 or < -1.5 and $p < 0.05$. An over-representation analysis on each DEG list using DAVID 6.8 software (Sherman, 2007) was performed.

4. RESULTS & DISCUSSION

4.1. Bed Rest Study

This Bed Rest study was designed in order to get a comprehensive figure, in young and elderly subjects, of mechanisms that regulate the mitochondria and energy metabolism adaptation, occurring in atrophic muscles following immobility and by a subsequent moderate exercise, suitable to detect differences in recovery response in both groups. Furthermore, to establish exercise as an important strategy to stimulate mitochondrial adaptations in older individuals, despite a diminished and delayed adaptation of mitochondria to exercise in senescent muscle.

In the present study, the expression levels of key proteins related to mitochondrial biogenesis and activity were analysed. In particular PGC1α, the master regulator gene in mitochondrial biogenesis, was analysed along with OXPHOS complexes, mitochondrial mass markers such as citrate synthase and TOM20 and the best characterized sirtuin in mitochondria Sirt3, that has emerged as the major regulator of mitochondrial protein deacetylation (Lombard et al., 2007), in the context of mitochondrial activity-regulating signalling "downstream" of PGC1α. Interestingly, Sirt3 has never been evaluated in Bed Rest studies, although it might be involved as reduction of OXPHOS function. "Upstream" of PGC1α, the energy sensor AMPK/LKB1 signalling pathway was evaluated. All these proteins will give a comprehensive picture of mitochondrial remodelling in young and elderly subjected to the same immobility/rehabilitation protocol.

4.1.1 Results

4.1.1.1. Protein Expression

All participants were able to comply with the study protocol. No dropouts and no medical complications occurred (see Pišot et al. 2016 for more details).

Data about the expression of PGC1α, the master regulator of mitochondrial biogenesis, are given in Figure 12 A. At BCD PGC1α protein levels in E and in Y groups were not different. Both in E and in Y bed rest (BR14) induced a decreased expression of PGC1α, but in these latter, the decline was not statistically significant. Both in Y and in E PGC1α levels "rebounded" during recovery, attaining values, than those observed at BCD. This rebound was

more pronounced in Y (2 times than BCD vs. 1.4 times than BCD in E). Overall, the effect caused on PGC1α protein expression in E was significantly affected by inactivity, but less marked by exercise, with respect to Y, although the differences were not so large.

The expression levels of Sirt3, which are known to be controlled by PGC1α in the nucleus (Brenmoehl & Hoeflich, 2013), follow a pattern similar to that of PGC1α (Fig. 12 B). Specifically, a decreased expression was observed at BR14 followed by a trend of recovery at R+14. Sirt3 levels, however, in E did not present the rebound at R+14 described for PGC1α, and were still lower than those determined at BCD. Conversely, in Y a full recovery of the Sirt3 protein at R+14 vs. BCD was observed.

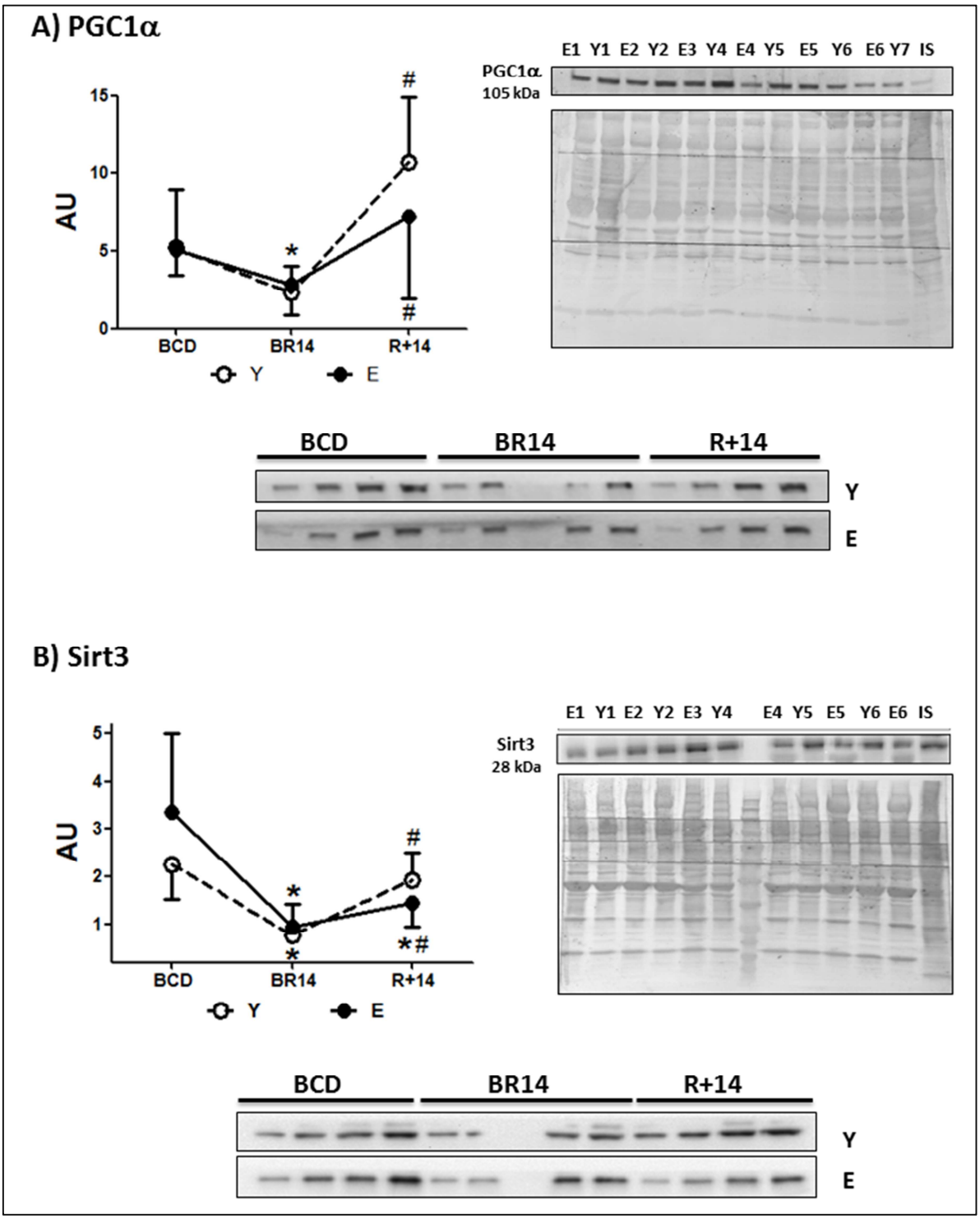

Figure 12: Changes in expression levels of PGC1α (A) and Sirt3 (B) in young and elderly subjects after bed rest and rehabilitation. In each A and B panels, on the left – graph represents means ± SD of samples from randomly taken 7 young (Y; aged 18-30 years) and 16 elderly (E; aged 55-65 years) subjects under the three conditions: BCD before bed rest, BR14 after bed rest, R+14 after rehabilitation. Values from single subjects were calculated as mean of three different assays of each sample where 20 µg of proteins were loaded. Continuous line: Elderly group; Dotted line: Young group). * represents statistical significance ($p < 0.05$) to BCD condition, # between BR14 and R+14 conditions and $ between BCD conditions. On the right – representative western blot image for randomly taken Y and E subjects, and below the Coomassie staining of the whole membrane used as loading measurement. On the central panels – representative western blot images from a single Y or E subject under BCD, BR14 and R+14 conditions; four different quantities (5 µg, 10 µg, 15 µg and 20 µg) were loaded on gel.

Then, the effects of bed rest and rehabilitation on the OXPHOS complexes protein expression were investigated (Fig. 13). The behaviour of the different complexes was rather heterogeneous. The respiratory chain carriers CII (probed as SDHB subunit), CIII (UQCRC2 subunit) and CIV (COX IV subunit) showed both in Y and in E a general pattern similar to that described above for PGC1α (although in some cases the differences did not reach statistical significance): i.e. a decrease at BR14 and a recovery with a rebound at R+14. Intriguingly, in the case of CII (SDHB subunit), smaller effects of bed rest and the same rehabilitation extent were observed in E subjects compared to Y, but a baseline protein abundance significantly greater (BR14 fold changes relative to BCD were 0.8 for E vs. 0.6 for Y, while R+14 fold changes relative to BR14 were 1.8 for E vs. 2.4 for Y). In contrast, the protein abundance of the respiratory chain carrier CI (probed as subunit NDUFB8) did not change in any condition, both in Y and in E.

Lastly, OXPHOS Complex V (CV), a main component of the phosphorylating system together with the ADP/ATP and Pi carriers, showed a peculiar pattern: both in Y and in E the expression decreased at BR14, and did not recover during R+14.

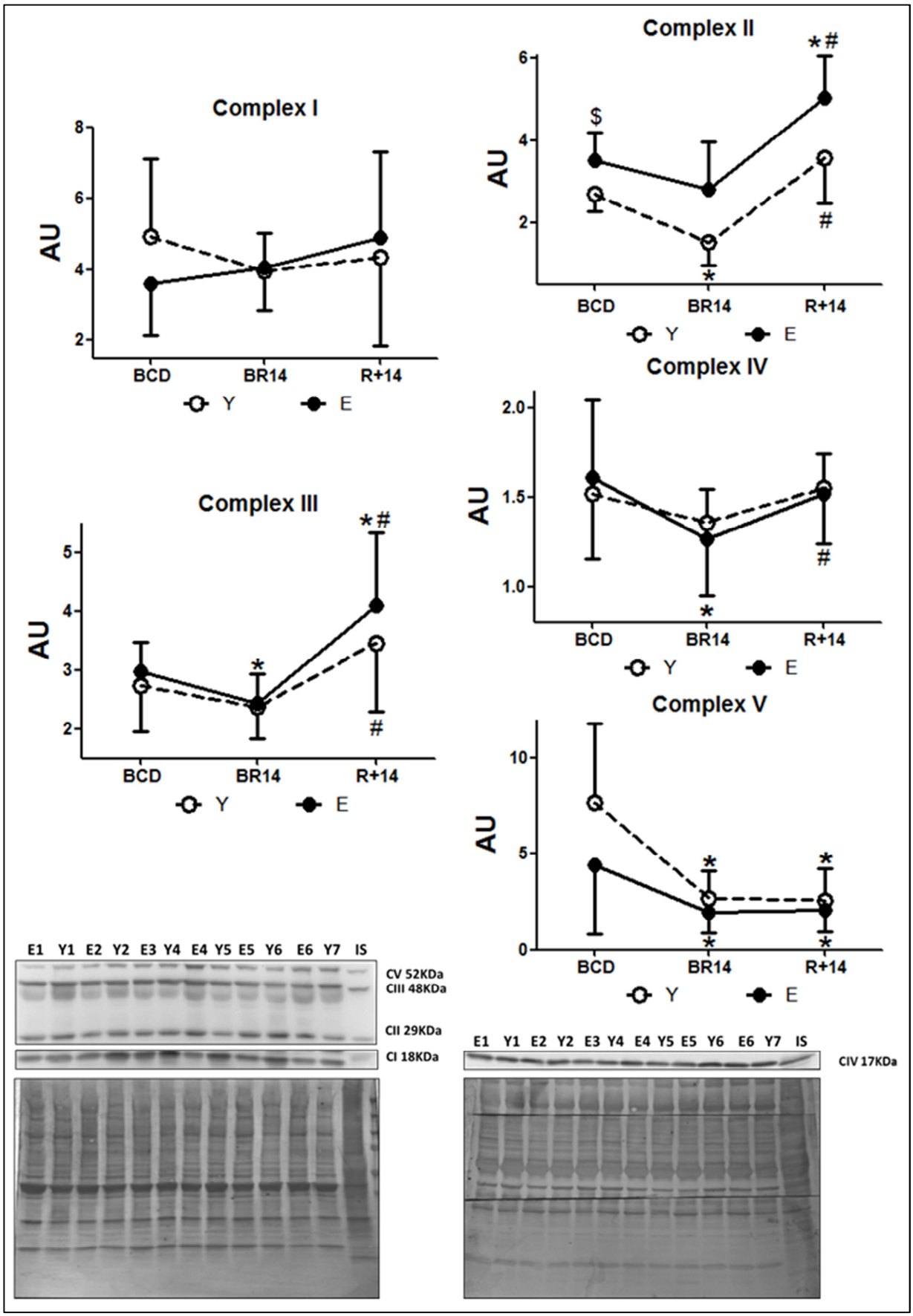

Fig 13. Changes of OXPHOS complexes expression levels in young and elderly subjects after bed rest and rehabilitation. For details, see Fig 12.

In order to estimate mitochondrial mass the expression levels of TOM20, a component of the translocase of the outer mitochondrial membrane and Citrate Synthase (CS) an enzyme of the mitochondrial matrix involved in the Krebs' cycle were determined (Figure 14 A and B). The pattern of TOM20 and CS protein abundance were similar, showing accordance between the two markers. In particular, in Y the expression levels of the two proteins were similar in all the conditions investigated. Conversely, in E they reflected the one of PGC1α, with a decrease at BR14 and a full recovery in R+14. CS activity was also evaluated and were found tiny and not significant changes with a tendency to decrease at BR14 and recover after R+14, at least in E group. Due to the scarcity of bioptic material, for CS activity analyses were used young control samples from another our study (see Salvadego et al., 2016) being similar in anthropometric characteristics with the original Y group and showing no change in CS protein abundance after similar bed rest protocol.

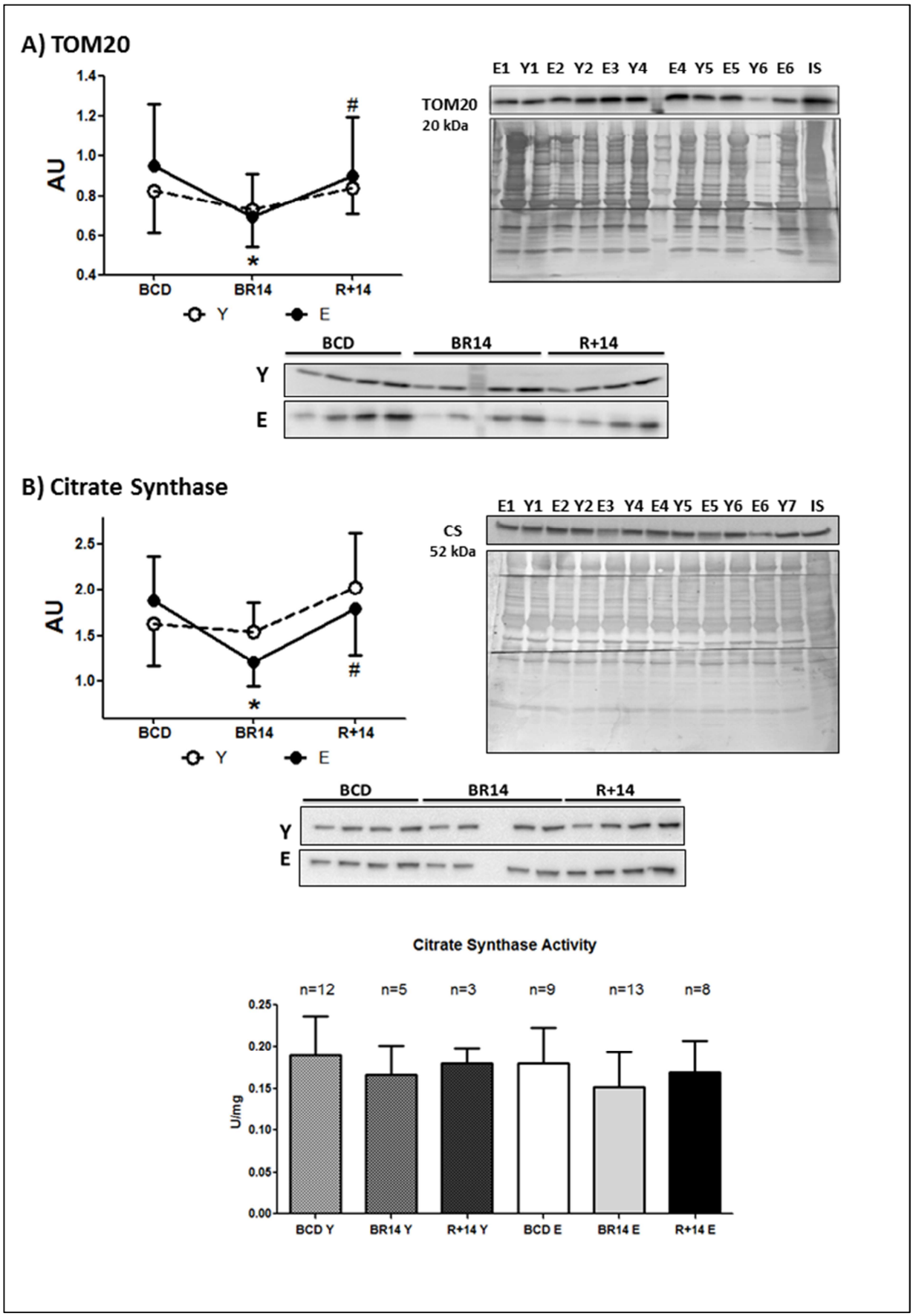

Fig 14. Changes of TOM20 (A) and CS (B) expression levels and CS activity in young and elderly subjects after bed rest and rehabilitation. For details, see Fig 12.

The expression levels of the key enzyme GAPDH (Fig. 15) were determined as an indicator of glycolytic metabolism. In Y subjects expression levels of GAPDH increased at BR14 suggesting a shift from oxidative to non-oxidative metabolism, and returned to BCD levels during R+14. In E GAPDH levels tended to increase during BR14, even if they did not reach statistical significance, and decreased at BCD after R+14.

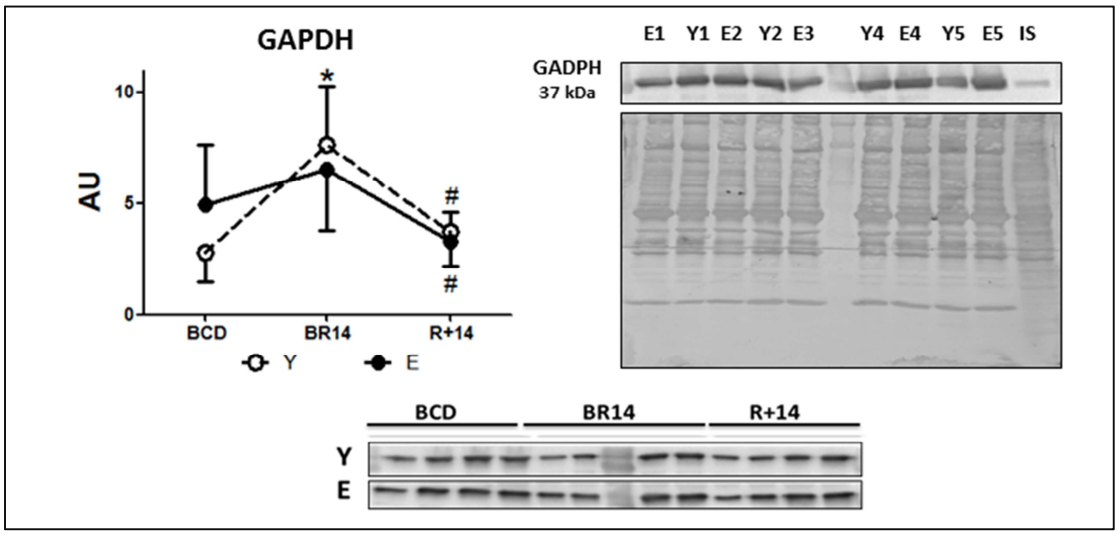

Fig 15. Changes of GAPDH expression levels in young and elderly subjects after bed rest and rehabilitation. For details, see Fig 12.

Finally, in order to evaluate if the observed changes were associated/driven by a condition of energy stress, and if LKB1-AMPK signalling pathway was triggered in concert with the PGC-1α-Sirt3 axis, p-AMPK/AMPK and p-LKB1/LKB1 ratios were assessed (Fig. 16), considering that LKB1 is a main upstream activator of AMPK. The results are in Figure 16, panels A and B. No significant changes in p-AMPK/AMPK ratios were observed in BR and in R+14, both in Y and in E. In accordance, no differences were observed also for the phosphorylation extent of LKB1 (pLKB1/LKB1 ratio).

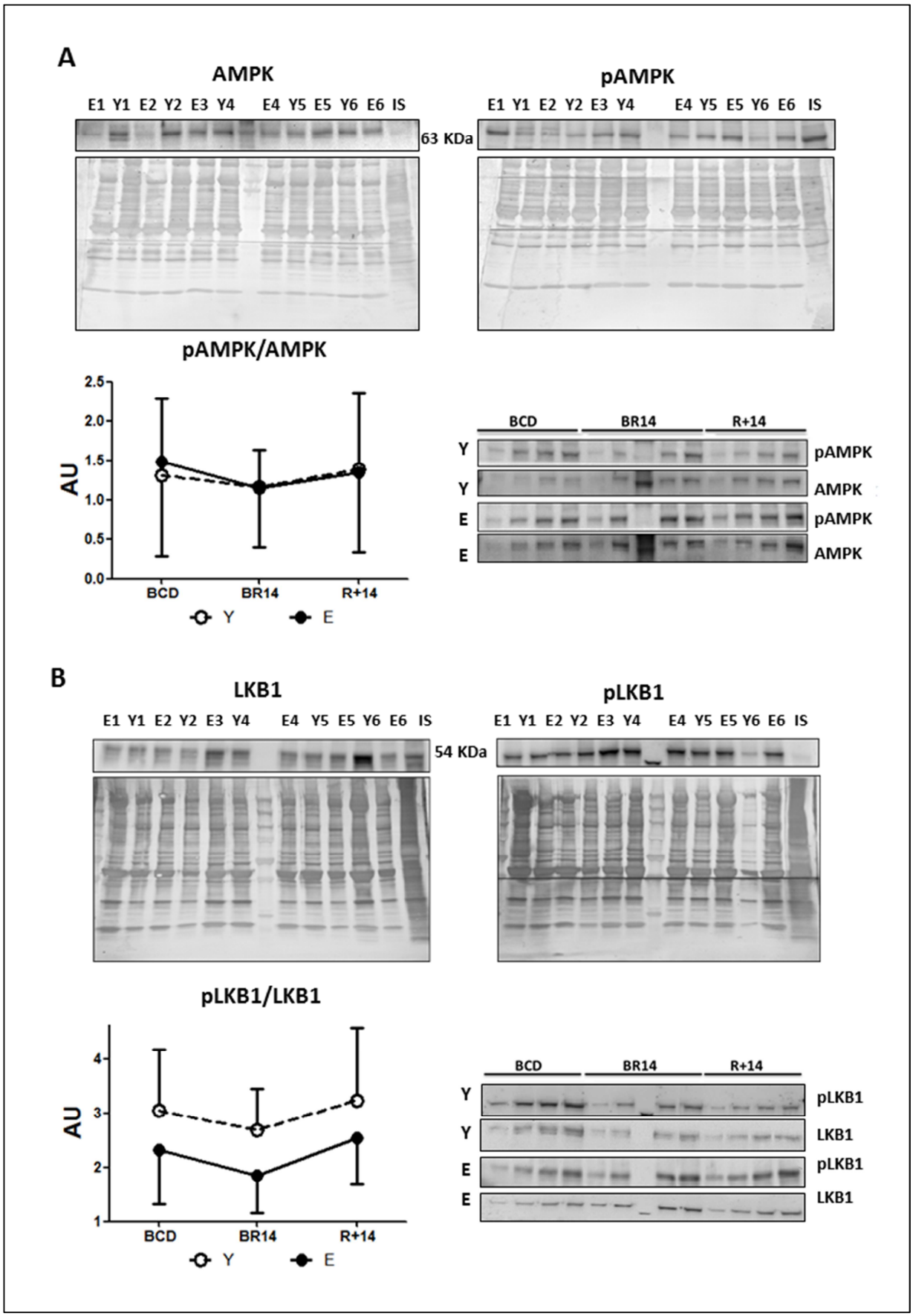

Fig 16. Changes expression levels of pAMPK/AMPK (A) and pLKB1/LKB1 (B) in young and elderly subjects after bed rest and rehabilitation. For details, see Fig 12.

4.1.1.2. Gene Expression

The analysis was principally focused on a public gene expression dataset, namely GSE24215 dataset (Alibegovic et al., 2010) as it is referred to an immobility protocol quite similar to the one used in this Thesis, in particular because of the number of subjects (20 healthy men), the timespan of the bed-rest (10 days) and the analysed muscle (*vastus lateralis*). Unfortunately, the associated rehabilitation protocol in (Alibegovic et al., 2010) was dissimilar due to the duration (4 *vs* 2 weeks) and the number of weekly training sessions (6 *vs* 3 days per week). Nevertheless, rehabilitation-related data were also analysed considering that the exercise intensity was moderate as in our study and GSE24215 represents the most comprehensive public dataset in this field.

Data were extensively analysed using DAVID 6.8 software (fold change > +1.5 or < -1.5 and $p < 0.05$ are considered significant). The results of the analysis focused on genes relevant for skeletal muscle structure/function, with particular attention to those of mitochondria and energy metabolism, are reported in Table I.

Table I. *Vastus lateralis* mitochondrial and energy metabolism gene expression data from GSE24215 dataset

Gene enrichment analysis of downregulated genes after immobility

Category	Term	Count	%	PValue	Benjamini	Fold Enrichment
UP_KEYWORDS	Mitochondrion	49	20,94	1,5E-16	3,14E-14	4,00
UP_KEYWORDS	Muscle protein	8	3,42	5E-06	0,00036	11,74
KEGG_PATHWAY	**hsa00190:Oxidative phosphorylation**	8	3,42	0,00303	0,03573	4,12
KEGG_PATHWAY	hsa04920:Adipocytokine signaling pathway	7	2,99	0,00049	0,01087	6,84
KEGG_PATHWAY	hsa01230:Biosynthesis of amino acids	7	2,99	0,00066	0,01282	6,47
GOTERM_CC_DIRECT	GO:0005753~mitochondrial proton-transporting ATP synthase complex	4	1,71	0,00200	0,05541	15,62

Gene enrichment analysis of upregulated genes after immobility

Category	Term	Count	%	PValue	Benjamini	Fold Enrichment
UP_SEQ_FEATURE	Signal peptide	87	25,74	2,8E-06	0,00147	1,62
UP_KEYWORDS	Collagen	9	2,66	0,00016	0,00963	5,79
UP_KEYWORDS	Muscle protein	6	1,78	0,00296	6,10567	0,08
UP_KEYWORDS	Acute phase	4	1,18	0,00313	0,08112	13,28

Gene enrichment analysis of downregulated genes after exercise

Category	Term	Count	%	PValue	Benjamini	Fold Enrichment
UP_SEQ_FEATURE	chain: Alcohol dehydrogenase 1A	3	2,36	0,00011	0,05012	164,45

Gene enrichment analysis of upregulated genes after exercise

Category	Term	Count	%	PValue	Benjamini	Fold Enrichment
UP_KEYWORDS	Mitochondrion	41	11,39	7,3E-06	0,00031	2,15
GOTERM_CC_DIRECT	GO:0031012~extracellular matrix	23	6,39	3,4E-08	4,83E-06	4,20
GOTERM_MF_DIRECT	GO:0008083~growth factor activity	12	3,33	0,00023	0,03796	3,97
KEGG_PATHWAY	hsa04115:p53 signaling pathway	8	2,22	0,00038	0,01285	5,85

Baseline condition with immobility were compared and in the latter were found downregulated 8 muscle protein genes, including subunits of myosin MYL3, MYL12B,

MYL12A, MYH7B and troponin TNNI3. Interestingly, 49 mitochondrial genes were also significantly downregulated. 8 are OXPHOS genes (hsa00190:Oxidative phosphorylation) codifying for subunits of OXPHOS complexes I, II, IV and V (namely, CI: NDUFB3, NDUFB10; CII: SDHC; CIV: COX7A2, COX7B; CV: ATP5F1, ATP5G1, ATP5G3). Moreover, 4 genes (PPIF, ATP5F1, ATP5G1, ATP5G3) are subunits of CV and of mitochondrial permeability transition pore (PTP) and are included in GO:0005753~mitochondrial proton-transporting ATP synthase complex. PGC1α gene, included in hsa04920:adipocytokine signalling pathway, was also downregulated along with subunits of TIM (TIMM8A) and TOM complexes (TOMM40L).

Among the upregulated genes after immobility there are 6 muscle proteins including troponin subunit TNNT2, and myosin chains MYL4, MYL5, MYH4 and MYH8. Myosin heavy chain upregulation is in accordance to a muscle switch from slow to fast fibers (Lynch et al., 2015 – Schiaffino & Reggiani, 2011).

After rehabilitative exercise training, 41 mitochondrial genes were found significantly upregulated with respect to immobility. Among these, there were genes encoding for subunits of mitochondrial proton-transporting ATP synthase complex V and mitochondrial PTP (ATP5E, ATP5G1, ATPG3, PPIF), of complex IV (COX7A2), complex II (SDHC), TIM (TIMM8A) and TOM complexes (TOMM40L). Nevertheless, taken into account the higher number of genes upregulated after rehabilitation with respect to those downregulated after immobility (386 *vs.* 252), gene ontology categories hsa00190:Oxidative phosphorylation and GO:0005753~mitochondrial proton-transporting ATP synthase complex resulted no longer significantly enriched.

Conversely, genes like alcohol dehydrogenase 1A were markedly downregulated after exercise in agreement with a switch towards oxidative phosphorylation.

Intriguingly, it was not observed any change in any condition for citrate synthase gene expression.

Furthermore, we analysed two different datasets involving shorter immobility protocols to see if there were changes in mitochondrial gene expression during the early response to inactivity. Specifically, we used GSE5110 (Urso et al., 2006) and GSE8872 (Chen et al., 2007) datasets, which reported only the response to immobility (2 – 5 days) of *vastus lateralis* and *medial gastrocnemius* muscles, respectively, in young subjects (20 – 30 years old). From this analysis emerged that just genes ascribed to ubiquitin-proteasome pathway were increased. On the contrary, metallothionein function (genes with antioxidant properties), extra cellular matrix (ECM) integrity proteins and OXPHOS complex I and V subunits (Complex I

NDUFS4/B3/B5; Complex V ATP5L/C1) were decreased (Urso et al., 2006 – Chen et al., 2007).

Finally, as no datasets were available relative to effects of immobility and rehabilitative exercise protocols on elderly people, some information was sought by analysing public databases for gene expression changes between young and old sedentary people. From the analysis of database of Asmann and colleagues (Asmann et al., 2007) resulted differences in methallothionein and PGC1α gene expression in *vastus lateralis* between young and elderly people. Furthermore, as fast fibers represent the majority of *vastus lateralis* composition, we analysed dataset from Raue's study focusing on differences established by ageing in fast fibers gene expression (Raue et al., 2011). Between young and elderly subjects were seen differences in gene expression of muscle structural proteins and mitochondrial translocators, but not in genes encoding for the proteins analysed in our bed-rest study.

4.1.2. Discussion

4.1.2.1. Down- and Up- regulation of PGC1α and Sirt3 protein expression by immobility and rehabilitation

Two-weeks bed rest period, in accordance to a decreased need of new mitochondrial membranes and active energetic metabolism to sustain energy demands in immobility, leads to a diminished expression level of PGC1α, a master regulator of mitochondrial biogenesis and structural/functional integrity during pathophysiological processes of muscle atrophy and aging (Finck et al., 2006). Likewise, a decrease of protein levels (which appears greater than PGC1α) is observed for Sirt3, a NAD^+-dependent protein deacetylase localized solely inside mitochondria (Scarpulla, 2002 – Brenmoehl & Hoeflich, 2013), that is known to be a main mitochondrial activity regulator with a prominent role in skeletal muscle (Jing et al., 2011 – Jing et al., 2013 – Vassilopoulos et al., 2014). After 14 days of rehabilitation program with a moderate exercise training, the levels of PGC1α and Sirt3 protein expression raise coherently with increased energy need, with PGC1α levels reaching values even beyond the baseline (Figure 12 A). Such immobility and rehabilitation effects on PGC1α protein are in line with previous proteomics and mRNA expression studies (Brocca et al., 2012 – Wall et al., 2014).

The similar pattern exhibited by PGC1α and Sirt3 is expected considering that i) PGC1α in the nucleus, when active, is recognised to regulate Sirt3 expression (Brenmoehl & Hoeflich, 2013), and ii) contractile activity during exercise is documented to trigger signalling pathways leading to Sirt3 induction by PGC1α (via oestrogen-related receptor binding

element) (Ventura-Clapier et al., 2008 and references therein). In turn, Sirt3 can enhance in a positive feedback system (via cAMP response element binding protein–dependent transcriptional signalling) PGC1α expression and the subsequent regulation of mitochondrial related proteins (Palacios et al., 2009 – Kong et al., 2010 – Hokari et al., 2010 – Brenmoehl & Hoeflich, 2013). In this respect, it should be emphasized that PGC1α-Sirt3 signalling pathway is documented to be triggered by contractile activity and to result in both biogenesis and activation of several enzymes of oxidative and energetic metabolism (Palacios et al., 2009 – Hokari F. et al., 2010).

Elderly subjects exhibit a more significant loss of PGC1α protein abundance after immobility, and a rise with exercise (2.6 times than BR14) inferior than the young group (4.7 times than BR14). In the case of Sirt3, a significant increase of protein levels were observed after exercise for elderly subjects, but not a full recovery as for young subjects.

In this regard, it may be hypothesized that the decrease in PGC1α levels during immobility may be due to a diminished intracellular calcium that may be counteracted by exercise recovery. In fact, it is known that the induction of PGC1α can be induced via Ca^{2+}-mediated signalling during muscle contraction (Irrcher et al., 2003). If this is the case, the greater sensitivity to immobility observed by us in elderly patients might be explained by the tendency of Ca^{2+} concentration to decrease during aging in skeletal muscle cells (Berchtold et al., 2000 and references therein). However, validation of this hypothesis requires additional studies, as alteration of intracellular Ca^{2+} concentration during immobility is still matter of debate due to contrasting reports (Ingalls et al., 1999 – Fraysse et al., 2003).

Regardless the biochemical mechanisms, together these results demonstrate that in the elderly the expression levels of PGC1α and Sirt3 were more significantly affected by inactivity and less responsive to exercise than in the young people. Moreover, it is worth mentioning the baseline expression level that is the same between young and elderly subjects in accordance to precedent studies (Lanza et al., 2008 – Irving et al., 2015). Specifically, Irving and colleagues study showed no age difference in the protein levels of PGC1α, NRF-1 or Tfam in the *vastus lateralis* muscle between old (59–76 years) and young (18–30 years) sedentary subjects. As for Sirt3 data (Figure 12 B), this is the first study that examines the expression levels of this mitochondrial sirtuin in relation to bed rest and subsequent rehabilitation in both young and elderly men. Nevertheless, several studies reported increased levels of Sirt3 (and PGC1α) in skeletal muscle after exercise training in both the elderly and young (Lanza et al., 2008 – Irving et al., 2015 – Hokari et al., 2010). Considering the PGC1α-Sirt3 mutual relationship, our data showing Sirt3's decreased expression level after bed rest

are perfectly consistent with PGC1α data from this and other bed rest studies (Brocca et al., 2012 – Wall et al., 2015), which confirm the decrease of protein levels after immobilization.

Moreover, the increased abundance of Sirt3 observed by us after rehabilitation in concert with PGC1α is supported also by studies in which the overexpression/knockdown of Sirt3 or PGC1α elicits in muscle similar effects and promotes in muscle the activity of several enzymes involved in oxidative and energetic metabolism and in antioxidant defence (Kong et al., 2010).

4.1.2.2. OXPHOS complexes protein abundance after immobility and rehabilitation

OXPHOS complexes elicit peculiar steady-state levels following immobility and exercise training (Fig. 13), which might evoke different imbalance between protein biogenesis and degradation for the single complexes. Data on respiratory chain complexes CII, CIII and CIV show an overall mild decrease in protein levels provoked by bed rest and a more marked and significant increase induced by exercise, that is a pattern similar to PGC1α. These data are in line with other studies using a protocol of two weeks of one-leg immobilization (Gram et al., 2014). Intriguingly, in our conditions complex I is completely unaffected. Conversely, OXPHOS complex V expression is markedly down-regulated by bed-rest, but not increased by rehabilitation (Fig. 13). This is a unique behaviour among the protein analysed in this study. Unfortunately, there are no data to explain the absence of recovery after exercise training. Nevertheless, it might be inferred that enhanced degradative processes of complex V subunits, realistically elicited by atrophy in addition to a repressed protein biogenesis, could be more extensive than for other proteins and not counteracted by the moderate exercise of our rehabilitation program, thereby maintaining a low steady-state level of the protein. Then, it might be speculated that in order to achieve reactivation of the protein synthesis fit for balance of its degradation should be recommended an endurance training protocol, which should be more efficient to activate mitochondrial protein synthesis in accordance to (Flück, 2012). These aspects need further investigations. Anyway, it should be considered that the ATP synthesis activity of complex V is fine regulated by many interactors including Sirt3 (Rahman et., 2014), which is more abundantly expressed after rehabilitation under our conditions in both elderly and young subjects (Fig. 12 B). Sirt3 was far away reported to activate different OXPHOS complexes, such as complexes II and III, through deacetylation thereby controlling energy production (Ahn et al., 2008 – Finley et al., 2011 - Brenmoehl & Hoeflich, 2013). Interestingly, in skeletal muscle it has been more recently reported a Sirt3-mediated

deacetylation of complex V subunits beta and Oligomycin Sensitivity Conferral Protein (OSCP) as occurring in response to nutrient- and exercise-induced stress (Vassilopoulos et al., 2014 – Rahman et al., 2014), although the function of Sirt3 in these conditions is still to be defined completely. Deacetylations on complex V proteins operated by Sirt3 are well characterised, and can regulate the cell's oxidative capacity (Lin et al., 2014 – Jing et al., 2011). Specifically, it has been shown a role of Sirt3 in the acetylation status of several complex V proteins (alpha, beta, gamma, OSCP, b, epsilon subunits), as well as a protein-protein interaction of Sirt3 with alpha, beta and OSCP (Vassilopoulos et al., 2014 – Rahman et al., 2014 – Ahn et al., 2008 – Bao et al., 2010 – Wu et al., 2013). In this scenario, further investigation is needed to verify the tempting hypothesis that exercise may be able to trigger Sirt3-mediated deacetylation of complex V facing the low protein abundance observed through up-regulation of their activity.

No difference is observed between the young and elderly groups in the response to the treatments of OXPHOS except for complex II, which is less affected by immobility and responds in the same way to exercise training in the elderly group compared to the young one. It is interesting to note that there are not any significant differences between young and elderly subjects neither in baseline levels of OXPHOS complexes, again except for complex II, which is higher in elderly subjects. CII is the only OXPHOS complex that in rodents tends to increase its expression associated with complex II-hyperactive aged fibers (Picard et al., 2010 – O'Connell et al., 2009 – Piec et al., 2005 - Brierley et al., 1996 - Wanagat et al., 2001). Moreover, even skeletal muscle from aged humans (Bua et al., 2006) showed an increase in electron transport chain aberrations which are normally identified as succinate dehydrogenase hyperactivity (Wanagat et al., 2001). This might explain the different BCD levels and treatment responses in E and Y groups.

Taken as a whole, the data here presented document that the single OXPHOS complexes show diverse patterns of expression, in some cases dissimilar from PGC1α. This is in contrast with the well-known ability of PGC1α to regulate the expression of mitochondrial- and nuclear- encoded subunits of OXPHOS (Scarpulla, 2002). This divergence might be imputed to a response by degradative pathways of OXPHOS complexes to the immobility and exercise stimuli different from the expression regulators linked to PGC1α. Indeed, it is recognised that disuse muscle atrophy is accompanied by activation of multiple catabolic pathways beside inhibition of protein synthesis (Sandri et al., 2008 – Brocca et al., 2012 – Bonaldo and Sandri 2013 – Cannavino et al., 2015). On the other hand, it may be inferred that under these conditions PGC1α may elicit different regulation of single proteins involved in

energy production, thereby controlling mitochondrial remodelling. Such an effect was described during osteogenic and motor neuron differentiation (Sanchez-Aragò et al., 2013 – O'Brien et al., 2015), as well as in several reports discussed in the review of (Chan et al., 2014) providing evidence that PGC1α in skeletal muscle may selectively and differently control the expression levels of several mitochondrial proteins. Unchanged expression levels of OXPHOS Complex I are in accordance.

4.1.2.3. Different responses of citrate synthase and TOM20 to immobility and rehabilitation in young and elderly subjects

The expression levels of the mitochondrial matrix protein citrate synthase, and of the outer mitochondrial membrane protein TOM20, two proteins usually recognized as reliable mitochondrial mass markers, seem not to be completely in accordance with that of PGC1α. Specifically, dissimilar from that of PGC1α is the different pattern shown by both proteins in young and elderly subjects (Fig. 14 A and B) suggesting a different impact of the treatments on the two populations, i.e. bed rest is more strongly evident in elderly compared to young subjects and exercise is effective. Intriguingly, in elderly subjects the pattern of TOM20 and CS protein abundance evokes the one of PGC1α, with a decrease after immobility and a full recovery after rehabilitation, whereas in young subjects the two proteins appear unaffected. Such diverse effects observed in the young group on TOM20 and CS protein abundance with respect to PGC1α might indicate that this does not simply reflect the modification of mitochondrial mass. Considering the direct correlation of TOM20 with PGC1α through NRF-1 and NRF-2 (Scarpulla, 2002), it is hard to explain the absence of effects in young subjects. As already postulated for OXPHOS complexes, specific effects on degradation and/or expression pathways of single proteins (mitochondrial remodelling) may be suggested as responsible for the differences observed for both TOM20 and citrate synthase.

The unchanged levels of citrate synthase here observed in the young group during immobility are in accordance with (Abadi et al., 2009), in which is used a similar immobilization timespan. Unfortunately, data on citrate synthase activity are not in accordance with protein expression levels, though in the elderly group there is a tendency to decrease with bed rest and increase with exercise (Fig. 14 B). It is not unexpected a mismatch between citrate synthase expression and activity. In fact, in several studies, data about citrate synthase protein, mRNA and activity are often in contrast (Abadi et al., 2009 – Wall et al., 2015 – Cannavino et al., 2015) and could be due to different sensitivity of the methods used for the

study and to different response of the activity and expression control pathways to the treatments. Also, the same baseline values of young and elderly subjects are not unexpected (Wall et al., 2015). It is known that mitochondrial content and activity decline with age (Short et al., 2005), but this is no longer true when are analysed healthy and active elderly subjects (Brierly et al., 1996 – Abadi et al., 2009).

4.1.2.4. Glycolytic marker GAPDH suggests a metabolism shift during Bed Rest counteracted by rehabilitation

Data here presented documenting that the glycolysis marker GAPDH increases during bed rest and decreases after rehabilitation in both groups, with a more pronounced effect in young subjects (Fig. 15), suggest an up-regulation of glycolytic metabolism during bed rest, may be as a compensatory response to the mitochondria impairment, and a subsequent return to a more oxidative metabolism after exercise. These results put themselves in the middle of the discussion on glycolytic and oxidative metabolism in muscle atrophy and immobility. There is not any agreement on this topic in literature. Different bed rest studies in humans (Brocca et al., 2012 – Alibegovic et al., 2010 – Ringholm et al., 2011 – Moriggi et al., 2010) showed a down regulation of both glycolytic and oxidative metabolism during disuse, but there are also many studies that affirmed the contrary, documenting the cell reliance on glycolysis (Acheson et al., 1995 – Fitts et al., 2000 – Stein & Wade, 2005).

4.1.2.5. No activation of LKB1-AMPK signalling pathway during Bed Rest and rehabilitation

It is known that, during cell stress events given by energy impairment, one of the upstream activators and inducers of PGC1α expression through phosphorylation is AMPK, a serine/threonine protein kinase that has emerged as a master sensor of cellular energy balance in mammalian cells including skeletal myocytes (Hardie et al., 2012). Moreover, one of the key upstream activators of AMPK signalling pathway is LKB1 when associated in complex with pseudokinase STRAD, and MO25 scaffold protein (Marignani, 2005). Indeed, the regulation of AMPK is quite complex and, in addition to allosteric regulation by AMP, also involves phosphorylation by upstream kinases and decreased dephosphorylation by protein phosphatases. Recent studies have found that the phosphorylation of AMPK on Thr172, led by the active form of LKB1 (phosphorylated on serine residue 428), consent the translocation of both from the nucleus to the cytosol (Shelly et al., 2007 – Barnes et al., 2007 – Xie et al.,

2008). AMPK activity is recognized to be increased by several endogenous stimuli leading to energy impairment including exercise/muscle contractile activity (Witczak et al., 2008 and references therein). Skeletal muscle expresses LKB1, STRAD and MO25, and LKB1 appears to be the primary AMPK upstream kinase under conditions of high energy stress (Witczak et al., 2008 and references therein). Conversely, it has been documented (Hardie and Sakamura, 2006) that in skeletal muscle calcium/calmodulin-dependent protein kinase kinases (CaMKKs), also key activators of AMPK, are not expressed significantly. Moreover, experiments with muscle-specific knockouts of LKB1 suggest that the CaMKK→AMPK pathway cannot be a major player in mediating the effects of muscle contraction, despite the fact that increases in cytosolic Ca^{2+} obviously occur (Berchtold et al., 2000).

On these bases, we decided to analyse in this study the LKB1-AMPK axis and we expected that it could be triggered in concert with the PGC1α-Sirt3 axis and involved to regulate PGC1α and OXPHOS protein expression during immobility and/or rehabilitation. In fact, it is known that Sirt3 may also regulate LKB1-AMPK axis under conditions of energy impairment (Giralt & Villaroya, 2012 – Kincaid & Bossy-Wetzel, 2013). In accordance, LKB1 was found to be de-acetylated (and thereby activated) by Sirt3 in the heart, with the activated LKB1 activating in turn AMPK, thus augmenting the activity of LKB1-AMPK pathway (Pillai et al., 2010).

The activation of the pathway through the evaluation of p-AMPK/AMPK and p-LKB1/LKB1 ratios was examined and any change was observed under the three conditions investigated in both young and elderly subjects (Figure 16). This may imply that energetic impairment, known to activate LKB1-AMPK axis, was not provoked to an extent sufficient by immobility as such, or together with exercise-linked energy spending, that was documented be at least 60% of $V'O_2$ peak (Mounier et al., 2015). Unfortunately, due the precariousness of AMP/ATP ratio after the excision of muscle sample (Hardie & Sakamoto, 2006), this hypothesis could not be verify in the conditions of this study. Nevertheless, it should be inferred that a lower energy demand may consent to maintain a normal muscle energy status during disuse, even in the presence of mitochondrial biogenesis/activity down-regulation, and that moderate exercise may not enhance the energy demand to a large extent. These results are in accordance with data from another bed rest study performed on *vastus lateralis* muscle biopsies (Brocca et al., 2012). Considering that rehabilitation protocol used in this study consisted in a mild continuous exercise, these data might be explained based on results of new studies in which it was demonstrated that a visible activation of AMPK signalling pathway is possible only right after interval training (Combes et al., 2015). In fact, Combes and

colleagues proved that AMPK, CaMKII and p38-MAPK may not be activated if the subject is undergone a continuous exercise at 70% of the V'O_2 peak. Conversely, activation of these pathways was seen after interval training and it already disappeared 3 hours after the last exercise, likely as consequence of possible downregulation or de-phosphorylation of LKB1/AMPK after exercise. Thus, it cannot be excluded that during this rehabilitation protocol LKB1-AMPK signalling pathway may be implicated but reverted due to its fast de-phosphorylation or downregulation. Consistently, it cannot be excluded an induction of PGC1α expression after rehabilitation by LKB1-AMPK signalling pathway. On the other hand, the hypothesis stated above of cytosolic Ca^{2+} fluctuation during contraction as possible trigger of PGC1α expression remains valid.

4.1.2.6. Gene Expression Analysis

Several studies have tried to comprehend through gene expression analyses the molecular mechanisms involved in skeletal muscle responses to immobility and rehabilitation in humans, as well as in changes associated to aging. Thus, in the present study were analysed some public gene expression datasets, taken from different studies, in which were investigated different muscles (*vastus lateralis* and *medial gastrocnemius*) and were applied different protocols of immobilization or immobilization followed by rehabilitation in 20-30 years old individuals.

The extensive response to immobility and rehabilitation of gene expression in GSE24215 dataset (see paragraph 4.1.1.2 – Alibegovic et al., 2010), concerning mitochondria and oxidative phosphorylation, supports the idea that modulation of gene expression may occur in humans as skeletal muscle response to immobility and rehabilitation for PGC1α and OXPHOS complexes, but not for citrate synthase. This is in accordance with the overall message of the results of protein abundance obtained for the young group of control of the bed rest study of this Thesis, where the most significant changes concerned single OXPHOS complexes, but not mitochondrial mass, suggesting that the effects were on PGC1α–mediated mitochondrial remodelling rather than biogenesis. Nevertheless, one must consider that data from diverse studies should be compared with caution due to differences in immobility and rehabilitative exercise protocols. Moreover, it should be noted that the data of gene expression from our bioinformatics analysis not always are related to the protein subunits analysed by immunoblot for the single complexes in the bed rest study of this Thesis. In particular, the dissimilar responses of ATP synthase complex V and TOM after immobility with respect to

our results on protein abundance could be justified by the different subunits tested. Similarly, is comprehensible a different response during rehabilitation, where we used a protocol shorter than Alibegovic and colleagues (2 *vs*. 4 weeks) that could differently affect the protein levels. Intriguingly in the case of Complex I, despite NDUFB3 and NDUFB10 gene expression resulted downregulated by immobility, the absence of changes for NDUFB8, a nuclear DNA-encoded subunit integral to the assembly of complex I, is in accordance with our WB data.

From our analysis of GSE5110 and GSE8872 public datasets involving 2 and 5 days of immobility (see paragraph 4.1.1.2 – Chen et al., 2007, Urso et al., 2006), it is also clear that, while only few OXPHOS gene expression was downregulated, a downregulation occurs of antioxidant defences with a likely increase of ROS generation causing upregulation of the ubiquitin-proteasome pathway and protein breakdown. This is common in atrophic muscle (Grune et al., 2003 – Powers et al., 2012 and references therein). Thus, based on literature data supporting the idea that degradative pathways are enhanced depending on length of immobility (Brocca et al., 2012), it may be inferred that the effects observed by us lowering the steady-state levels of mitochondrial oxidative proteins might be due to a greater impact of degradative pathways. Results from our analysis of GSE24215 dataset do not conflict with such hypothesis because gene expression of Atrogin-1 and FOXO3A (genes involved in ubiquitin-proteasome pathway) are up- and down- regulated in immobility and rehabilitation respectively, although near to the threshold.

Finally, based on the analysis of Asmann database (Asmann et al., 2007) comparing young and elderly sedentary subjects, the lower PGC1α gene expression in old people might be ascribed to lower level of physical activity and recall the downregulation caused by immobility. Anyway, in the bed rest study of this Thesis PGC1α protein abundance at baseline was similar regardless of the subjects' age. This apparently conflicting finding might be explained considering that the subjects of the elderly group were moderately active, and not just sedentary. Indeed, in elderly sedentary subjects moderate exercise could restore PGC1α levels to the ones of young people (Koltai et al., 2012).

In conclusion, combining data from the bioinformatics analysis of gene expression with those of protein abundance from the bed rest study conducted in this Thesis, it seems that immobility and exercise can affect mitochondrial protein expression levels by both gene expression regulation and protein degradative pathways.

4.1.4. Conclusions

Using an *ex vivo* experimental design in the present report were provided evidence, based on quantitative immunoblot analyses, for different expression patterns exhibited in *vastus lateralis* muscle after immobility and rehabilitation by a choice of key proteins involved in mitochondria and energy metabolism regulation, with some worthwhile peculiarities in elderly compared to young patients.

Disuse atrophy and recovery were associated with different expression patterns of connected signalling proteins suggesting an involvement of PGC1α-Sirt3 axis in regulation of mitochondrial protein biogenesis, but not activation of the energy sensing LKB1-AMPK pathway. OXPHOS complexes showed peculiar patterns evoking different imbalance between protein biogenesis and degradation for the single complexes.

Overall, exercise training was capable to counteract the effect of immobility, when present, except for OXPHOS complex V whose degradation had to be likely prevalent over biogenesis down-regulation in atrophic muscle. The moderate exercise training protocol applied in our study may explain the absence of recovery of disuse-impaired protein abundance in this case, as well as the unexpected lack of differences in activating phosphorylation of LKB1-AMPK.

Comparing the young and elderly subjects, was observed a difference only for PGC1α and Sirt3 proteins, whose expression levels in the elderly were more affected by immobility and less responsive to exercise in line with the greater loss in muscle mass and contractile function.

It should be mentioned a limit of this study. In fact, only protein expression was analysed as no functional measurements were performed due to shortage of fresh samples. Whereas the functional data presented in (Pišot et al., 2016) are systemic.

*4.2. Effects of exercise in healthy and Tgαq*44 transgenic CHF mice*

An impairment of skeletal muscle oxidative metabolism, with functional consequences involving other organs and systems, seems to play a key role in the pathogenesis of exercise intolerance in CHF patients (Poole et al. 2012). The role of skeletal muscle is even more pronounced in patients with CHF and preserved ejection fraction (Haykowski et al. 2015). Although the positive effects of exercise training in clinically stable CHF patients are well established (Hirai et al. 2015), the role of exercise interventions on skeletal muscle oxidative metabolism during the critical period of the transition from compensated to uncompensated CHF is not clear.

The aim of this project was to evaluate the effect of prolonged endurance training, in particular voluntary exercise performed on running wheels, on muscle mitochondrial biogenesis and oxidative function in *soleus* muscle from a mice model of dilated cardiomyopathy (Tgαq*44) and wild type mice (FVB). In particular, wild type and Tgαq*44 (at 10-12 months of age, during the transition from the compensated to the uncompensated phase of CHF) mice were divided into two groups, one with sedentary animals and one with animals who performed 2 weeks of voluntary exercise training on a wheel. With this study design, the oxidative function was evaluated along with the effect of exercise by high resolution respirometry.

4.2.1 Results

The data presented in this Thesis on mitochondrial respiration *ex vivo* from *soleus* muscle of healthy and cardiomyopathy mice, sedentary and trained, were obtained by high-resolution Respirometry (see Fig 17 for representative oxygraph trace).

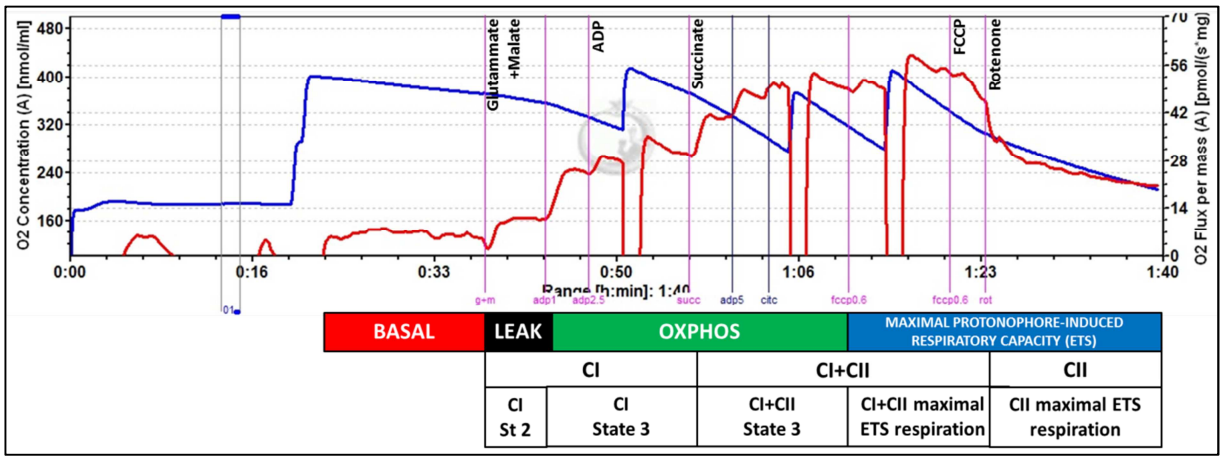

Fig 17. Representative HRR trace. The blue trace represents the oxygen concentration (in nmol/ml) in the chamber and the red one the oxygen consumption (pmol/s*mg wet weight). The magenta and dark blue marks represent the substrates/inhibitors addition in the chamber. On the bottom of the graph a summary of the investigated conditions during the used protocol.

The collected data were carefully analysed, normalized by CS activity and evaluated by outer mitochondrial membrane intactness. Intactness was evaluated during the Respirometry measure adding cytochrome C in the O2K chamber. If the membrane is broken, the respiration is stimulated by cytochrome C. On the contrary, if the membrane is intact the response to the substrate is null. In this study all measures have a variation < 14% (range -13% to +14%). No experiment exceeded the cut-off value of +15% (Wüst et al., 2012) (Fig 18 A). All data were also normalized by correspondent citrate synthase activity assay, expressed as U (nanomoles/min) per g of wet weight tissue, as marker of mitochondrial mass (Fig 18 B). Citrate synthase activity showed no significant difference in the analysed groups (11.9±2.7 in WT-CTRL, 10.9±3.1 in WT-T, 14±2.5 in Tg-CTRL and 13.1±3.9 in TG-T).

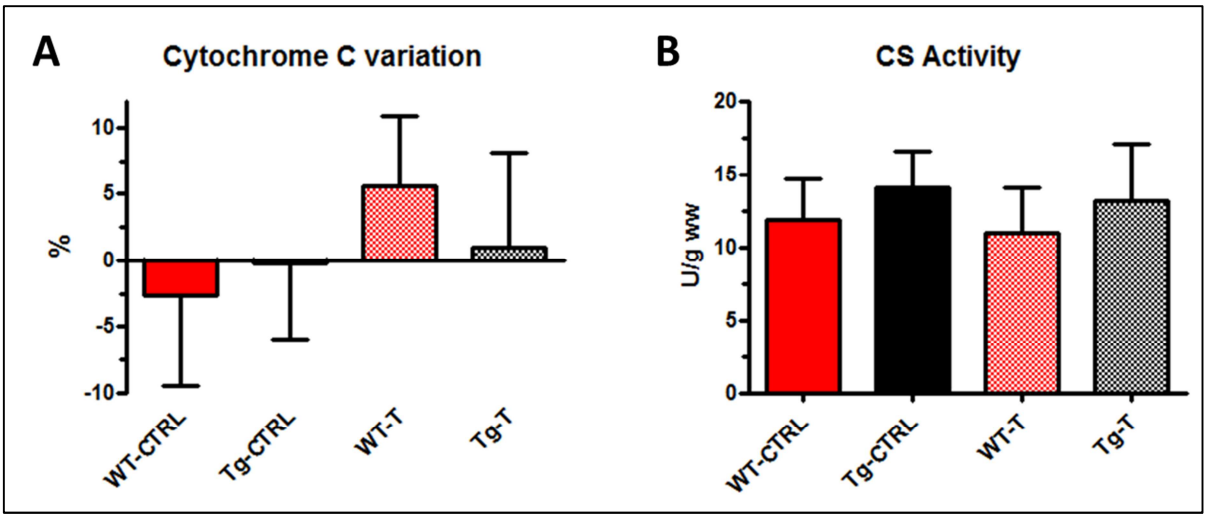

Fig 18. Cytochrome C variation (%) and Citrate Synthase activity (U/g wet weight).
All data are represented as mean±SD.

The main data on mitochondrial respiration *ex vivo*, obtained by high-resolution respirometry, are presented in Figure 19. In the untrained groups oxidative phosphorylation capacity (P) was lower in Tg-CTRL than in WT-CTRL both when normalized by mg of wet weight and CS and showed no increase after 2 months training in both WT and Tg groups (Fig 19 A).

For all the analysed groups addition of adenylates triggers a 2-3 fold increase in oxygen consumption sustained by complex I (CI State 3 respiration), in accordance with (Gnaiger, 2014), suggesting a good ETS - PS coupling even in Tg-mice. CI State 2 leak respiration does not differ. On the contrary, values of CI State 3 respiration are significantly lower in Tg sedentary mice with respect to WT-CTRL mice (Fig 19 B).

ETS capacity (E) and ETS residual rotenone-insensitive respiration, sustained by complex II, do not have any significant change in the groups (Fig 19 C).

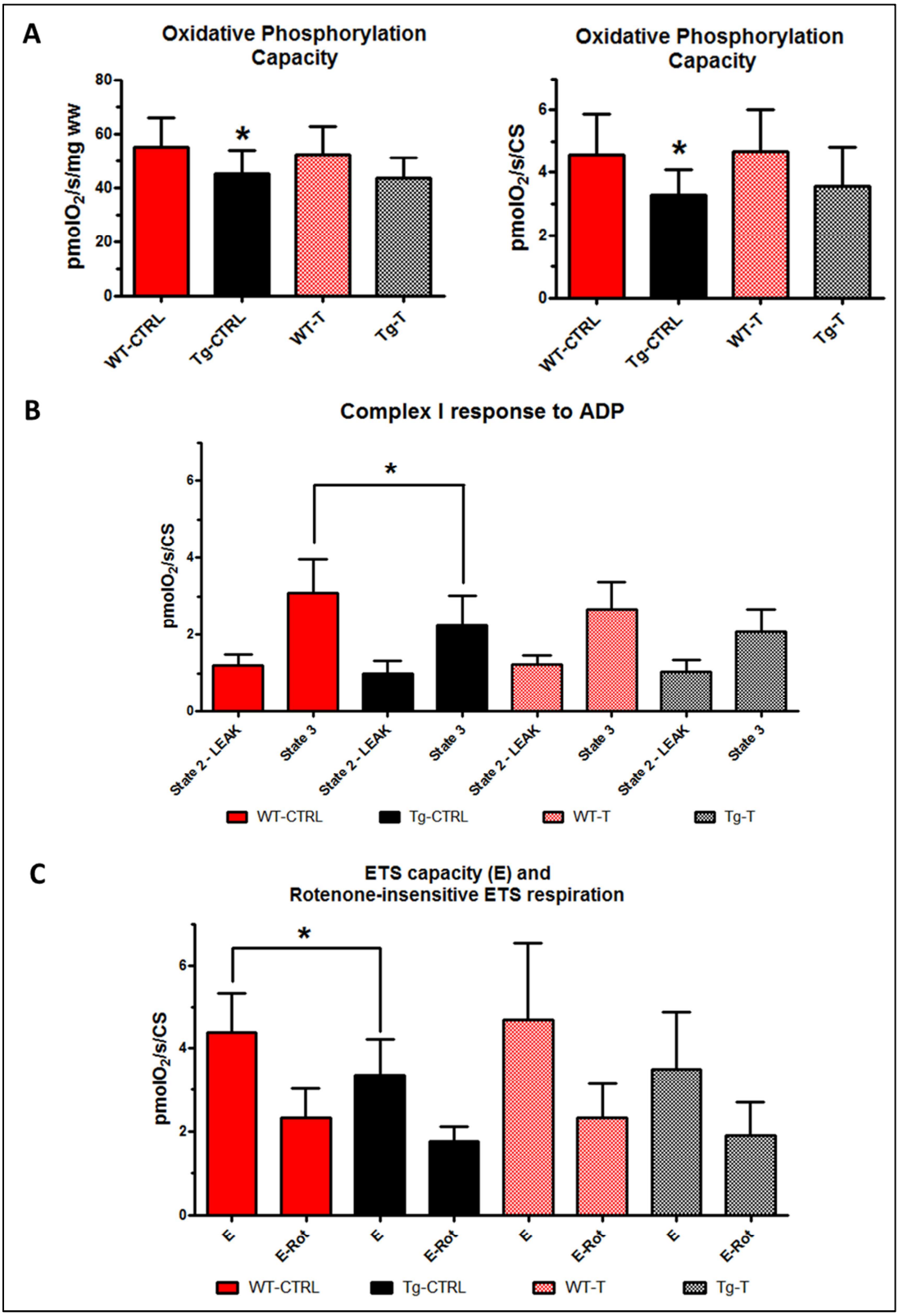

Fig 19. Mitochondrial respiration *ex vivo* in *soleus* muscle from WT-CTRL, Tg-CTRL, WT-T and Tg-T mice. Panel A shows values of Oxidative Phosphorylation Capacity (P) normalized on tissue wet weight and citrate synthase activity (CS). In panel B is reported ADP stimulation of Complex I respiration (from State 2 – leak to State 3 respiration). In panel C is reported the ETS capacity (E) measured by titration addition of FCCP, and the residual ETS respiration after addition on rotenone (E-Rot). All data are reported as mean ± SD; n = 15 for WT-CTRL and Tg-CTRL, 9 for WT-T and 14 for Tg-T mice, except for ADP- response of C I which were: n=10 for WT-CTRL and Tg-CTRL, 8 for WT-T and 13 for Tg-T mice. Statistical significance is reported as * if $p<0.05$.

It was detected also an inexistent spare capacity in mice due to no increase, compared to oxidative phosphorylation capacity, of the total respiration after the addition of the protonophore FCCP, which is used to evaluate the phosphorylating and the electron transport system (Fig 20 A). The P/E phosphorylation system control ratio, that is reported to decrease with limitation by the phosphorylation system (Pesta & Gnaigner, 2012), is the same in all the investigated condition (P/E = 1 with C I + II substrates) and in accordance with data reported for mouse skeletal muscle (Gnaiger, 2009) (Fig 20 B). This means that, even in Tg-mice, PS does not exert control over coupled respiration and does not limit oxidative phosphorylation capacity relative to ETS capacity.

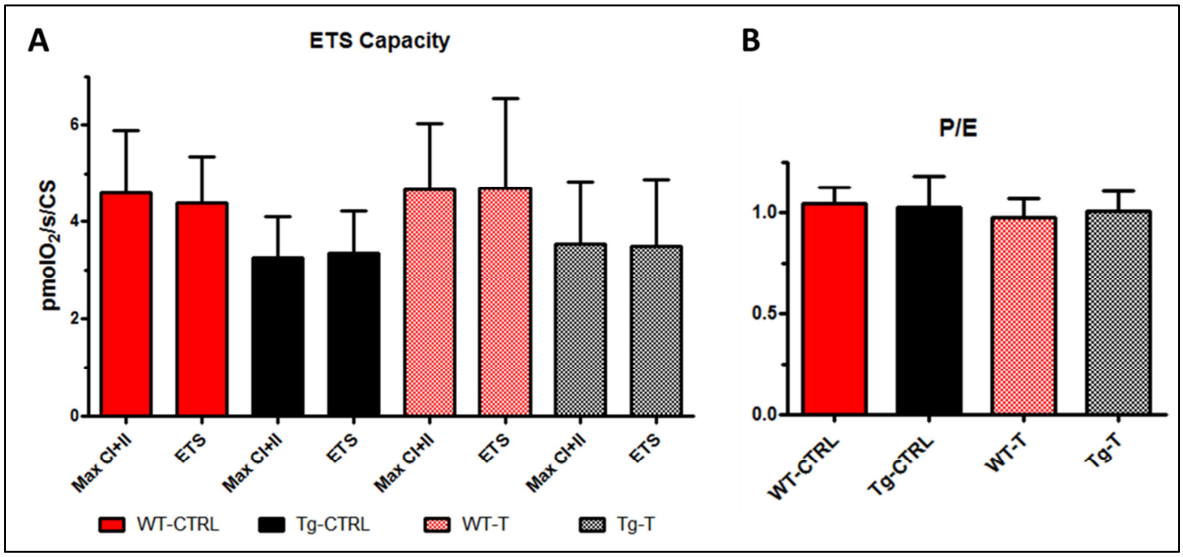

Fig 20. ETS Capacity (A) and Phosphorylating system control ratio (B) in the investigated groups. A) In the histograms are showed both the maximal ADP-stimulated respiration (Max CI+II) and ETS respiration (ETS) in the 4 groups; B) The graph represents P/E ratio given by maximal respiration in phosphorylating conditions (P – maximal ADP-stimulated respiration) and electron transport system respiration (E – ETS). All data are represented as mean ± SD.

Moreover, in all the considered variables (oxidative phosphorylation capacity, complex I response to ADP, ETS capacity, rotenone-insensitive ETS respiration and CS activity) there was no increase or amelioration of the respiration after the training protocol.

To strengthen this point, Figure 21 shows that in both WT-T and in TG-T no significant correlations were observed between oxidative phosphorylation capacity and the total distance covered during the 2 months of training, despite the fact that the latter variable varied by a factor of ~3 in WT-T and by a factor of ~8 in TG-T.

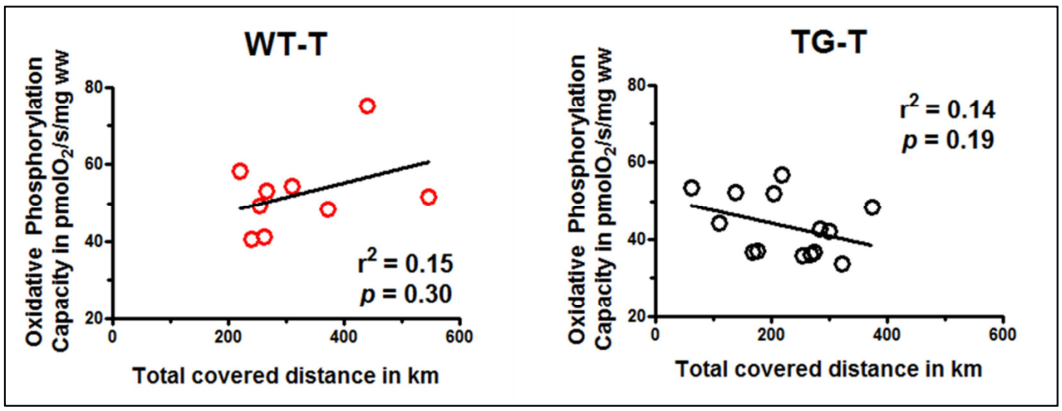

Fig 21. Correlation slopes between oxidative phosphorylation capacity and total distance run by mice (WT-T and TG-T) in ≈ 2 months in [km].

Training performance over 56 days was further analysed. The distances covered daily (mean ± SD values calculated over 3 days) at the beginning and at the end of the training period are shown in Figure 22. At the beginning of training values in Tg-T were significantly lower (less than half) than those obtained in WT-T. In Tg-T the daily covered distance increased significantly during the training period, whereas in WT-T it did not significantly change. At the end of the training period, the difference between the two groups substantially disappeared. The total time spent running on the wheels at the beginning of the training period was higher in WT-T (5.13 ± 1.40 hours day-1) than in Tg-T (2.80 ± 1.48 hours day-1). At the end of the training period, the difference between the two groups did not reach statistical difference (3.50 ± 1.10 hours day-1 in WT-T vs. 3.72 ± 1.29 hours day-1 in Tg-T). The total covered distance during training was higher in WT-T (344.6 ± 107.5 km) than in Tg-T (238.8 ± 76.7 km). In summary, at the beginning of training Tg mice had a lower level of habitual physical activity, suggesting a lower exercise tolerance and performance, compared to WT mice. At the end of the training period this difference disappeared.

One WT-T mouse and one Tg-T mouse were excluded from the analyses since the animals, for unknown reasons, did not train significantly (one of them run only 5 km and the other one 63 km over 2 months). Another WT-T mouse died before the end of training period.

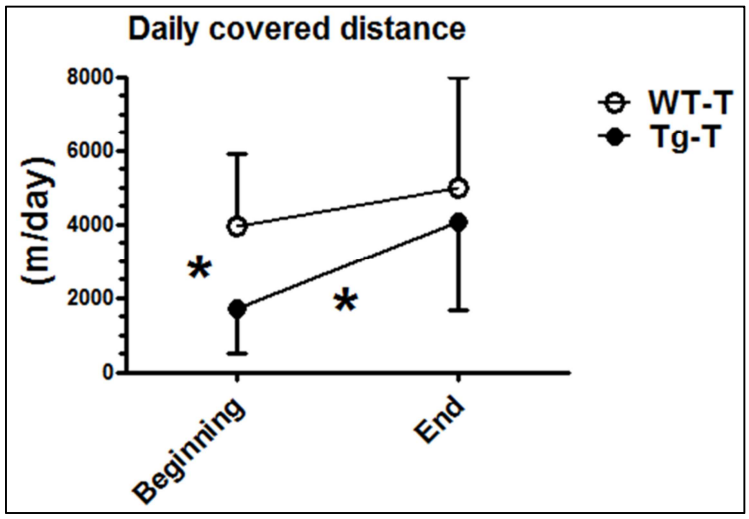

Fig 22. Distance covered daily calculated over 3 days at the beginning and at the end of the training period, in the wild type (WT) and Tgαq*44 mice (Tg) training groups (WT-T and Tg-T, respectively). All data are reported as mean ± SD. * indicates $p < 0.05$.

Moreover, to identify changes in *soleus* muscle fiber structure myosin heavy chain (MHC) isoforms was analysed (Fig. 23). As expected for a highly oxidative muscle like the *soleus*, in WT-CTRL MHC isoforms content was ~75% type 1, ~20% type 2A and ~5% type 2X. No significant differences were observed between Tg-CTRL and WT-CTRL. The data are compatible with those showing no significant differences between WT-CTRL and Tg-CTRL in terms of CS activity (see above). No significant differences (vs. WT-CTRL) were observed with training in WT-T, whereas in Tg-T a higher (vs. Tg-CTRL) content of type 1 and a lower content of type 2A MHC isoforms were observed.

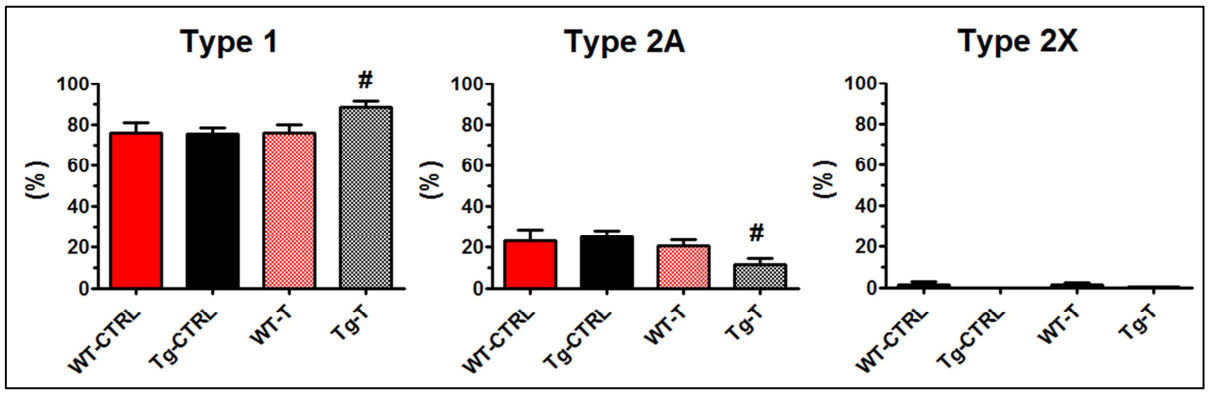

Fig 23. Myosin heavy chain (MHC) isoforms (type 1, type 2A, type 2X) content in *soleus* muscle from WT-CTRL, Tg-CTRL, WT-T and Tg-T mice. Data are expressed as a percentage (mean ± SD values) of total MHC. # $p < 0.05$ vs. Tg-CTRL.

Finally, to investigate cells energy status and further confirm data about mitochondrial mass, p-AMPK/AMPK ratio and PGC-1α protein expression levels were analysed by immunoblotting (Fig. 24). The ratio between phosphorylated and non-phosphorylated AMPK

levels (p-AMPK/AMPK) was not significantly different in WT-CTRL vs. Tg-CTRL. p-AMPK/AMPK levels were not different in WT-T vs. WT-CTRL, whereas they were higher in Tg-T vs. Tg-CTRL. No significant differences in PGC1α protein levels were observed between groups.

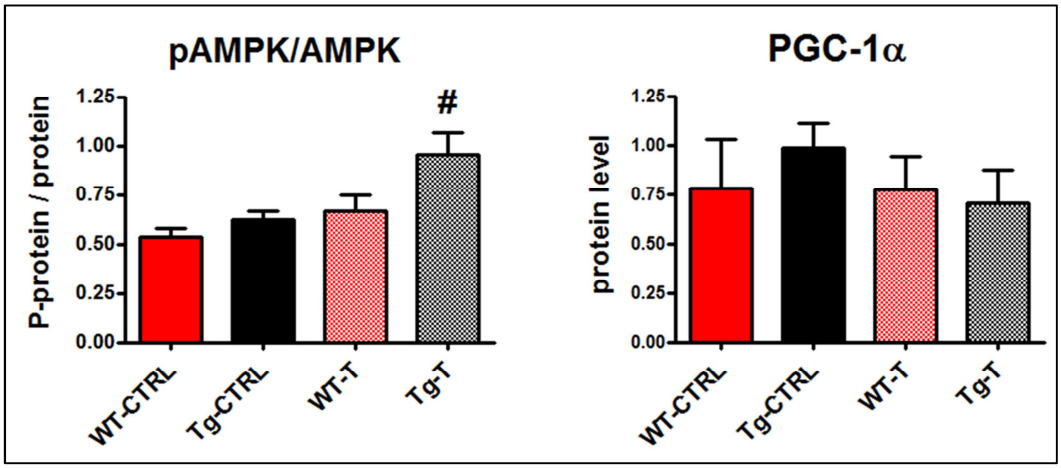

Fig 24. p-AMPK/AMPK ratio and PGC1α protein levels in WT-CTRL, Tg-CTRL, WT-T and Tg-T mice.
All data are represented as mean ± SD values. # $p < 0.05$ vs. Tg-CTRL.

4.2.2. Discussion

4.2.2.1. Mitochondrial respiration impairment is present in *soleus* muscle of CHF transgenic mice model

The study described in this Thesis was performed in Tgαq*44 mice (TG) at ~12 months of age, that is in the critical period of the transition from the compensated to the uncompensated phase of CHF. During the functional evaluation by high-resolution respirometry some of the valuated variables showed an impairment of *soleus* muscle mitochondrial respiration *ex vivo* in Tg-CTRL mice with respect to WT-CTRL mice. All data were normalized by CS activity, a valid estimator of mitochondrial content, both in humans (Larsen et al. 2012) and in mice (Jacobs et al. 2013).

The functional evaluation was carried out by determining the following main variables (Pesta & Gnaiger 2012 – Salvadego et al. 2016): Complex I "leak" respiration (state 2 respiration, O_2 consumption not associated with the phosphorylation of ADP but with the leaking of protons across the inner mitochondrial membrane); maximal ADP-stimulated mitochondrial respiration (state 3) through respiratory complex I and complexes I + II (often termed "oxidative phosphorylation capacity"); ETS respiration, also in presence of rotenone to discriminate the contribution of Complex I and II; phosphorylating system control ratio (P/E) calculated as the ratio of "oxidative phosphorylation capacity" and "ETS capacity".

In summary, in myofibers from Tg-CTRL vs. WT-CTRL (the groups of animals which did not undergo the training program) when electron transport was activated through complex I, or both complexes I and II, and excess ADP was added, a reduction of respiration was observed, a symptom of an impaired mitochondrial function. This impairment was not attributable to changes in mitochondrial content, which was presumably not different between the two groups, as suggested by the data on CS activity and MHC isoforms content.

Interesting data were given by values of P/E ratio. This ratio is known to be near 1 in mouse skeletal muscle at difference from humans (P/E = 0.7-0.8) and rat (P/E = 0.56-0.88) (Gnaiger et al., 2009 and reference herein), indicating an inexistent spare respiratory capacity. The values of P/E ratio observed indicate that PS did not exert control over coupled respiration and did not limit "oxidative phosphorylation capacity" relative to ETS capacity, even in Tg-mice. This may suggests that PS impairment, if any, had not to exceed the one of ETS.

The respiratory defect may be ascribed to complex I. Indeed, ETS respiration sustained by complex II, measured as rotenone-insensitive uncoupled respiration, did not show any significant reduction, suggesting no impairment of complex II, III and IV. This is in accordance with previous reports and in particular with (Wüst et al., 2012), which described in CHF rats impairments of mitochondrial complex I respiration. Anyway, a dysfunction of Complex I is very common in human cardiac muscle affected by HF (Ide et al., 1999 – Kuznetsov et al., 2004 – Drose et al., 2016). With (Wüst et al., 2012) study, here we reported an oxidative function alteration in skeletal muscle that it is likely a downstream effect of the main damage in cardiac muscle, where mitochondrial dysfunction was documented by (Elas et al., 2008).

Complex I can have two catalytically active (open) forms, i.e. active (A-form) and deactivated (D-form), and an inactive closed form (Vinogradov, 1998). A- and D- forms are reversibly converted each other and the latter can be converted in the active form in presence of NADH and ubiquinone (Galkin et al., 2009). On the contrary, the closed form is irreversible and is reported to result from D-form as a consequence of S-nitrosylation on a critically exposed cysteine 39 residue on the surface of ND3 subunit (Galkin, 2008). This residue is not accessible in the A-form. According to other reports, the activity of Complex I in failing myocardium seems to be depressed by an S-nitrosylation on ND3 subunit enhanced by a lowered antioxidant defence and nitric oxide (NO) formation (Scheuble et al., 2002). The latter, in particular, is recognized to be linked to an increased tumor necrosis factor-α (TNF-α), NO-synthase expression and inflammation documented in failing heart and in skeletal muscle

cachexia (Scheuble et al., 2002 – Babot et al., 2004 – Galkin et al., 2009 – Remels et al., 2010).

On these bases, it is hypothesized an irreversible (see also below the discussion about the effects of training) damage of complex I occurring in the *soleus* of Tg mice in the transition from compensated to uncompensated CHF. The damage could be attributable to a transition from the silent D-form to an inactivated (closed) form of the enzyme, in which complex I is not capable to respond to activation stimuli. The molecular mechanisms responsible for such inactivation remain to be explored.

4.2.2.2. Exercise performance is increased by exercise training in CHF mice

In the Tg-T group the functional impairments of mitochondrial respiration discussed above were associated with a reduced exercise performance, as indicated by the lower (by ~60%) spontaneous free wheel running activity observed in Tg-T vs. WT-T at the beginning of the training period (Figure 21). The availability of a running wheel in the cage in which the training groups of mice were kept for ~2 months was associated, in all Tg-T animals (with the exception of one, which was excluded from the analysis), with a substantial increase, from the beginning to the end of the training period, of the level of spontaneous free wheel running activity, determined as the distance covered daily by the animal. Overall, in Tg-T this variable more than doubled over the 2-month period. In WT-T the spontaneous level of physical activity did not significantly change over the training period, whereas the total covered distance was significantly higher in WT-T vs. Tg-T. In short, in both WT-T and Tg-T the availability of the running wheel in the cage represented a valid training intervention. During the last 3 days of training the daily covered distances were substantially the same in WT-T and in Tg-T. In other words, the difference in exercise performance and exercise tolerance between the two groups, observed before training, substantially disappeared following training.

4.2.2.3. Improvement of exercise performance in CHF mice involves mechanisms located "upstream" of mitochondria

In the absence of changes in mitochondrial respiratory function, it is hard to explain the increased exercise performance following training observed in Tg-T. As mentioned above, indeed, in both WT and Tg mice the training intervention did not have any significant effect on these variables, which were not significantly different in WT-T vs. WT-CTRL, and in Tg-T vs. Tg-CTRL (see Fig. 2).

Exercise training in CHF enhances O_2 delivery to and O_2 utilization by skeletal muscle, thereby improving variables of functional evaluation of oxidative metabolism strictly related

to exercise tolerance (Grassi et al. 2015) such as peak $V'O_2$, the "ventilatory" or "lactate" threshold, critical power, the various phases of the $V'O_2$ kinetics (Hirai et al. 2015). These improvements may occur by several mechanisms, which ultimately act by enhancing microvascular PO_2 ($P_{mv}O_2$) and peripheral O_2 diffusing capacity (D_mO_2). Strictly speaking, both these variables are independent from mitochondrial respiratory function. Both these variables, moreover, are markedly depressed in CHF (Poole et al. 2012, Hirai et al. 2015). $P_{mv}O_2$ represents the driving force for peripheral O_2 diffusion from capillaries to mitochondria, whereas D_mO_2 describes the diffusive capacity for O_2 from Hb to mitochondria (Wagner 1996, Esposito et al. 2010, Esposito et al. 2011, Poole et al. 2012, Hirai et al. 2015). Exercise training in CHF patients improves also other factors, intrinsically associated with the disease, which can negatively impact at several levels on skeletal muscle oxidative metabolism, such as an increased production of pro-inflammatory cytokines and ROS (Reid & Moylan 2011), endothelial dysfunction (Wisløff et al. 2007), decreased vascular/muscle NO bioavailability (Hirai et al. 2014, 2015). Some of these factors represent the target of specific therapeutic interventions (see e.g. Sperandio et al. 2009, Chirinos & Zanami 2016).

Improvements of exercise performance obtained by training in the present study presumably involved, along the pathway for O_2 from ambient air to the mitochondria of skeletal muscles (Wagner, 1996), mechanisms located "upstream" of mitochondria. The present study demonstrated that this general conclusion applies to Tg mice during the critical period between compensated cardiac muscle hypertrophy and uncompensated overt CHF. The sites at which training-induced improvements may take place in CHF are several, and may comprehend an improved cardiac function and an enhanced capacity of cardiovascular O_2 delivery (Poole et al. 2012 – Hirai et al. 2015), skeletal muscle neo-angiogenesis (Mezzani et al. 2013), a redistribution of blood flow towards oxidative muscles (Musch et al. 1992), a reduced humoral and sympathetically-mediated vasoconstriction (Negrao & Middlekauff 2008, Zucker et al. 2015), an improved endothelial function, an improved microvascular O_2 delivery and an improved intramuscular matching between O_2 delivery and O_2 utilization (Hirai et al. 2014), an increased vascular and tissue NO availability (Hirai et al. 2014 – Chirinos & Zanami 2016). Unpublished observations by Tyrankiewicz et al. obtained in Tgαq*44 mice undergoing the same training protocol utilized in the present study, observed an enhanced cardiac function. All these mechanisms would result in an increased $P_{mv}O_2$ and in a decreased D_mO_2, which would enhance skeletal muscle oxidative metabolism independently from changes occurring at the mitochondrial level. This concept is discussed in detail in the review by Hirai et al. (2015), and has been confirmed by the studies on CHF patients by

Esposito et al. (2010, 2011). The overall scenario and the responses to training may be substantially different when the animals reach the uncompensated phase of the disease, and overt cardiac failure ensues.

4.2.2.4. Unchanged mitochondrial function could be due to voluntary exercise training protocol

Unexpectedly the voluntary exercise protocol did not have any effect on respiratory variables in the two groups. *Soleus* muscle seems to be in both the trained groups analysed insensible to exercise. It is the case to remember that *soleus* muscle is a 80% type I fiber muscle and manly possesses an oxidative metabolism. In a study of Hoppe and colleagues it was proved the inability of *soleus* muscle to synthetize new proteins after training proving to be a muscle resistant to exercise as seen in many studies (Hoppe et al., 2004).

The unchanged mitochondrial respiratory function following training described (also in WT mice) in the present study, however, should be put in a broader perspective. In recent years the concept has indeed emerged that both in healthy subjects (MacInnis et al. 2016) and in cardiac patients (Wisløff et al. 2007) high-intensity aerobic interval training (e.g., four 4-min intervals at 90-95% of peak heart rate, separated by 3-min of moderate-intensity recovery, 3 times per week [Wisløff et al. 2007]) is more effective than prolonged moderate-intensity exercise training in improving skeletal muscle mitochondrial function (as well as other variables, such as maximal aerobic power, endothelial function, etc.). According to a study carried out by (Boushel et al., 2014) in healthy subjects, following moderate-intensity prolonged exercise training increases in peak muscle $V'O_2$ are associated with increases in blood flow, capillary volume, peripheral O_2 diffusing capacity, in the presence of an unchanged mitochondrial oxidative phosphorylation capacity. Although comparisons of the training protocol adopted in the present study with training protocols in humans may not be straightforward, after considering that in the present study training was carried out by the animals for 3-5 hours per day, the training stimulus seems similar to a prolonged submaximal exercise training approach. It cannot be excluded, therefore, that different results could have been obtained by adopting a training regimen characterized by shorter and more intense training bouts.

4.2.2.5. AMPK signalling pathway is activated after training in CHF mice, but does not induce PGC1α protein expression

In Tg-CTRL the impaired mitochondrial function did not presumably determine a significant energy unbalance. This would be compatible with a relatively low level of habitual

physical activity. As a consequence of this, p-AMPK/AMPK (the intracellular "sensor" of energy stress) levels were not different in Tg-CTRL vs. WT-CTRL. This may explain the absence of differences, between the two groups, in terms of the levels of PGC1α (the master controller of mitochondrial proliferation and function), of CS activity (taken as an estimate of mitochondrial mass) and of MHC isoforms content, which showed values typical for a highly oxidative muscle.

Conversely, following the prolonged and intense training stimulus an energy unbalance emerged in Tg-T (these animals were characterized by an impaired mitochondrial function), and p-AMPK/AMPK levels rose. This increase, however, was not associated with increased levels of PGC1α, but with a shift of the content of MHC isoforms towards an even more oxidative phenotype (increased type 1 MHC isoform, decreased type 2A). Previous experimental evidence suggests that endurance exercise-induced fiber-type transformation in skeletal muscle can occur independently from the function of PGC1α. For example, (Geng et al., 2010) showed that voluntary exercise-induced type IIb-to-IIa transformation was not affected by the deletion of the PGC1α gene in knockout mice. The MHC isoforms shift in the present study did not relieve the functional impairment of mitochondrial respiration, but it might have contributed, possibly in association with other factors occurring upstream of mitochondria (see discussion above), to the improved exercise performance observed following training in Tg-T.

4.2.3. Conclusions

In conclusion, functional impairments in exercise performance and in *soleus* muscle mitochondrial respiration were observed in transgenic CHF mice during the critical period of transition from compensated hypertrophy to uncompensated CHF. The impairment of mitochondrial respiration was mainly qualitative, since it was not associated with differences in CS activity, MHC isoforms content, p-AMPK/AMPK and PGC1α levels. The impairment was presumably related to the function of complex I of the mitochondrial respiratory chain. Exercise training improved exercise performance, but it did not affect mitochondrial respiration, even in the presence of an increased % of type 1 MHC isoforms. Factors "upstream" of mitochondria were likely mainly responsible for the functional improvement.

The overall scenario and the responses to training could be different after the animals reach the uncompensated phase of the disease, and overt cardiac failure ensues.

4.3. ATPase-Inhibitory Factor 1 (IF1) as Prognostic Factor in LGA. An ex vivo Study

Astrocytomas are the most common and lethal tumors of the CNS. They can evolve from low grade lesions (WHO II grade) to anaplastic lesions (WHO III grade) and then even to glioblastomas (WHO grade IV). All astrocytomas derive from glial astrocytic cells that are the support cells of CNS in order to maintain nervous structures and to transport nutrient to neurons. This study focuses on Low Grade Astrocytomas (LGA, WHO grade II) because these are usually well differentiated, slow-growing, but treatment-resistant tumors. In fact, LGA are clinically heterogeneous and can either recur relatively shortly after surgery or not and patients can become long-survivors. At the present moment there are not definitive molecular criteria to classify a lesion as at high or low risk to relapse and/or to progress. In this scenario, it is important to identify new biomarkers for LGA. Recently ATPase-Inhibitory Factor 1 (IF1), a basic, fibrillar protein that reversibly binds to the catalytic β-F1-ATPase subunit of OXPHOS Complex V, was identified in many types of carcinomas as an important biomarker of prognosis (Sánchez-Aragó et al., 2013 – Gao et al., 2016 – Song et al., 2014 – Yin et al., 2015). Moreover, in some carcinomas IF1 was described as a factor in defining the glycolytic phenotype (Sánchez-Aragó et al., 2013 – Song et al., 2014). In fact, it was found that IF1 expression levels in colorectal, lung, breast and liver cancer are upregulated if compared with healthy tissues and could be a prognostic factor for these tumors. Moreover, in breast cancer the expression levels are associated with the staging of the disease (Sánchez-Cenizo, 2014). The purpose of the study was to investigate the expression levels and the prognostic value of IF1 in human LGA. In this thesis also the expression levels of OXPHOS complexes along with mitochondrial mass markers (HSP60 and CS) were assessed, together with IF1, in both LGA and in a subgroup of LGA with suspected early anaplastic signs (LGA*), in order to have some indications of their bioenergetic phenotype. Unfortunately, to this aim it was impossible to carry out functional respirometric measurements due to difficulty to get fresh surgical specimens.

4.3.1. Results

IF1 expression was investigated by IHC in 13 LGA and 14 high-grade astrocytomas (HGA) and by IF in 12 LGA and 9 high-grade astrocytomas (HGA). Both techniques confirmed an up regulation of the protein in HGA compared to LGA (Fig 25).

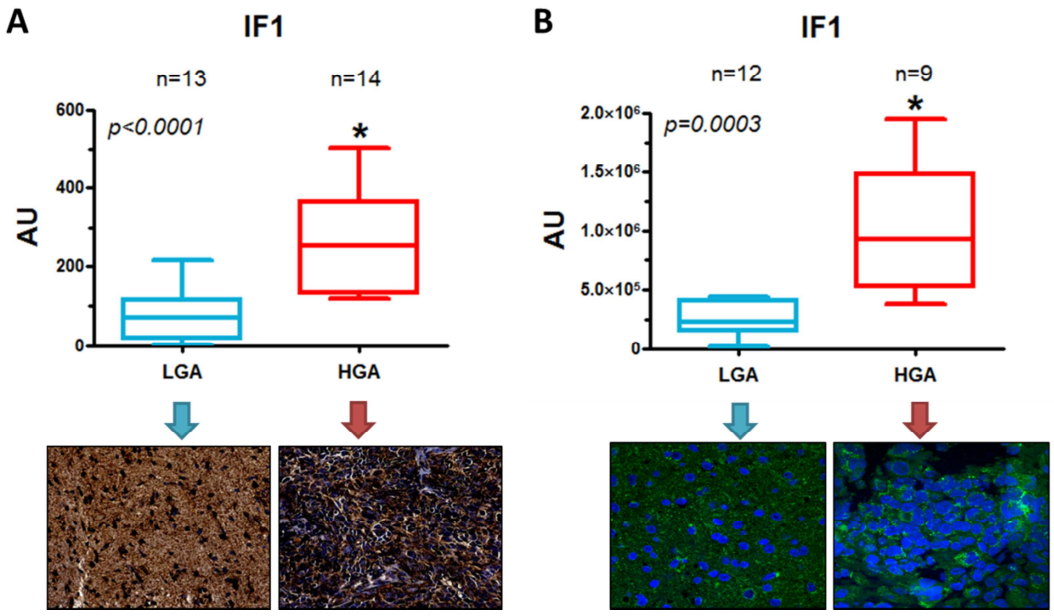

Fig 25. IF1 expression levels in LGA and HGA evaluated by IHC (A) and IF (B).
Representative images of LGA and HGA of both techniques are pictured below the correspondent graph. All data are represented as whisker and box plot, where the whiskers represent minimum and maximum values and the box the 50% of the population along with median, 25 and 75 percentile values.

Because of the importance of finding new prognostic markers in LGA and based on our evidence for the increase of the protein abundance with tumor grading, the attention of the study was focused on the LGA in order to verify if IF1 can be proposed as a molecular biomarker to classify the lesions. First, the expression values of IF1 were evaluated by IHC in 19 pairs of tumoral and border zone tissues to verify if there is an increase of the protein levels switching from healthy to neoplastic tissue. In these samples, there was a significant upregulation in the protein expression levels in the tumoral compared to border zone (Fig 26).

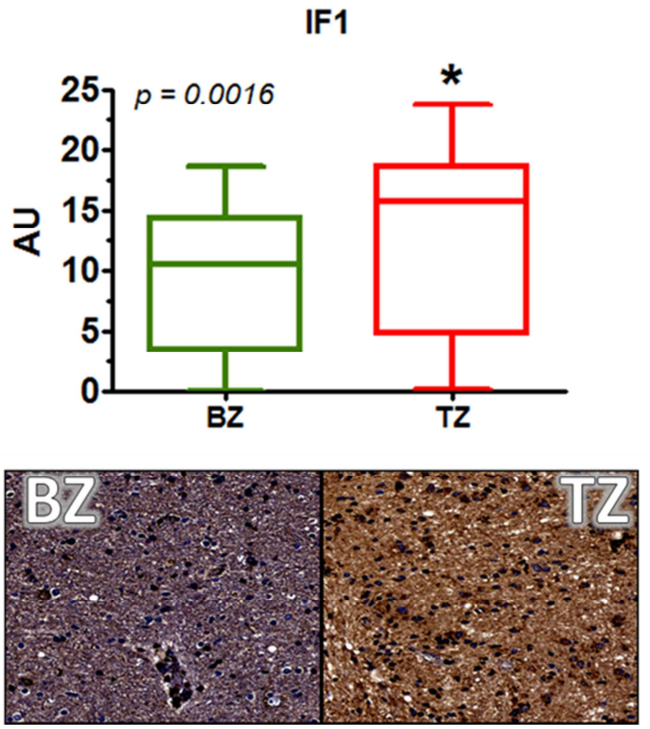

Fig 26. IF1 expression values in tumoral border zone (BZ) vs tumoral zone (TZ).
IHC representative images are pictured below the graph. All data are represented as whisker and box plot (for details see Fig 25), n=19 for both BZ and TZ.

Further, among very recently collected LGA samples, still without clinical follow-up, were identified two different subgroups: canonical LGA and still low-grade astrocytomas but with suspected early anaplastic signs (LGA*). IF1 expression levels were evaluated in these two subgroups by IHC (6 LGA vs 7 LGA*), IF (7 vs 5) and immunoblotting (5 vs 4). All three techniques confirmed an up regulation of the protein levels in the LGA* compared to LGA (Fig 27), thereby validating each other despite the low numbers of samples and difference in their sensitivity.

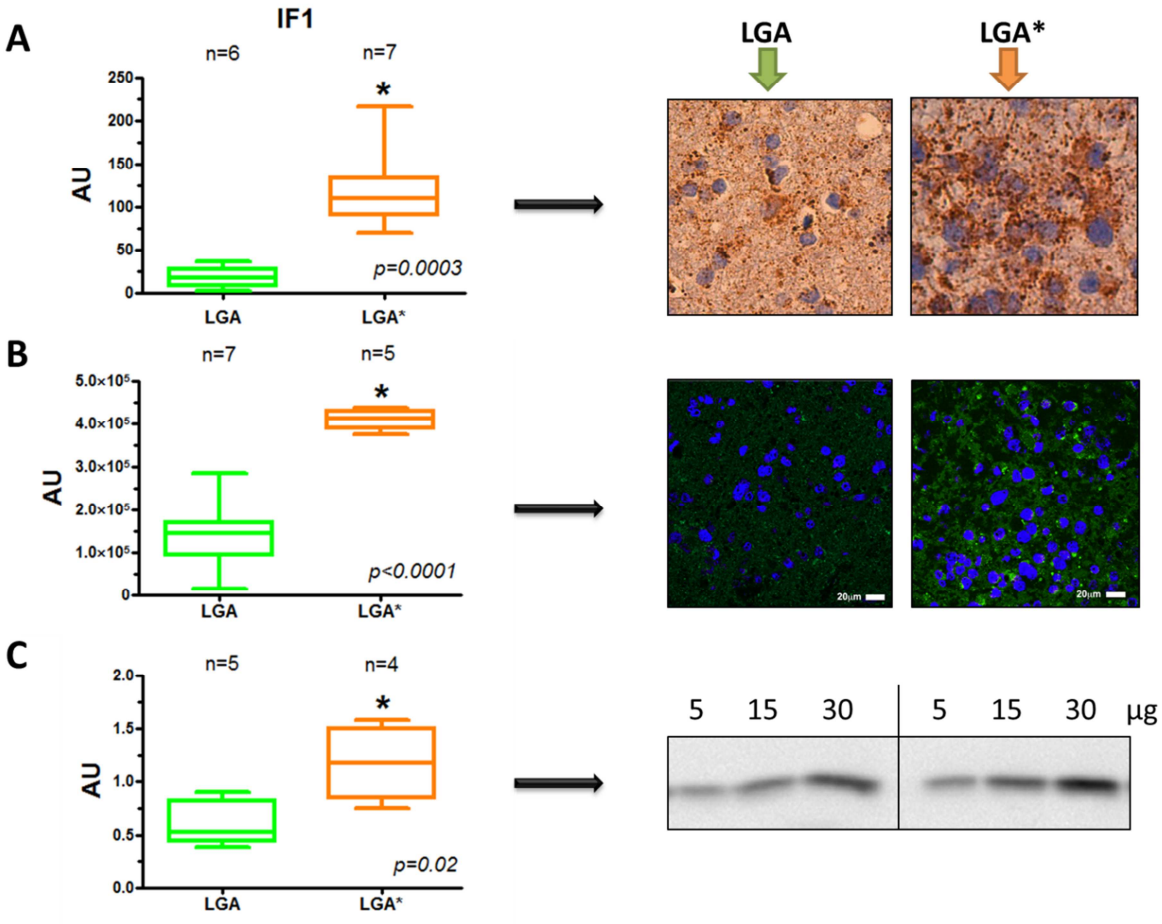

Fig 27. IF1 expression levels in LGA and LGA* samples analysed by IHC (A), IF (B) and WB (C). On the left side of each panel IF1 expression level is represented with whisker and box plot along with the number of samples and statistical p value. On the right side of each panel representative images of the three techniques of IF1 expression in LGA and LGA* samples.

The examined population of LGA was further expanded to 68 samples from which all clinical charts and follow-up were available. They were analysed by IHC using TMA, an approach which consents high-throughput analyses of many samples at once and by different techniques (IHC, IF or *in situ* hybridization), thereby minimizing the size of the biopsy from the donor/patient and to reduce variation among replicates.

The prognostic value of IF1 was assessed by analysing the 68 samples by Kaplan-Meier estimator (Fig 28). The IF1 median value of the population was chose as cut-off value for this analysis and there were identified two different populations in LGA stratifying for overall survival values in relation to IF1 expression levels. More expressed is IF1, more severe is the prognosis of the patients as confirmed by Log-Rank statistical analysis ($p = 0.01$). Unfortunately, with the numbers of the analysed cohort, it was not possible to define if IF1 is an independent prognostic factor. An independent prognostic factor is defined by Multivariate

statistical analysis, which indicates if the proposed prognostic factor has independent value compared to other, already established, biomarkers (Schwab, 2011).

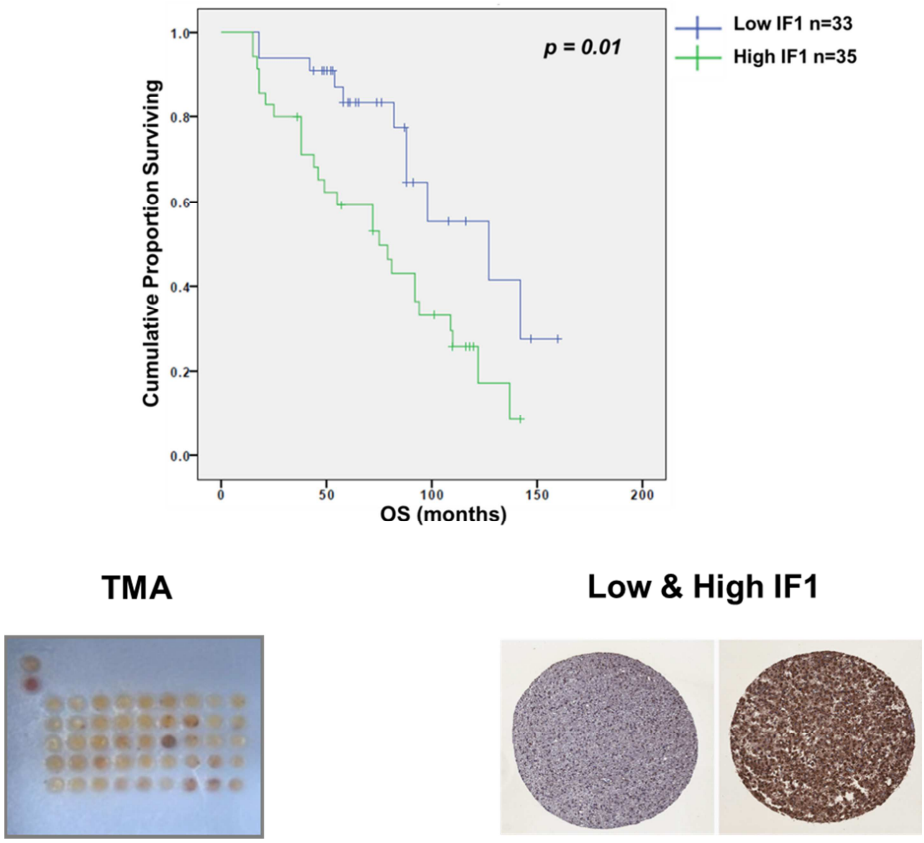

Fig 28. Overall survival in LGA patients with respect to IF1 expression levels. Kaplan Meier curves were used to represent the OS (in months) in LGA patients. The blue curve represents patients that have a low expression of IF1 (cut-off value: 10 AU). On the contrary, the green one represents the patients with high expression of the protein. On the lower part of the picture are represented one of the TMA used for the study and two representative samples with low and high expression of IF1.

Furthermore it was evaluated the correlation between IF1 and other recognized glioma markers. Very interestingly, results showed IF1 to be significantly, though weakly, associated with consolidated radiological prognosis indexes of tumor resection and infiltration, i.e. extent of resection (EOR) ($p = 0.0005$; $r = -0.413$) and ΔVT2T1 ($p = 0.038$; $r = 0.255$) (Skrap et al., 2012) (Fig 29 A and B). These indexes are based on magnetic resonance imaging (MRI) before and after surgery. In particular, EOR is based on pre- and post- operative images in order to evaluate the tumor resection performed by surgery. On the other hand, ΔVT2T1 is based on two different pre-operative images in order to evaluate the tumoral mass and its infiltration among near tissues (see paragraph 4.3.2.3).

It is also very interesting the finding that IF1 is likewise weakly associated ($r = 0.21$), though not significantly ($p = 0.0867$), with p65 nuclear subunit of NF-kB (Fig 29 C).

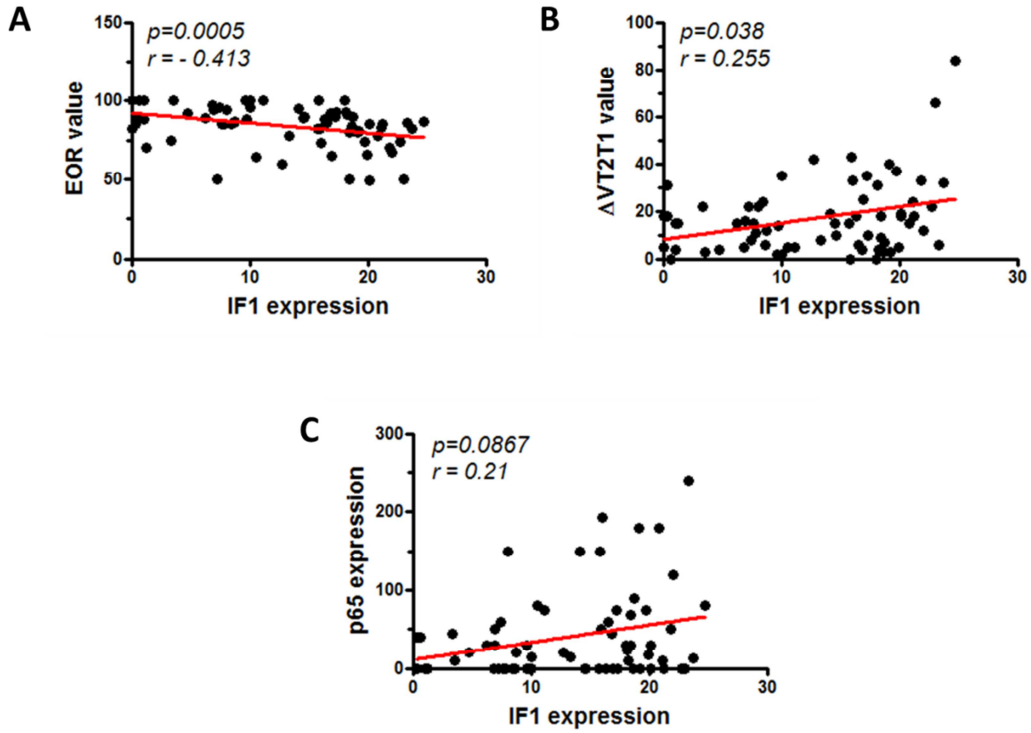

Fig 29. IF1expression levels correlation with EOR index (A), ΔVT2T1 index (B) and p65 expression levels (C). In each panel statistical significance (p) and correlation (r) values are reported.

In order to have some indications, although not functional, of LGA bioenergetic phenotype, the expression levels of GAPDH, Citrate Synthase, HSP60 and OXPHOS complexes I-V were evaluated by immunoblotting in the same LGA and LGA* samples (5 vs 4). The analyses revealed no changes in GAPDH, CS and HSP60, suggesting an unchanged glycolytic metabolism and mitochondrial mass, although a tendency to an increase of CS and HSP60, even if not significant, was observed (Fig 30 A, B and D). Mitochondrial mass was further evaluated by IHC (6 vs 7 samples), targeting a non-glycosylated protein on the outer mitochondrial membrane of 60 KDa, showing a significant increase in LGA* group not in accordance with WB data (Fig 30 C).

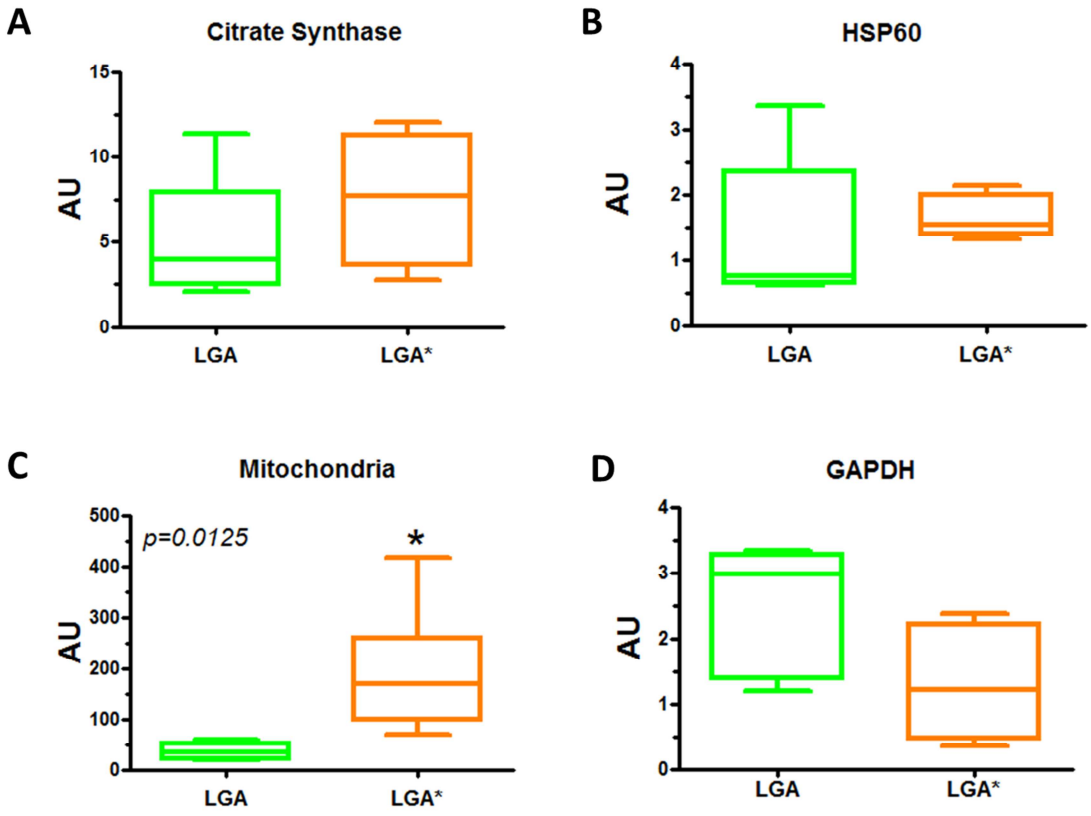

Fig 30. Mitochondrial mass and glycolytic markers in LGA vs LGA*.
In panels A and B CS and HSP60 results of WB are presented. In panel C ICH results of a commercial Ab that evaluated mitochondrial mass marker (MTC-02 clone Ab, Thermo Scientific) are showed. In panel D results of glycolytic marker GAPDH, obtained by WB are showed. * $p < 0.05$

As far as concerns the OXPHOS subunits expression levels, all complexes, except for complex II, revealed an intense up regulation of the investigated subunits (NDUFB8 of CI, SDHB of CII, UQCRC2 of CIII, COXII of CIV and Complex V α) in LGA* vs LGA (Fig 31).

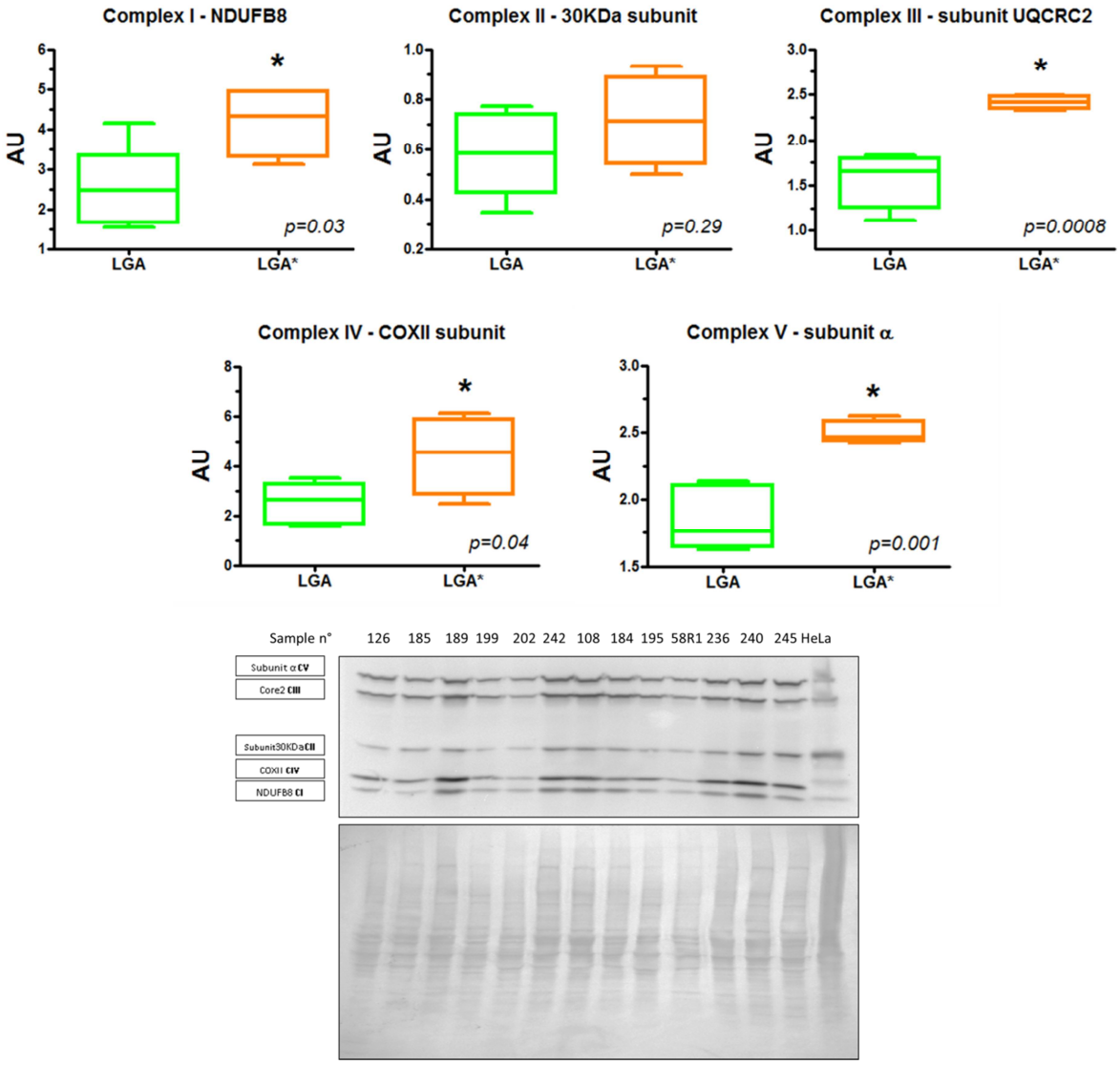

Fig 31. OXPHOS complexes expression levels in LGA vs LGA*.
Whisker and box plots for each complex subunit are represented for LGA vs LGA*, along with p value (* p< 0.05). On the bottom of the picture a representative WB picture of a series of randomly taken specimens from both LGA and LGA* groups is shown. Loaded protein quantities are normalized on densitometric values obtained from lower Coomassie stained PVDF membrane.

The same LGA samples divided into two subgroups and analysed by IHC and WB for IF1 and mitochondrial mass (see above) were also separately evaluated for β subunit of complex V. These analyses revealed a tendency for β to be up regulated in LGA* (Fig 32).

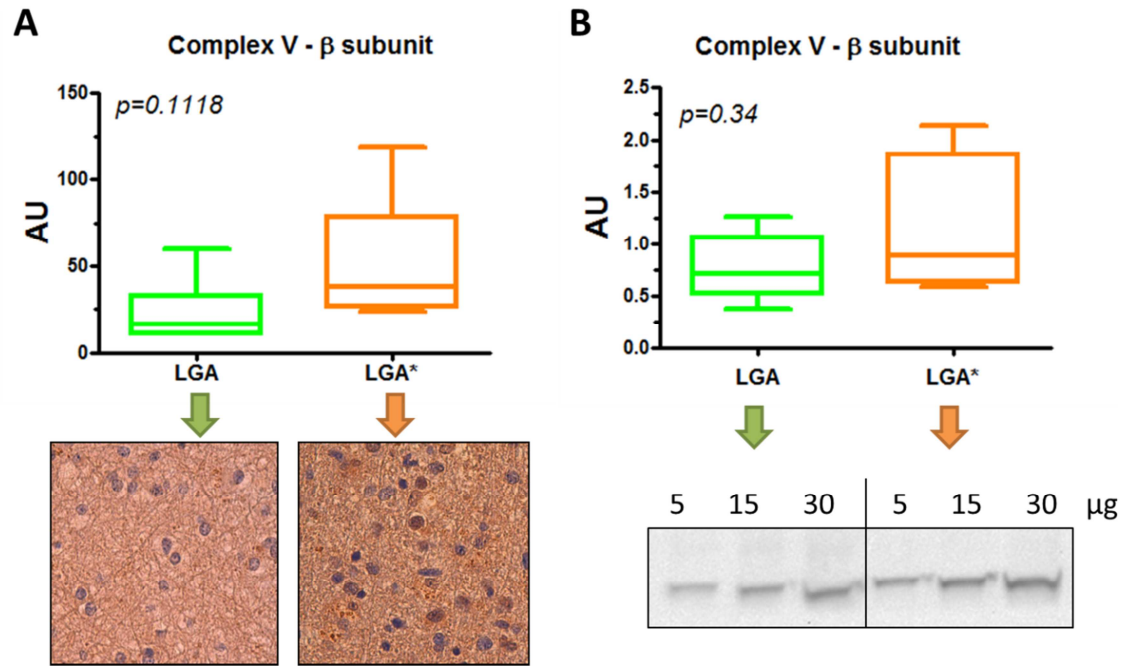

Fig 32. Complex V - β subunit in LGA vs LGA*.
In panel A are showed the results of IHC for the investigated subunit along with representative images (6 vs 7 samples). In panel B are showed the results of WB experiments (5 vs 4) along with one representative image.

4.3.2. Discussion

4.3.2.1. IF1 is Up-Regulated in High Grade Astrocytomas

In this study IF1 expression was evaluated by IHC and IF on LGA (WHO II grade astrocytomas) and HGA (WHO III-IV grade astrocytomas) samples. Immunoblot analyses in HGA samples were not performed due to large necrotic areas inside tumor tissue. In fact, in this case data from tissue homogenates would reflect all the tissue heterogeneity, tumor and necrotic tissues, and thereby creating an artefact. On the contrary, IHC and IF permit to analyse only vital cells. IHC and IF techniques confirmed an up regulation of the protein in HGA compared to LGA, in accordance with a previous report in which was proved an increase in IF1 content in relation to the WHO grading in gliomas also compared to healthy brain tissue samples (Wu et al., 2015). Wu and colleagues proved the correlation between IF1 expression and tumor grading independently from the histological derivation of the tumoral cells, comparing also healthy brain tissue that was not possible to collect for the present study. They also showed that IF1 protein levels consistently matched mRNA expression levels.

Notably the study here presented was able to determine with different techniques that IF1 upregulation was still true in a more restricted group of gliomas (9-14) but all deriving from the same cell type, namely astrocytes.

4.3.2.2. IF1 is Up-Regulated in LGA* with Suspected Anaplastic Evolution vs. canonical LGA and in Tumoral vs. Border Zone

LGA group was divided into two subgroups, identified during the histopathological analysis of recently collected biopsies, namely canonical low-grade astrocytomas not showing any sign of abnormal proliferation and anaplastic evolution (LGA) and low-grade astrocytomas with suspected early signs of anaplastic evolution (LGA*). In these subgroups the expression levels of IF1 were investigated by IHC (6 vs 7 samples), IF (7 vs 5) and immunoblotting (5 vs 4). All the techniques confirmed an upregulation of IF1 symptomatic of the possibility that it may be used as a prognostic marker also in this glioma subset. Unfortunately, because the analysed samples were in a small number, due to the low incidence of this tumor, and without clinical follow-up, as recently collected, it was not possible to verify this hypothesis until now.

IF1 expression levels were further investigated in different zones of same LGA surgical specimens. In particular, the tumoral border zone, near to healthy tissues, and the proper tumoral zone were analysed in 19 pair of bioptic samples. Also in this case IF1 is upregulated, even if slightly, in the tumoral zone compared to the border zone, demonstrating a gradual increase in the protein levels since early stages of the disease and an upregulation from healthy brain tissue to low-grade in accordance with (Wu et al., 2015). Commenting on such slight but significant increase of IF1 in this case, it should be reminded that the tumoral border zone is still a cancer zone that shows tumoral characteristics even if “diluted” in healthy tissues. Progressing from healthy brain tissue to the necrotic area of the tumor there is a gradient of healthy and cancer cells that sometimes in border zones could be difficult to distinguish.

4.3.2.3. IF1 is a Prognostic Factor in LGA and is Associated with Radiologic Markers of Tumor Resection & Infiltration

Finding new prognostic factors in early stages of a neoplasia is becoming a major task in order to better direct clinical therapy that will fit better the patient disease characteristics. This aspect is even more important in low-grade gliomas after the last revision in 2016 of the

WHO classification of CNS tumors (Louis et al., 2016). Genetic features are now evaluated beside the histopathological characteristics of the gliomas, in order to choose the best therapeutic approach to treat the tumors. In LGG the outcome has traditionally been considered to be more favourable in oligodendrogliomas and less favourable in astrocytomas, whereas oligoastrocytomas has been attributed as an intermediate prognosis (Hartmann et al., 2011). Nowadays no molecular parameter is a sensitive prognostic biomarker in WHO grade II glioma patients, who do not receive radiotherapy or chemotherapy after surgery (Hartmann et al., 2011), neither in case of astrocytoma despite the less favourable outcome. Regardless of histology, IDH1 mutation status is the strongest prognostic marker for OS in high-grade gliomas, but the prognostic role in low-grade diffuse gliomas (WHO grade II) is not clear (Iwadate et al., 2015). It should be noted that, even if LGA occur less frequently than glioblastomas, still 70% of grade II gliomas evolve to anaplasia or recur at higher grade after surgery, in turn leading to death within 5-10 years (Furnari et al., 2007). Thus, there is a necessity to find out a predictive factor that could suggest a worse prognosis and/or progression of the lesion.

As noticed above, IF1 in the last years has become a protein of common interest as prognostic factor in different carcinomas. After the first encouraging phases of the study here reported on a small sample number, IF1 appeared to be not just a prognostic factor in gliomas, but in an even more restricted group with large clinical interest, low-grade astrocytomas. Thus, it was decided to enlarge the investigated cohort to 68 samples of LGA, all with clinical charts and follow-up, in order to determine if IF1 could be a marker of overall survival in these patients. The samples, divided into two groups discriminated by low or high expression of IF1 on the basis of a cut-off value, given by the median value of the investigated population, were evaluated by Kaplan-Meier estimator. IF1 turned out to be a prognostic factor in LGA-patients as seen in gliomas (Wu et al., 2015) and in carcinomas (Gao et al., 2016 – Yin et al., 2015 – Song et al., 2014 – Sanchez-Aragó et al., 2013). Since 2013, when IF1 was first identified as biomarker in colon and breast cancer (Sanchez-Aragó et al., 2013), other studies followed, confirming that report, but no one focused specifically on low-grade gliomas.

In the present study IF1 expression was correlated with two radiological indexes of tumor resection and infiltration. Extent of resection (EOR) is an index established by analysing the pre- and postoperative volumes of the gliomas on T2-weighted MRI studies and is calculated as: (preoperative tumor volume - postoperative tumor volume)/preoperative tumor volume, as previously described by (Smith et al., 2008). EOR is also known to have an important impact in overall survival (OS). In fact, an early resection of most of the tumoral mass is the main

factor in enhancing OS, but also in preventing the anaplastic transformation of low-grade gliomas (Ius et al., 2012). In the investigated samples, EOR has a weak but significant inverse association to IF1 expression levels. This suggests that more expressed IF1 is, more difficult is to completely take away the tumor, compatible with possible infiltration of the mass with irregular edges.

The second index analysed was ΔVT2T1, a preoperative estimation of the difference between tumor volumes on T2-weighted MRI studies and on contrast-enhanced T1-weighted MRI studies. ΔVT2T1 is calculated as: preoperative volumetric tumor volume segmented on T2-weighted images – preoperative volumetric tumor volume segmented on T1-weighted images (Skrap et al., 2012). ΔVT2T1 is a marker of tumor infiltration and proliferation that is known to be inversely correlated with EOR (Ius et al., 2012 – Skrap et al., 2012). In this study ΔVT2T1 proved to be directly associated, though weakly, with IF1. This suggests that IF1 might be associated to tumor infiltration and proliferation, in line with EOR results.

Infiltration and angiogenesis in tumors seem to be directed by NF-kB pathway. The activation of this pathway could be canonical or non-canonical (Razani et al., 2011). The canonical one is represented by NF-kB1 complex made by RelA/p50 dimers. On the other hand, the non-canonical pathway is triggered by NF-kB2 complex formed by RelB/p52 dimers. Angiogenesis and endothelial-mesenchymal transition (EMT) in cancer seem to be promoted by the stabilization of NF-kappa-B-inducing kinase (NIK) in complex with TNF receptor-associated factor 1 (TRAF1), which has the ability to activate NF-kB and in turn the vascular endothelial growth factor (VEGF) and Zinc finger protein SNAI1 (Snail1). Thus, infiltration and EMT (loss of cell polarity, loss of intracellular junctions and increased cell migration) are stimulated (Song et al., 2014 – Wu et al., 2015). Different studies on liver, colon, breast and even glioma have found out a connection between these processes and NF-kB (Song et al., 2014 – Wu et al., 2015 – Sanchez-Aragó et al., 2013). Moreover, in these studies were observed a link between IF1 and NF-kB. Sanchez-Aragó and colleagues found out that the inhibitory action of IF1 on ATP synthase could promote, togheter with the downregulation of oxidative phosphorylation, ROS production thereby activating NF-kB (Sanchez-Aragó et al., 2013 – García-Bermúdez & Cuezva, 2016 and references herein). In addition, the groups of Song and Wu have discovered a connection between IF1 and subunits p50 or p65 of NF-kB (Song et al., 2014 – Wu et al., 2015). As demonstrated by Song and colleagues, IF1 can induce proliferation and tumor metastatization through the activation of NF-kB, Snail1 and VEGF. Moreover, NF-kB is able to induce in a positive feedback loop the expression of IF1 continuing the promotion of tumor infiltration. In particular, they showed that p65 could

actively bind to IF1 promoter in the nucleus inducing its expression. In gliomas, Wu and colleagues investigated the relationship between IF1 and NF-kB p50 subunit. They found out that IF1 knockdown in glioma cell lines inhibited the expression of NF-kB, Snail1 and VEGF, increased the expression of E-cadherin and reduced vimentin levels, according to a diminished ability to metastasize. In this perspective, in this thesis was analysed the correlation between IF1 and p65 expression levels detected by IHC. Even though the correlation did not reach statistical significance, maybe due to a still low number of samples, there is a weak association between the two proteins. This is in line with data mentioned above by other groups (Song et al., 2014 – Wu et al., 2015) and might give an explanation of the direct association between IF1 and ΔVT2T1, an index of tumor infiltration. It might be inferred that more IF1 is expressed, more NF-kB may be activated along with Snail1 and VEFG, promoting proliferation and angiogenesis and resulting in a greater tumor infiltration, as testified by the radiological markers. This aspect should be further investigated in a greater sample cohort.

4.3.2.4. OXPHOS Complexes Expression Levels in LGA vs LGA*

Cancer bioenergetics in the last few years revealed itself to be not an easy topic. In fact, several findings showed that the matter is not as simple as Warburg thought and that cancer metabolism is more than just aerobic glycolysis. In particular, for gliomas, there seems not to be an accordance on which kind of metabolism tumor cells prefer. Some reports described they prefer a glycolytic metabolism as healthy astrocytic cells (Oudard et al., 1996), others documented increased levels of oxidative metabolism proteins with glioma grading (Marin-Valencia et al., 2012 – Griguer et al., 2005). It is unquestionable that there is a large OXPHOS heterogeneity in gliomas as seen in various proteomic and gene expression studies (Hu et al., 2013 – Ordys et al., 2010).

For this part of the study the same LGA and LGA* samples that were previously mentioned in this thesis were analysed.

First, it was analysed the expression level of GAPDH, a major enzyme involved in the glycolytic pathway. The expression of this protein, analysed by western blot, does not change in the two groups and it might be in agreement with no upregulation of glycolysis. Interestingly, it should be noted that astrocytes have a high metabolic capacity, supporting neurons through glycolysis-derived ATP and lactate, and producing ATP by mitochondrial metabolic pathways for their own survival and energy demands. Therefore, healthy astrocytes exhibit a double metabolic phenotype due to an enhanced glycolysis and oxidative

phosphorylation compared to healthy neurons. In this regard, also astrocytic tumor cell lines show this peculiarity with respect to neuroblastoma cell lines (Kim et al., 2015). Thus, it could be reasonable to suggest that cancer cells originated from cellular types with a strong glycolytic phenotype would not enhance this pathway further.

Moreover, as mitochondrial mass markers were analysed the expression levels of both citrate synthase and HSP60 protein by immunoblotting, and a 60kDa non-glycosylated protein component of mitochondria found in human cells (Ab2- MTC02 Clone, Thermo Fisher, see datasheet) by IHC. CS and HSP60 are referred as established mitochondrial mass markers in many reports (Cuezva et al., 2009), but did not show significant differences in this study between the two groups. On the contrary IHC analyses with Ab2- MTC02 Clone showed a significant increase in mitochondrial content for LGA* with respect to LGA. This might be considered unusual in tumor cells, but also another study found out that mitochondria are up regulated in astrocytomas in contrast to healthy tissue (Feichtinger et al., 2014). The discrepancy between immunoblotting and IHC data could be caused by different sensitivity of the two methods and/or by fewer number of samples analysed in immunoblotting that, nevertheless, showed that HSP60 and CS protein expression levels tend to increase in LGA*, even if not significantly. An apparent upregulation of mitochondria should not be so unexpected in astrocytic tumors considering the upregulation of OXPHOS proteins documented during glioma grading (Scrideli et al., 2008 – Marie et al., 2008), as well as the proposed theory of genic waves of metabolic reprogramming in tumors, with the first stages relying on glycolytic metabolism and the later phases accompanied by switch to a more oxidative metabolism (Smolkova et al., 2010). In accordance with the hypothesis that astrocytoma cells are both mitochondria- and glycolysis-proficient there are data which our laboratory recently obtained on three different glioblastoma (high-grade astrocytoma) cell lines, namely SF767, U87MG and A172, documenting a mitochondrial oxidative phosphorylation ATP supply of ~30%.

Finally, OXPHOS complexes I, II, III, IV and V were evaluated by immunoblotting, documenting that LGA* samples showed a general upregulation, except for complex II. These results are in agreement with the data showing increase of mitochondrial mass. A tendency towards an increase of some OXPHOS complexes was previously described by Feichtinger and colleagues (Feichtinger et al., 2014) in grade II and III astrocytic tumors with respect to normal brain tissue, finding out in particular an increase in complex V levels. Moreover, Xu and colleagues found a significant increase in complex V expression levels in low-grade astrocytomas (Xu et al., 2016). The upregulation of OXPHOS protein expression could be due

to a compensatory response to an inhibited function, if any. Unfortunately, it was not possible to test the activity of the complexes in order to have an answer to this question, due to difficulty to get fresh surgical specimens and insufficiency of cryopreserved material. In this thesis there were reported also results on β subunit of ATP synthase expression levels that showed a tendency to increase in LGA* *vs.* LGA in both IHC and immunoblotting, though without any statistical significance different from α subunit whose increase was more marched and significant. In literature there are reports of upregulation of both complex V α and β subunits mRNAs and protein expression, observed by IHC, in blood vessels and cells of glioblastoma with respect to healthy tissues (Xu et al., 2016). Xu and colleagues reported also in low-grade astrocytomas an increase in these two mRNA concluding that these two proteins are not a reliable biomarker to separate LGA to HGA, due to their high expression in both groups. The reason of this upregulation might be the downregulation of miRNAs, which target ATP5A1 and ATP5B mRNAs. In fact, these miRNAs seem to be downregulated in astrocytomas and glioblastoma, also in brain blood vessels. The same miRNAs were shown to be involved in the proliferation and invasion of glioma (Yan et al., 2015). Also in colorectal cancer (Geyik et al., 2014) were found high levels of ATP5B mRNA in accordance with data on GBM presented in Xu study. The discrepancy of the data here presented between α and β subunits protein expression might be due to different translation control mechanisms. In fact, it is known from literature that the expression of β subunit in carcinomas can be downregulated by different mechanism, both by limiting number of mRNA due to the hyper-methylation of ATP5B gene promoter and the regulation of 3' untranslated region (3'UTR), and by reducing mRNA translation by specific mechanisms such as the one exploited by G3BP1 protein (Ortega et al., 2010 – Willers et al., 2010).

Some limits of this part of the study should be underlined, in particular the low number of analysed samples, due to the low incidence of LGA, and the lack of functional studies, due to difficulty of having fresh tissues from patients.

4.3.3. Conclusions

IF1 expression levels increase in LGA with worse prognosis and could be proposed as a biomarker of OS as in HGG and other cancers. Including IF1 among biomarkers to support radio-diagnostic characterisation by indexes of tumor infiltration and resection might be also proposed to assist patient management in the case of LGA, rare tumors with a good prognosis in general, which could nonetheless evolve in anaplastic lesions and are still without an

adjuvant therapy. Moreover, our preliminary data from recently collected samples, still without patients follow-up, showed an upregulation of IF1 expression in low-grade astrocytomas with suspected early anaplastic signs. If confirmed with samples from greater number of patients, these data could be useful in LGA-patients treatment choice.

5. BIBLIOGRAPHY

A.A.V.V. Central Brain Tumor Registry of the United States: CBTRUS Statistical Report: Primary Brain and Central Nervous System Tumors Diagnosed in the United States in 2004- 2007. (http://www.cbtrus.org/2011-NPCR-SEER/WEB-0407-Report-3-3-2011.pdf)

A.A.V.V. MitoMiner 4.0v - A database of mammalian mitochondrial localisation evidence, phenotypes and diseases. 2016 http://mitominer.mrc-mbu.cam.ac.uk/release-4.0/begin.do.

Abadi A, Glover EI, Isfort RJ, Raha S, Safdar A, Yasuda N, Kaczor JJ, Melov S, Hubbard A, Qu X, Phillips SM, Tarnopolsky M. Limb immobilization induces a coordinate down-regulation of mitochondrial and other metabolic pathways in men and women. PLoS One. 2009 Aug 5;4(8):e6518. doi: 10.1371/journal.pone.0006518.

Acheson KJ, Décombaz J, Piguet-Welsch C, Montigon F, Decarli B, Bartholdi I, Fern EB. Energy, protein, and substrate metabolism in simulated microgravity. Am J Physiol. 1995 Aug;269(2 Pt 2):R252-60.

Agnihotri S, Burrell KE, Wolf A, Jalali S, Hawkins C, Rutka JT, Zadeh G. Glioblastoma, a brief review of history, molecular genetics, animal models and novel therapeutic strategies. Arch Immunol Ther Exp (Warsz). 2013 Feb;61(1):25-41. doi: 10.1007/s00005-012-0203-0.

Ahn BH, Kim HS, Song S, Lee IH, Liu J, Vassilopoulos A, Deng CX, Finkel T. A role for the mitochondrial deacetylase Sirt3 in regulating energy homeostasis. Proc Natl Acad Sci U S A. 2008 Sep 23;105(38):14447-52. doi: 10.1073/pnas.0803790105. Epub 2008 Sep 15.

Alibegovic AC, Højbjerre L, Sonne MP, van Hall G, Alsted TJ, Kiens B, Stallknecht B, Dela F, Vaag A. Increased rate of whole body lipolysis before and after 9 days of bed rest in healthy young men born with low birth weight. Am J Physiol Endocrinol Metab. 2010 Mar;298(3):E555-64. doi: 10.1152/ajpendo.00223.2009. Epub 2009 Dec 8.

Alibegovic AC, Sonne MP, Højbjerre L, Bork-Jensen J, Jacobsen S, Nilsson E, Faerch K, Hiscock N, Mortensen B, Friedrichsen M, Stallknecht B, Dela F, Vaag A. Insulin resistance induced by physical inactivity is associated with multiple transcriptional changes in skeletal muscle in young men. Am J Physiol Endocrinol Metab. 2010 Nov;299(5):E752-63. doi: 10.1152/ajpendo.00590.2009. Epub 2010 Aug 24.

Asmann YW, Nair KS, Lanza IR, Short DK, Short KR, Bigelow ML, Joyner MJ. Skeletal Muscle Transcript Profiles in Trained or Sedentary Young and Old Subjects. 2007. GEO DataSet GSE9103

Austin S, St-Pierre J. PGC-1α and mitochondrial metabolism--emerging concepts and relevance in ageing and neurodegenerative disorders. J Cell Sci 2012, 125: 4963-4971.

Azarias G, Perreten H, Lengacher S, Poburko D, Demaurex N, Magistretti J, Chatton J. Glutamate transport decreases mitochondrial pH and modulates oxidative metabolism in astrocytes. J Neurosci 2011, 31: 3550-3559.

Babot M, Birch A, Labarbuta P, Galkin A. Characterisation of the active/de-active transition of mitochondrial complex I. Biochim Biophys Acta. 2014 Jul;1837(7):1083-92. doi: 10.1016/j.bbabio.2014.02.018. Epub 2014 Feb 22.

Balss J, Meyer J, Mueller W, Korshunov A, Hartmann C, von Deimling A. Analysis of the IDH1 codon 132 mutation in brain tumors. Acta Neuropathol. 2008; 116:597–602.

Bao J, Scott I, Lu Z, Pang L, Dimond CC, Gius D, Sack MN. SIRT3 is regulated by nutrient excess and modulates hepatic susceptibility to lipotoxicity. Free Radic Biol Med. 2010 Oct 15;49(7):1230-7. doi: 10.1016/j.freeradbiomed.2010.07.009. Epub 2010 Jul 18.

Barnes AP, Lilley BN, Pan YA, Plummer LJ, Powell AW, Raines AN, Sanes JR, Polleux F. LKB1 and SAD kinases define a pathway required for the polarization of cortical neurons. Cell 2007, 129: 549-63.

Barrett T, Troup DB, Wilhite SE, Ledoux P, Evangelista C, et al. NCBI GEO: archive for functional genomics data sets—10 years on. Nucleic Acids Res. 2011 Jan;39:D1005–1010.

Berchtold MW, Brinkmeier H, Müntener M. Calcium ion in skeletal muscle: its crucial role for muscle function, plasticity, and disease. Physiol Rev. 2000 Jul;80(3):1215-65.

Berg JM, Tymoczko JL, Stryer L, Biochimica 6th ed., Zanichelli, Bologna. 2008

Bergouignan A, Rudwill F, Simon C, Blanc S. Physical inactivity as the culprit of metabolic inflexibility: evidence from bed-rest studies. J Appl Physiol (1985). 2011 Oct;111(4):1201-10. doi: 10.1152/japplphysiol.00698.2011. Epub 2011 Aug 11.

Bergouignan A, Trudel G, Simon C, Chopard A, Schoeller DA, Momken I, Votruba SB, Desage M, Burdge GC, Gauquelin-Koch G, Normand S, Blanc S. Physical inactivity differentially alters dietary oleate and palmitate trafficking. Diabetes. 2009 Feb;58(2):367-76. doi: 10.2337/db08-0263. Epub 2008 Nov 18.

Bethke L, Webb E, Murray A, Schoemaker M, Johansen C, Christensen HC, et al: Comprehensive analysis of the role of DNA repair gene polymorphisms on risk of glioma. Hum Mol Genet 2008; 17:800–805.

Bonnet S, Archer SL, Allalunis-Turner J et al., A mitochondria-K+ channel axis is suppressed in cancer and its normalization promotes apoptosis and inhibits cancer growth. Cancer Cell. 2007 11(1):37–51.

Boushel R, Ara I, Gnaiger E, Helge JW, Gonzalez-Alonso J, Munck-Andersen T, Sondergaard H, Damsgaard R, van Hall G, Saltin B, Calbet JA. Low-intensity training increases peak arm V'O2 by enhancing both diffusive and convective O2 delivery. Acta Physiol. (Oxf.) 2014; 211: 122-134.

Bowling N, Walsh RA, Song G, Estridge T, Sandusky GE, Fouts RL et al, Increased protein kinase C activity and expression of Ca2+-sensitive isoforms in the failing human heart. Circulation. 1999;99:384–391.

Boyer PD. The binding change mechanism for ATP synthase - some probabilities and possibilities. Biochim. Biophys. Acta 1993 1140 215–250.

Brault JJ, Jespersen JG, Goldberg AL. Peroxisome proliferator-activated receptor gamma coactivator 1alpha or 1beta overexpression inhibits muscle protein degradation, induction of ubiquitin ligases, and disuse atrophy. Journal of Biological Chemistry. 2010;285:19460–19471.

Braunwald E. Heart failure. JACC: Heart Failure 1: 1-20, 2013.

Bravo C, Minauro-Sanmiguel F, Morales-Ríos E, Rodríguez-Zavala JS, García JJ. Overexpression of the inhibitor protein IF(1) in AS-30D hepatoma produces a higher association with mitochondrial F(1)F(0) ATP synthase compared to normal rat liver: functional and cross-linking studies. J Bioenerg Biomembr 2004; 36(3):257-64.

Brenmoehl J, Hoeflich A. Dual control of mitochondrial biogenesis by sirtuin 1 and sirtuin 3. Mitochondrion. 2013 Nov;13(6):755-61. doi: 10.1016/j.mito.2013.04.002. Epub 2013 Apr 11.

Brierley EJ, Johnson MA, James OF, Turnbull DM. Effects of physical activity and age on mitochondrial function. QJM. 1996 Apr;89(4):251-8

Brocca L, Cannavino J, Coletto L, Biolo G, Sandri M, Bottinelli R, Pellegrino MA. The time course of the adaptations of human muscle proteome to bed rest and the underlying mechanisms. J Physiol. 2012 Oct 15;590(Pt 20):5211-30. doi: 10.1113/jphysiol.2012.240267. Epub 2012 Jul 30.

Brocca L, Pellegrino MA, Desaphy JF, Pierno S, Camerino DC, Bottinelli R. Is oxidative stress a cause or consequence of disuse muscle atrophy in mice? A proteomic approach in hindlimb-unloaded mice. Exp Physiol. 2010 Feb;95(2):331-50. doi: 10.1113/expphysiol.2009.050245. Epub 2009 Oct 9.

Brower RG. Consequences of bed rest. Crit Care Med. 2009 Oct;37(10 Suppl):S422-8. doi: 10.1097/CCM.0b013e3181b6e30a.

Bua E, Johnson J, Herbst A, Delong B, McKenzie D, Salamat S, Aiken JM (2006) Mitochondrial DNA–deletion mutations accumulate intracellularly to detrimental levels in aged human skeletal muscle fibers. Am. J. Hum. Genet. 79, 469–480.

Cabezon E, Butler PJG, Runswick MJ, Walker JE. Modulation of the Oligomerization State of the Bovine F1-ATPase Inhibitor Protein, IF1, by pH. J. Biol. Chem. 2000; 275:25460-25464.

Calvo SE, Mootha VK. The mitochondrial proteome and human disease. Annu Rev Genomics Hum Genet. 2010;11:25-44. doi: 10.1146/annurev-genom-082509-141720.

Cannavino J, Brocca L, Sandri M, Grassi B, Bottinelli R, Pellegrino MA. The role of alterations in mitochondrial dynamics and PGC-1α over-expression in fast muscle atrophy following hindlimb unloading. J Physiol. 2015 Apr 15;593(8):1981-95. doi: 10.1113/jphysiol.2014.286740. Epub 2015 Feb 4.

Cantó C, Auwerx J. PGC-1alpha, SIRT1 and AMPK, an energy sensing network that controls energy expenditure. Curr Opin Lipidol. 2009 Apr;20(2):98-105. doi: 10.1097/MOL.0b013e328328d0a4.

Cantó C, Gerhart-Hines Z, Feige JN, Lagouge M, Noriega L, Milne JC, Elliott PJ, Puigserver P, Auwerx J. AMPK regulates energy expenditure by modulating NAD+ metabolism and SIRT1 activity. Nature 2009, 458: 1056-1060.

Carter HN, Chen CC, Hood DA. Mitochondria, muscle health, and exercise with advancing age. Physiology (Bethesda). 2015 May;30(3):208-23. doi: 10.1152/physiol.00039.2014.

Chan MC, Arany Z. The many roles of PGC-1a in muscle – recent developments. Metabolism 2014, 63: 441-451.

Chen H, Vermulst M, Wang YE, Chomyn A, Prolla TA, McCaffery JM, Chan DC. Mitochondrial fusion is required for mtDNA stability in skeletal muscle and tolerance of mtDNA mutations. Cell. 2010 Apr 16; 141(2):280-9.

Chen Y, Fu LL, Wen X, Wang XY, Liu J, Cheng Y, Huang J. Sirtuin-3 (SIRT3), a therapeutic target with oncogenic and tumor-suppressive function in cancer. Cell Death Dis 2014, 5: e1047, doi: 10.1038/cddis.2014.14.

Chirinos JA, Zanami P. The nitrate-nitrite-NO pathway and its implications for heart failure and preserved ejection fraction. Curr. Heart Fail. Rep. 2016, doi: 10.1007/s11897-016-0277-9.

Civitarese AE, Carling S, Heilbronn LK, Hulver MH, Ukropcova B, Deutsch WA, Smith SR, Ravussin E; CALERIE Pennington Team. Calorie restriction increases muscle mitochondrial biogenesis in healthy humans. PLoS Med. 2007 Mar;4(3):e76.

Combes A, Dekerle J, Webborn N, Watt P, Bougault V, Daussin FN. Exercise-induced metabolic fluctuations influence AMPK, p38-MAPK and CaMKII phosphorylation in human skeletal muscle. Physiol Rep. 2015 Sep;3(9). pii: e12462. doi: 10.14814/phy2.12462.

Cuezva JM, Ortega AD, Willers I, Sánchez-Cenizo L, Aldea M, Sánchez-Aragó M. The tumor suppressor function of mitochondria: translation into the clinics. Biochim Biophys Acta 2009, 1792: 1145-1158.

Czarnowska E, Bierla JB, Toczek M, Tyrankiewicz U, Pajak B, Domal-Kwiatkowska D, Ratajska A, Smolenski RT, Mende U, Chlopicki R. Narrow time window of metabolic changes associated with transition to overt heart failure in Tgaq*44 mice. Pharmacol. Reports 2016; 68: 707-714.

Daga A, Bottino C, Castriconi R, Gangemi R, Ferrini S. New perspectives in glioma immunotherapy. Curr Pharm Des. 2011. 17: 2439-2467.

Dai M, Wang P, Boyd AD, Kostov G, Athey B, et al. Evolving gene/ transcript definitions significantly alter the interpretation of GeneChip data. Nucleic Acids Res. 2005 33:e175.

Däpp C, Schmutz S, Hoppeler H, Flück M. Transcriptional reprogramming and ultrastructure during atrophy and recovery of mouse soleus muscle. Physiol Genomics. 2004 Dec 15;20(1):97-107. Epub 2004 Oct 12.

de Jonge HW, Dekkers DH, Houtsmuller AB, Sharma HS, Lamers JM. Differential signaling and hypertrophic responses in cyclically stretched vs endothelin-1 stimulated neonatal rat cardiomyocytes. Cell Biochem. Biophys. 2007;47:21–32.

DeFronzo RA. Lilly lecture 1987. The triumvirate: beta-cell, muscle, liver. A collusion responsible for NIDDM. Diabetes. 1988; 37: 667–687.

Dirks ML, Wall BT, Nilwik R, Weerts DH, Verdijk LB, van Loon LJ. Skeletal muscle disuse atrophy is not attenuated by dietary protein supplementation in healthy older men. J Nutr. 2014 Aug;144(8):1196-203. doi: 10.3945/jn.114.194217. Epub 2014 Jun 11.

Drexler H, Riede U, Munzel T, Konig H, Funke E, et al. Alterations of skeletal muscle in chronic heart failure. Circulation. 1992;85:1751–1759.

Dröse S, Stepanova A, Galkin A. Ischemic A/D transition of mitochondrial complex I and its role in ROS generation. Biochim Biophys Acta. 2016 Jul;1857(7):946-57. doi: 10.1016/j.bbabio.2015.12.013. Epub 2016 Jan 9.

Düvel K, Yecies JL, Menon S, Raman P, Lipovsky AI, Souza AL, Triantafellow E, Ma Q, Gorski R, Cleaver S, Vander Heiden MG, MacKeigan JP, Finan PM, Clish CB, Murphy LO, Manning BD. Activation of a metabolic gene regulatory network downstream of mTOR complex 1. Mol Cell. 2010 Jul 30;39(2):171-83. doi: 10.1016/j.molcel.2010.06.022.

Edes IF, Tóth A, Csányi G, Lomnicka M, Chłopicki S, Edes I, Papp Z. Late-stage alterations in myofibrillar contractile function in a transgenic mouse model of dilated cardiomyopathy (Tgalphaq*44). J Mol Cell Cardiol. 2008 Sep;45(3):363-72. doi: 10.1016/j.yjmcc.2008.07.001. Epub 2008 Jul 12.

Ehrenborg E, Krook A. Regulation of skeletal muscle physiology and metabolism by peroxisome proliferator-activated receptor delta. Pharmacol Rev. 2009 Sep;61(3):373-93. doi: 10.1124/pr.109.001560.

Eisner V, Lenaers G, Hajnóczky G. Mitochondrial fusion is frequent in skeletal muscle and supports excitation-contraction coupling. J. Cell Biol. 2014; 205, 179–195. 10.1083/jcb.201312066

Elas M, Bielanska J, Pustelny K, Plonka PM, Drelicharz L, Skorka T, Tyrankiewicz U, Wozniak M, Heinze-Paluchowska S, Walski M, Wojnar L, Fortin D, Ventura-Clapier R, Chlopicki S. Detection of mitochondrial

dysfunction by EPR technique in mouse model of dilated cardiomyopathy. Free Radic Biol Med. 2008 Aug 1;45(3):321-8. doi: 10.1016/j.freeradbiomed.2008.04.016. Epub 2008 Apr 20.

Esposito F, Mathieu-Costello O, Shabetai R, Wagner PD, Richardson RS. Limited maximal exercise capacity in patients with heart failure. Partitioning the contributors. J. Am. Coll. Cardiol. 2010; 55: 1945-1954.

Esposito F, Reese V, Shabetai R, Wagner PD, Richardson RS. Isolated quadriceps training increases maximal exercise capacity in chronic heart failure. The role of skeletal muscle convective and diffusive oxygen transport. J. Am. Coll. Cardiol. 2011; 58: 1353-1362.

Fan W, Wang W, Mao X, Chu S, Feng J, Xiao D, Zhou J, Fan S. Elevated levels of p-Mnk1, p-eIF4E and p-p70S6K proteins are associated with tumor recurrence and poor prognosis in astrocytomas. J Neurooncol. 2016 Nov 29.

Feichtinger RG, Weis S, Johannes AM, Zimmermann F, Geilberger R, Sperl W, Kofler B. Alterations of oxidative phosphorylation complexes in astrocytomas. Glia 2014, 62: 514–525.

Finck BN, Kelly DP. PGC-1 coactivators: inducible regulators of energy metabolism in health and disease. J Clin Invest 2006; 116:615–622.

Finley LW, Carracedo A, Lee J, Souza A, Egia A, Zhang J, Teruya-Feldstein J, Moreira PI, Cardoso SM, Clish CB, Pandolfi PP, Haigis MC. SIRT3 opposes reprogramming of cancer cell metabolism through HIF1α destabilization. Cancer Cell. 2011 Mar 8;19(3):416-28. doi: 10.1016/j.ccr.2011.02.014.

Finley LW, Haas W, Desquiret-Dumas V, Wallace DC, Procaccio V, Gygi SP, Haigis MC. Succinate dehydrogenase is a direct target of sirtuin 3 deacetylase activity. PLoS One. 2011;6(8):e23295. doi: 10.1371/journal.pone.0023295. Epub 2011 Aug 17.

Fitts RH, Riley DR, Widrick JJ. Physiology of a microgravity environment invited review: microgravity and skeletal muscle. J Appl Physiol (1985). 2000 Aug;89(2):823-39.

Flück M. Regulation of Protein Synthesis in Skeletal Muscle. Dtsch Z Sportmed. 2012; 63: 75-80. doi: 10.5960/dzsm.2012.001

Formentini L, Pereira MP, Sánchez-Cenizo L, Santacatterina F, Lucas JJ, Navarro C, Martínez-Serrano A, Cuezva JM. In vivo inhibition of the mitochondrial H+-ATP synthase in neurons promotes metabolic preconditioning. EMBO J. 2014 Apr 1;33(7):762-78. doi: 10.1002/embj.201386392.

Formentini L, Sánchez-Aragó M, Sánchez-Cenizo L, Cuezva JM. The mitochondrial ATPase inhibitory factor 1 triggers a ROS-mediated retrograde prosurvival and proliferative response. Mol Cell. 2012 Mar 30;45(6):731-42. doi: 10.1016/j.molcel.2012.01.008

Fraysse B, Desaphy JF, Pierno S, De Luca A, Liantonio A, Mitolo CI, Camerino DC. Decrease in resting calcium and calcium entry associated with slow-to-fast transition in unloaded rat soleus muscle. FASEB J. 2003 Oct;17(13):1916-8. Epub 2003 Aug 15.

Frey TG, Renken CW, Perkins GA. Insight into mitochondrial structure and function from electron tomography. Biochim. Biophis. Acta. 2002; 1555:196-203.

Fulda S, Exploiting mitochondrial apoptosis for the treatment of cancer. Mitochondrion. 2010 10(6):598–603.

Furnari FB, Fenton T, Bachoo RM, Mukasa A, Stommel JM, Stegh A, Hahn WC, Ligon KL, Louis DN, Brennan C, Chin L, DePinho RA, Cavenee WK. Malignant astrocytic glioma: genetics, biology, and paths to treatment. Genes Dev 2007, 21: 2683-2710.

Galkin A, Abramov AY, Frakich N, Duchen MR, Moncada S. Lack of oxygen deactivates mitochondrial complex I: implications for ischemic injury? J Biol Chem 284: 36055–36061, 2009.

Galkin A, Meyer B, Wittig I, Karas M, Schägger H, Vinogradov A, Brandt U, Identification of the mitochondrial ND3 subunit as a structural component involved in the active/deactive enzyme transition of respiratory complex I. J Biol Chem. 2008 Jul 25;283(30):20907-13. doi: 10.1074/jbc.M803190200. Epub 2008 May 23.

Gao YQ, Yang W, Karplus M. A structure-based model for the synthesis and hydrolysis of ATP by F1-ATPase. Cell. 2005 Oct 21;123(2):195-205.

Gao YX, Chen L, Hu XG, Wu HB, Cui YH, Zhang X, Wang Y, Liu XD, Bian XW. ATPase inhibitory factor 1 expression is an independent prognostic factor in non-small cell lung cancer. Am J Cancer Res. 2016 May 1;6(5):1141-8. eCollection 2016.

García-Bermúdez J, Cuezva JM. The ATPase Inhibitory Factor 1 (IF1): A master regulator of energy metabolism and of cell survival. Biochim Biophys Acta. 2016; 1857(8):1167-82.

Gautier L, Cope L, Bolstad BM, Irizarry RA. affy--analysis of Affymetrix GeneChip data at the probe level. Bioinformatics. 2004 Feb 12;20(3):307-15.

Geng T, Li P, Okutsu M, Yin X, Kwek J, Zhang M, Yan Z. PGC-1alpha plays a functional role in exercise-induced mitochondrial biogenesis and angiogenesis but not fiber-type transformation in mouse skeletal muscle. Am J Physiol Cell Physiol. 2010 Mar;298(3):C572-9. doi: 10.1152/ajpcell.00481.2009. Epub 2009 Dec 23.

George J, Ahmad N. Mitochondrial sirtuins in cancer: emerging roles and therapeutic potential. Cancer Re2 2016, 76: 2500–2506.

Geyik E, Igci YZ, Pala E, Suner A, Borazan E, Bozgeyik I, Bayraktar E, Bayraktar R, Ergun S, Cakmak EA, Gokalp A, Arslan A. Investigation of the association between ATP2B4 and ATP5B genes with colorectal cancer. Gene. 2014 May 1;540(2):178-82. doi: 10.1016/j.gene.2014.02.050.

Gibbons C, Montgomery MG, Leslie AG, Walker JE, The structure of the central stalk in bovine F(1)-ATPase at 2.4 a resolution. Nat Struct Biol. 2000 7(11):1055-61.

Giralt A, Villarroya F. SIRT3, a pivotal actor in mitochondrial functions: metabolism, cell death and aging. Biochem J 2012; 444: 1-10.

Giresi PG, Stevenson EJ, Theilhaber J, Koncarevic A, Parkington J, Fielding RA, Kandarian SC. Identification of a molecular signature of sarcopenia. Physiol Genomics. 2005 Apr 14; 21(2):253-63.

Gledhill JR, Walker JE. Inhibitors of the catalytic domain of mitochondrial ATP synthase. Biochem Soc Trans. 2006; 34:989–992.

Gnaiger E, Capacity of oxidative phosphorylation in human skeletal muscle: new perspectives of mitochondrial physiology. Int J Biochem Cell Biol. 2009 Oct;41(10):1837-45. doi: 10.1016/j.biocel.2009.03.013. Epub 2009 Apr 2.

Gnaiger E. MitoPathways at the Q-junction: mouse skeletal muscle fibres. Mitochondrial Physiology Network 12.01(02): 1-3 (2014). O2k-Workshop Report, IOC39, Schroecken, Austria.

Go AS, Mozaffarian D, Roger VL, et al. Heart disease and stroke statistics--2013 update: a report from the American Heart Association. Circulation. 2013 Jan 1;127(1):e6-e245. doi: 10.1161/CIR.0b013e31828124ad.

Gram M, Vigelsø A, Yokota T, Hansen CN, Helge JW, Hey-Mogensen M, Dela F. Two weeks of one-leg immobilization decreases skeletal muscle respiratory capacity equally in young and elderly men. Exp Gerontol. 2014 Oct;58:269-78. doi: 10.1016/j.exger.2014.08.013. Epub 2014 Sep 2.

Grassi B, Rossiter HB, Zoladz JA. Skeletal muscle fatigue and decreased efficiency: two sides of the same coin? Exerc. Sport Sci Rev. 2015; 43: 75-83.

Green DW, Grover GJ. The IF(1) inhibitor protein of the mitochondrial F(1)F(0)-ATPase. Biochim Biophys Acta. 2000 May 31;1458(2-3):343-55.

Grier JT, Batchelor T. Low-grade gliomas in adults. Oncologist. 2006 Jun;11(6):681-93.

Griguer CE, Oliva CR, Gillespie GYJ. Glucose metabolism heterogeneity in human and mouse malignant glioma cell lines. Neurooncol 2005, 74: 123-133.

Grune T, Merker K, Sandig G, Davies KJ. Selective degradation of oxidatively modified protein substrates by the proteasome. Biochem. Biophys. Res. Commun. 2003; 305, 709–718.

Hagland H, Nikolaisen J, Hodneland LI, Gjertsen BT, Bruserud Ø, Tronstad KJ. Targeting mitochondria in the treatment of human cancer: a coordinated attack against cancer cell energy metabolism and signalling. Expert Opinion on Therapeutic Targets. 2007 11 (8):1055–1069.

Hardie DG, Ross FA, Hawley SA. AMPK: a nutrient and energy sensor that maintains energy homeostasis. Nat Rev Mol Cell Biol. 2012 Mar 22;13(4):251-62. doi: 10.1038/nrm3311.

Hardie DG, Sakamoto K. AMPK: a key sensor of fuel and energy status in skeletal muscle. Physiology (Bethesda). 2006 Feb;21:48-60.

Hardie DG. AMP-activated protein kinase: an energy sensor that regulates all aspects of cell function. Genes Dev 2011, 25: 1895-908.

Hartmann C, Hentschel B, Tatagiba M, Schramm J, Schnell O, Seidel C, Stein R, Reifenberger G, Pietsch T, von Deimling A, Loeffler M, Weller M; German Glioma Network. Molecular markers in low-grade gliomas: predictive or prognostic? Clin Cancer Res. 2011 Jul 1;17(13):4588-99. doi: 10.1158/1078-0432.CCR-10-3194. Epub 2011 May 10.

Haykowski MJ, Tomczak CR, Scott JM, Paterson DI, Kitzman DW. Determinants of exercise tolerance in patients with heart failure and reduced or preserved ejection fraction. J. Appl. Physiol. 2015; 119: 739-744.

Hirai DM, Copp SW, Holdsworth CT, Ferguson SK, McCullough DJ, Behnke BJ, Musch TI, Poole DC. Skeletal muscle microvascular oxygenation dynamics in heart failure: exercise training and nitric oxide-mediated function. Am. J. Physiol. Heart Circ. Physiol. 2014; 306: H690-698.

Hirai DM, Musch TI, Poole DC. Exercise training in chronic heart failure: improving skeletal muscle O2 transport and utilization. Am. J. Physiol. Heart Circ. Physiol. 2015; 309: H1419-H1439.

Hock MB, Kralli A. Transcriptional control of mitochondrial biogenesis and function. Annu Rev Physiol. 2009;71:177-203. doi: 10.1146/annurev.physiol.010908.163119.

Hokari F, Kawasaki E, Sakai A, Koshinaka K, Sakuma K, Kawanaka K. Muscle contractile activity regulates Sirt3 protein expression in rat skeletal muscles. J Appl Physiol (1985). 2010 Aug;109(2):332-40. doi: 10.1152/japplphysiol.00335.2009. Epub 2010 Apr 22.

Housley MP, Udeshi ND, Rodgers JT, Shabanowitz J, Puigserver P, Hunt DF, Hart GW. A PGC-1alpha-O-GlcNAc transferase complex regulates FoxO transcription factor activity in response to glucose. J Biol Chem. 2009 Feb 20;284(8):5148-57. doi: 10.1074/jbc.M808890200.

Hu J, Locasale JW, Bielas JH, O'Sullivan J, Sheahan K, Cantley LC, Vander Heiden MG, Vitkup D. Heterogeneity of tumor-induced gene expression changes in the human metabolic network. Nature Biotechnology 2013.

Huang L, Wolska BM, Montgomery DE, Burkart EM, Buttrick, PM, Solaro RJ. Increased contractility and altered Ca2+ transients of mouse heart myocytes conditionally expressing PKCbeta. Am. J. Physiol. Cell Physiol. 2001;280:C1114–C1120.

Hughes VA, Frontera WR, Wood M, Evans WJ, Dallal GE, Roubenoff R, Fiatarone Singh MA. Longitudinal muscle strength changes in older adults: influence of muscle mass, physical activity, and health. J Gerontol A Biol Sci Med Sci. 2001 May;56(5):B209-17.

Huss JM, Kelly DP. Mitochondrial energy metabolism in heart failure: a question of balance. J. Clin. Invest. 2005; 115:547–555.

Hvid L, Aagaard P, Justesen L, Bayer ML, Andersen JL, Ørtenblad N, Kjaer M, Suetta C. Effects of aging on muscle mechanical function and muscle fiber morphology during short-term immobilization and subsequent retraining. J Appl Physiol (1985). 2010 Dec;109(6):1628-34. doi: 10.1152/japplphysiol.00637.2010. Epub 2010 Sep 23.

Ide T, Tsutsui H, Kinugawa S, Utsumi H, Kang D, Hattori N, Uchida K, Arimura K, Egashira K, Takeshita A. Mitochondrial electron transport complex I is a potential source of oxygen free radicals in the failing myocardium. Circ Res 85: 357–363, 1999.

Imamura K, Ogura T, Kishimoto A, Kaminishi M, Esumi H. Cell cycle regulation via p53 phosphorylation by a 5'-AMP activated protein kinase activator, 5-aminoimidazole- 4-carboxamide-1-beta-D-ribofuranoside, in a human hepatocellular carcinoma cell line. Biochem Biophys Res Commun, 2001, 287: 562-567.

Ingalls CP, Warren GL, Armstrong RB. Intracellular Ca2+ transients in mouse soleus muscle after hindlimb unloading and reloading. J Appl Physiol (1985). 1999 Jul;87(1):386-90.

Ino Y, Zlatescu MC, Sasaki H, Macdonald DR, Stemmer-Rachamimov AO, Jhung S, et al: Long survival and therapeutic responses in patients with histologically disparate high-grade gliomas demonstrating chromosome 1p loss. J Neurosurg. 2000; 92:983–990.

Irizarry RA, Hobbs B, Collin F, Beazer-Barclay YD, Antonellis KJ, Scherf U, Speed TP. Exploration, normalization, and summaries of high density oligonucleotide array probe level data. Biostatistics. 2003 Apr;4(2):249-64.

Irrcher I, Adhihetty PJ, Joseph AM, Ljubicic V, Hood DA. Regulation of mitochondrial biogenesis in muscle by endurance exercise. Sports Med. 2003;33(11):783-93.

Irving BA, Lanza IR, Henderson GC, Rao RR, Spiegelman BM, Nair KS. Combined training enhances skeletal muscle mitochondrial oxidative capacity independent of age. J Clin Endocrinol Metab. 2015 Apr;100(4):1654-63. doi: 10.1210/jc.2014-3081. Epub 2015 Jan 19.

Ius T, Isola M, Budai R, Pauletto G, Tomasino B, Fadiga L, Skrap M. Low-grade glioma surgery in eloquent areas: volumetric analysis of extent of resection and its impact on overall survival. A single-institution experience in 190 patients: clinical article. J Neurosurg. 2012 Dec;117(6):1039-52. doi: 10.3171/2012.8.JNS12393. Epub 2012 Oct 5.

Iwadate Y, Matsutani T, Hirono S, Ikegami S, Shinozaki N, Saeki N. IDH1 mutation is prognostic for diffuse astrocytoma but not low-grade oligodendrogliomas in patients not treated with early radiotherapy. J Neurooncol. 2015 Sep;124(3):493-500. doi: 10.1007/s11060-015-1863-5. Epub 2015 Aug 5.

Jacobs RA, Diaz V, Meinild AK, Gassmann M, Lundby C. The C75Bl/6 mouse serves as a suitable model of human skeletal muscle mitochondrial function. Exp. Physiol. 2013; 98: 908-921.

Jäger S, Handschin C, St-Pierre J, Spiegelman BM. AMP-activated protein kinase (AMPK) action in skeletal muscle via direct phosphorylation of PGC-1alpha. Proc Natl Acad Sci USA 2007, 104: 12017-12022.

Jing E, Emanuelli B, Hirschey MD, Boucher J, Lee KY, Lombard D, Verdin EM, Kahn CR. Sirtuin-3 (Sirt3) regulates skeletal muscle metabolism and insulin signaling via altered mitochondrial oxidation and reactive oxygen species production. Proc Natl Acad Sci U S A. 2011 Aug 30;108(35):14608-13. doi: 10.1073/pnas.1111308108. Epub 2011 Aug 22.

Jing E, O'Neill BT, Rardin MJ, Kleinridders A, Ilkeyeva OR, Ussar S, Bain JR, Lee KY, Verdin EM, Newgard CB, Gibson BW, Kahn CR. Sirt3 regulates metabolic flexibility of skeletal muscle through reversible enzymatic deacetylation. Diabetes. 2013 Oct;62(10):3404-17. doi: 10.2337/db12-1650. Epub 2013 Jul 8.

Jose C, Bellance N, Rossignol R. Choosing between glycolysis and oxidative phosphorylation: a tumor's dilemma? Biochim Biophys Acta. 2011 Jun;1807:552.

Kim J, Han J, Jang Y, Kim SJ, Lee MJ, Ryu MJ, Kweon GR, Heo JY. High-capacity glycolytic and mitochondrial oxidative metabolisms mediate the growth ability of glioblastoma. Int J Oncol 2015, 47: 1009-1016.

Kincaid B, Bossy-Wetzel E. Forever young: SIRT3 a shield against mitochondrial meltdown, aging, and neurodegeneration. Front Aging Neurosci. 2013 Sep 6;5:48. doi: 10.3389/fnagi.2013.00048.

Koltai E, Hart N, Taylor AW, Goto S, Ngo JK, Davies KJ, Radak Z. Age-associated declines in mitochondrial biogenesis and protein quality control factors are minimized by exercise training. Am J Physiol Regul Integr Comp Physiol. 2012 Jul 15;303(2):R127-34. doi: 10.1152/ajpregu.00337.2011. Epub 2012 May 9.

Kong X, Wang R, Xue Y, Liu X, Zhang H, Chen Y, Fang F, Chang Y. Sirtuin 3, a new target of PGC-1alpha, plays an important role in the suppression of ROS and mitochondrial biogenesis. PLoS One. 2010 Jul 22;5(7):e11707. doi: 10.1371/journal.pone.0011707.

Koppenol WH, Bounds PL, Dang CV. Otto Warburg's contributions to current concepts of cancer metabolism. Nat Rev Cancer. 2011 May;11(5):325-37. doi: 10.1038/nrc3038. Review. Erratum in: Nat Rev Cancer. 2011 Aug;11(8):618.

Kramer DM, Roberts AG, Muller F, Cape J, Bowman MK. Q-cycle bypass reactions at the Q site of cyochrome bc1 (and related) complexes. Methods Enzymol. 2004; 382:21-45.

Kuhlbrandt W. Structure and function of mitochondrial membrane protein complexes. BMC Biology. 2015;1-11.

Kuznetsov AV, Kunz WS, Saks V, Usson Y, Mazat JP, Letellier T, Gellerich FN, Margreiter R. Cryopreservation of mitochondria and mitochondrial function in cardiac and skeletal muscle fibers. Anal Biochem 319: 296–303, 2003.

Kuznetsov AV, Schneeberger S, Seiler R, Brandacher G, Mark W, Steurer W, Saks V, Usson Y, Margreiter R, Gnaiger E. Mitochondrial defects and heterogeneous cytochrome c release after cardiac cold ischemia and reperfusion. Am J Physiol Heart Circ Physiol 286: H1633–H1641, 2004.

Laemmli UK. Cleavage of structural proteins during the assembly of the head of bacteriophage T4. Nature. 1970 Aug 15;227(5259):680-5.

Lagouge M, Argmann C, Gerhart-Hines Z et al., Resveratrol improves mitochondrial function and protects against metabolic disease by activating SIRT1 and PGC-1α. Cell. 2006 127 (6):1109–1122.

Lanza IR, Short DK, Short KR, Raghavakaimal S, Basu R, Joyner MJ, McConnell JP, Nair KS. Endurance exercise as a countermeasure of aging. Diabetes 2008; 57: 2933–2942. doi: 10.2337/db08-0349. Epub 2008 Aug 20.

Lanza IR, Sreekumaran Nair K. Functional Assessment of Isolated Mitochondria In Vitro. Methods Enzymol. 2009; 457: 349–372. doi: 10.1016/S0076-6879(09)05020-4

Larsen S, Nielsen J, Hansen CN, Nielsen LB, Wibrand F, Stride N, Schroder HD, Boushel R, Helge JW, Dela F, Hey-Morgensen M. Biomarkers of mitochondrial content in skeletal muscle of healthy young human subjects. J. Physiol. 2012; 590: 3349-3360.

LeBleu VS, O'Connell JT, Gonzalez Herrera KN, Wikman H, Pantel K, Haigis MC, de Carvalho FM, Damascena A, Domingos Chinen LT, Rocha RM, Asara JM, Kalluri R. PGC-1α mediates mitochondrial biogenesis and oxidative phosphorylation in cancer cells to promote metastasis. Nat Cell Biol. 2014 Oct;16(10):992-1003, 1-15. doi: 10.1038/ncb3039. Erratum in: Nat Cell Biol. 2014 Nov;16(11):1125.

Lenaz G, Baracca A, Fato R, Genova ML, Solaini G. Mitochondrial Complex I: structure, function, and implications in neurodegeneration. Ital J Biochem. 2006; 55:232-53.

Liang BC, Grootveld M.The importance of mitochondria in the tumourigenic phenotype: Gliomas as the paradigm (Review). International Journal of Molecular Medicine 2011; 27: 159-171.

Lin J, Wu H, Tarr PT, Zhang CY, Wu Z, Boss O, Michael LF, Puigserver P, E, Olson EN, Lowell BB, Bassel-Duby R, Spiegelman BM. Transcriptional co-activator PGC-1a drives the formation of slow-twich muscle fibers. Nature 418: 797-801, 2002.

Lin L, Chen K, Abdel Khalek W, Ward JL 3rd, Yang H, Chabi B, Wrutniak-Cabello C, Tong Q. Regulation of skeletal muscle oxidative capacity and muscle mass by SIRT3. PLoS One. 2014 Jan 15;9(1):e85636. doi: 10.1371/journal.pone.0085636. eCollection 2014.

Lippe G, Sorgato MC, Harris DA. Kinetics of the release of the mitochondrial inhibitor protein. Correlation with synthesis and hydrolysis of ATP. Biochim. Biophys. Acta 933 1-11. (1988a)

Lippe G, Sorgato MC, Harris DA. The binding and release of the inhibitor protein are governed independently by ATP and membrane potential in ox-heart submitochondrial vesicles. Biochim. Biophys. Acta 933 12-21. (1988b)

Lombard DB, Alt FW, Cheng HL, Bunkenborg J, Streeper RS, Mostoslavsky R, Kim J, Yancopoulos G, Valenzuela D, Murphy A, Yang Y, Chen Y, Hirschey MD, Bronson RT, Haigis M, Guarente LP, Farese RV Jr, Weissman S, Verdin E, Schwer B. Mammalian Sir2 homolog SIRT3 regulates global mitochondrial lysine acetylation. Mol Cell Biol. 2007 Dec;27(24):8807-14. Epub 2007 Oct 8.

López-Lluch G, Hunt N, Jones B, Zhu M, Jamieson H, Hilmer S, Cascajo MV, Allard J, Ingram DK, Navas P, de Cabo R. Calorie restriction induces mitochondrial biogenesis and bioenergetic efficiency. Proc Natl Acad Sci U S A. 2006 Feb 7;103(6):1768-73. Epub 2006 Jan 30.

Louis DN, Ohgaki H, Wiestler OD, Cavenee WK (eds): WHO Classification of Tumours of the Central Nervous System. Lyon, France: IARC Press, 2007

Louis DN, Perry A, Reifenberger G, von Deimling A, Figarella-Branger D, Cavenee WK, Ohgaki H, Wiestler OD, Kleihues P, Ellison DW. The 2016 World Health Organization Classification of Tumors of the Central Nervous System: a summary. Acta Neuropathol. 2016 Jun;131(6):803-20. doi: 10.1007/s00401-016-1545-1. Epub 2016 May 9.

Lowry OH, Rosebrough NJ, Farr AL, Randall RJ. Protein measurement with the Folin phenol reagent. J Biol Chem. 1951; 193(1):265-75.

Lynch CJ, Xu Y, Hajnal A, Salzberg AC, Kawasawa YI. RNA sequencing reveals a slow to fast muscle fiber type transition after olanzapine infusion in rats. PLoS One. 2015 Apr 20;10(4):e0123966. doi: 10.1371/journal.pone.0123966. eCollection 2015.

MacInnis MJ, Zacharewicz E, Martin BJ, Haikalis ME, Skelly LE, Tarnopolski MA, Murphy RM, Gibala MJ. Superior mitochondrial adaptations in human skeletal muscle after interval compared to continuous single-leg cycling matched for total work. J. Physiol. 2016 Jul 11. doi: 10.1113/JP272570.

Mancini DM, Henson D, LaManca J, Levine S. Respiratory muscle function and dyspnea in patients with chronic congestive heart failure. Circulation. 1992;86:909–918.

Mancini DM, Walter G, Reichek N, Lenkinski R, McCully KK, et al. Contribution of skeletal muscle atrophy to exercise intolerance and altered muscle metabolism in heart failure. Circulation. 1992;85:1364–1373.

Margareto J, Leis O, Larrarte E, Idoate MA, Carrasco A, Lafuente JV. Gene expression profiling of human gliomas reveals differences between GBM and LGA related to energy metabolism and notch signaling pathways. J Mol Neurosci 2007; 32: 53-63.

Marie SK, Okamoto OK, Uno M, Hasegawa AP, Oba-Shinjo SM, Cohen T. Maternal embryonic leucine zipper kinase transcript abundance correlates with malignancy grade in human astrocytomas. Int J Cancer. 2008 122:807-15.

Marignani PA. LKB1, the multitasking tumour suppressor kinase. J Clin Pathol. 2005 Jan;58(1):15-9.

Marin-Valencia I, Yang C, Mashimo T, Cho S, Baek H, Yang XL, Rajagopalan KN, Maddie M, Vemireddy V, Zhao Z, Cai L, Good L, Tu BP, Hatanpaa KJ,Mickey BE, Matés JM, Pascual JM, Maher EA, Malloy CR,

Deberardinis RJ, Bachoo RM. Analyses of tumor metabolism reveals mitochondrial glucose oxidation in genetically diverse human glioblastomas in the mouse brain in vivo. Cell metab 2012, 15: 827–837.

Mavelli I, Mondovi B, Federico R, Rotilio G. Superoxide dismutase activity in developing rat brain. J Neurochem. 1978 Jul;31(1):363-4.

Mende U, Samsarian C, Martins DC, Kagen A, Duffy C, Schoen FJ, Neer EJ. Dilated cardiomyopathy in two transgenic mouse lines expressing activated G protein alfa (q): lack of correlation between phospholipase C activation and the phenotype. J. Mol. Cell. Cardiol. 2001; 33: 1477-1491.

Menz RI, Walker JE, Leslie AGW. Structure of bovine mitochondrial Fl-ATPase with nucleotide bound to all three catalytic sites: Implications for the mechanism of rotary catalysis. Cell. 2001; 106:331–341.

Menzies K, Auwerx J. An acetylation rheostat for the control of muscle energy homeostasis. J Mol Endocrinol. 2013 Nov 26;51(3):T101-13. doi: 10.1530/JME-13-0140. Print 2013 Dec.

Mettauer B, Zoll J, Sanchez H, Lampert E, Ribera F, et al. Oxidative capacity of skeletal muscle in heart failure patients versus sedentary or active control subjects. J Am Coll Cardiol. 2001;38:947–954.

Mezzani A, Grassi B, Jones AM, Giordano A, Corrà U, Porcelli S, Della Bella S, Tedesco A, Giannuzzi P. Speeding of pulmonary V'O2 on-kinetics by light-to-moderate intensity aerobic exercise training in chronic heart failure: clinical and pathophysiological correlates. Int. J. Cardiol. 167: 2189-2195, 2013.

Min K, Smuder AJ, Kwon OS, Kavazis AN, Szeto HH, Powers SK. Mitochondrial-targeted antioxidants protect skeletal muscle against immobilization-induced muscle atrophy. J Appl Physiol (1985). 2011 Nov;111(5):1459-66. doi: 10.1152/japplphysiol.00591.2011. Epub 2011 Aug 4.

Mitchell P, Moyle J. Chemiosmotic hypothesis of oxidative phosphorylation. Nature. 1967 213(5072): 137-139.

Mitchell P. Coupling of phosphorylation to electron and hydrogen transfer by a chemiosmotic type of mechanism. Nature. 1961 191:144-148.

Mootha VK, Lindgren CM, Eriksson KF, Subramanian A, Sihag S, Lehar J, Puigserver P, Carlsson E, Ridderstråle M, Laurila E, Houstis N, Daly MJ, Patterson N, Mesirov JP, Golub TR, Tamayo P, Spiegelman B, Lander ES, Hirschhorn JN, Altshuler D, Groop LC. PGC-1alpha-responsive genes involved in oxidative phosphorylation are coordinately downregulated in human diabetes. Nat Genet. 2003 Jul; 34(3):267-73.

Moreno-Sánchez R, Rodríguez-Enríquez S, Marín-Hernández A, Saavedra E. Energy metabolism in tumor cells. FEBS J 2007, 274: 1393-1418.

Moriggi M, Vasso M, Fania C, Capitanio D, Bonifacio G, Salanova M, Blottner D, Rittweger J, Felsenberg D, Cerretelli P, Gelfi C. Long term bed rest with and without vibration exercise countermeasures: effects on human muscle protein dysregulation. Proteomics. 2010 Nov;10(21):3756-74. doi: 10.1002/pmic.200900817.

Mounier R, Théret M, Lantier L, Foretz M, Viollet B. Expanding roles for AMPK in skeletal muscle plasticity. Trends Endocrinol Metab. 2015 Jun;26(6):275-86. doi: 10.1016/j.tem.2015.02.009. Epub 2015 Mar 26.

Musch TI, Nguyen CT, Pham HW, Moore RL. Training effects on the regional blood flow response to exercise in myocardial infarcted rats. Am. J. Physiol. Heart Circ. Physiol. 262: H1846-H1852, 1992.

Myers J, Prakash M, Froelicher V, Do D, Partington S, Atwood JE. Exercise capacity and mortality among men referred for exercise testing. N. Engl. J. Med. 346: 793-801, 2002.

Negrao CE, Middlekauff HR. Adaptations in autonomic function during exercise training in heart failure. Heart Fail. Rev. 13: 51-60, 2008.

Nisoli E, Carruba MO. Nitric oxide and mitochondrial biogenesis. J Cell Sci. 2006 Jul 15;119(Pt 14):2855-62.

Obre E, Rossignol R. Emerging concepts in bioenergetics and cancer research: metabolic flexibility, coupling, symbiosis, switch, oxidative tumors, metabolic remodeling, signaling and bioenergetic therapy. Int J Biochem Cell Biol 2015, 59: 167-181.

O'Brien LC, Keeney PM, Bennett JP Jr. Differentiation of human neural stem cells into motor neurons stimulates mitochondrial biogenesis and decreases glycolytic flux. Stem Cells Dev 2015, 24: 1984-1994. 2015 May 20.

O'Connell K, Ohlendieck K. Proteomic DIGE analysis of the mitochondria-enriched fraction from aged rat skeletal muscle. Proteomics. 2009 Dec;9(24):5509-24. doi: 10.1002/pmic.200900472.

O'Hagan KA, Cocchiglia S, Zhdanov AV, Tambuwala MM, Cummins EP, Monfared M, Agbor TA, Garvey JF, Papkovsky DB, Taylor CT, Allan BB. PGC-1alpha is coupled to HIF-1alpha-dependent gene expression by

increasing mitochondrial oxygen consumption in skeletal muscle cells. Proc Natl Acad Sci U S A. 2009 Feb 17;106(7):2188-93. doi: 10.1073/pnas.0808801106. Epub 2009 Jan 28.

Ohgaki H, Kleihues P, The Definition of Primary and Secondary Glioblastoma. Clin Cancer Res. 2013; 19:764-772.

Opasich C, Aquilani R, Dossena M, Foppa P, Catapano M, et al. Biochemical analysis of muscle biopsy in overnight fasting patients with severe chronic heart failure. Eur Heart J. 1996;17:1686–1693.

Ordys BB, Launay S, Deighton RF, McCulloch J, Whittle IR, The Role of Mitochondria in Glioma Pathophysiology. Mol Neurobiol. 2010; 42:64–75.

Ortega AD, Willers IM, Sala S, Cuezva JM. Human G3BP1 interacts with the β-F1-ATPase mRNA and inhibits its translation. J. Cell Sci. 2010; 123 2685–2696.

Oudard S, Arvelo F, Miccoli L, Apiou F, Dutrillaux AM, Poisson M, Dutrillaux B, Poupon MF. High glycolysis in gliomas despite low hexokinase transcription and activity correlated to chromosome 10 loss. Br J Cancer. 1996 Sep; 74(6):839-45.

Oyedotun KS, Lemire BD. The quaternary structure of the Saccharomyces cerevisiae succinate dehydrogenase. Homology modeling, cofactor docking, and molecular dynamics simulation studies. J. Biol. Chem. 2004; 5:9424-31.

Palacios OM, Carmona JJ, Michan S, Chen KY, Manabe Y, Ward JL 3rd, Goodyear LJ, Tong Q. Diet and exercise signals regulate SIRT3 and activate AMPK and PGC-1alpha in skeletal muscle. Aging (Albany NY). 2009 Aug 15;1(9):771-83.

Parkinson H, Kapushesky M, Shojatalab M, Abeygunawardena N, Coulson R, et al. ArrayExpress a public database of microarray experiments and gene expression profiles. Nucleic Acids Res. 2007;35:747–750.

Pellegrino MA, Canepari M, Rossi R, D'Antona G, Reggiani C, Bottinelli R. Orthologous myosin isoforms and scaling of shortening velocity with body size in mouse, rat, rabbit and human muscle. J. Physiol. 546: 677-698, 2003.

Pesta D, Gnaiger E. High-resolution respirometry. OXPHOS protocols for human cell cultures and permeabilized fibers from small biopsies of human muscle. Methods Mol. Biol. 2012; 810: 25–58.

Peterson CM, Johannsen DL, Ravussin E. Skeletal muscle mitochondria and aging: a review. J Aging Res. 2012;2012:194821. doi: 10.1155/2012/194821. Epub 2012 Jul 19.

Picard M, Ritchie D, Wright KJ, Romestaing C, Thomas MM, Rowan SL, Taivassalo T, Hepple RT. Mitochondrial functional impairment with aging is exaggerated in isolated mitochondria compared to permeabilized myofibers. Aging Cell. 2010 Dec;9(6):1032-46. doi: 10.1111/j.1474-9726.2010.00628.x.

Piec I, Listrat A, Alliot J, Chambon C, Taylor RG, Bechet D. Differential proteome analysis of aging in rat skeletal muscle. FASEB J. 2005 Jul;19(9):1143-5. Epub 2005 Apr 14.

Piepoli MF, Stewart Coats AJ. The 'skeletal muscle hypothesis in heart failure' revised. Eur Heart J. 2013 Feb;34(7):486-8. doi: 10.1093/eurheartj/ehs463

Pillai VB, Sundaresan NR, Kim G, Gupta M, Rajamohan SB, Pillai JB, Samant S, Ravindra PV, Isbatan A, Gupta MP. Exogenous NAD blocks cardiac hypertrophic response via activation of the SIRT3-LKB1-AMP-activated kinase pathway. J Biol Chem 2010, 285: 3133-3144.

Pišot R, Marusic U, Biolo G, Mazzucco S, Lazzer S, Grassi B, Reggiani C, Toniolo L, di Prampero PE, Passaro A, Narici M, Mohammed S, Rittweger J, Gasparini M, Gabrijelčič M, Šimunič B. Greater loss in muscle mass and function but smaller metabolic alterations 2 in older compared to younger men following two weeks of bed rest and recovery. J Appl Physiol (1985). 2016 Jan 28:jap.00858.2015. doi: 10.1152/japplphysiol.00858.2015.

Poole DC, Hirai DM, Copp SW, Musch TI. Muscle oxygen transport and utilization in heart failure: implications for exercise (in)tolerance. Am. J. Heart Circ. Physiol. 2012; 302: H1050-H1063.

Power J, Cross RL, Harris DA. Interaction of F1-ATPase, from ox heart mitochondria with its naturally occurring inhibitor protein. Studies using radio-iodinated inhibitor protein". Biochim. Biophys. Acta. 1983 724 128-141.

Powers SK, Wiggs MP, Duarte JA, Zergeroglu AM, Demirel HA. Mitochondrial signaling contributes to disuse muscle atrophy. Am J Physiol Endocrinol Metab. 2012 Jul 1;303(1):E31-9. doi: 10.1152/ajpendo.00609.2011. Epub 2012 Mar 6.

Pullman ME, Monroy GC. A Naturally Occurring Inhibitor of Mitochondrial Adenosine Triphosphatase. J. Biol. Chem. 1963 238 3762-3769.

Rahman M, Nirala NK, Singh A, Zhu LJ, Taguchi K, Bamba T, Fukusaki E, Shaw LM, Lambright DG, Acharya JK, Acharya UR. Drosophila Sirt2/mammalian SIRT3 deacetylates ATP synthase β and regulates complex V activity. J Cell Biol. 2014 Jul 21;206(2):289-305. doi: 10.1083/jcb.201404118. Epub 2014 Jul 14.

Rato L, Duarte AI, Tomás GD, Santos MS, Moreira PI, Socorro S, Cavaco JE, Alves MG, Oliveira PF. Pre-diabetes alters testicular PGC1-α/SIRT3 axis modulating mitochondrial bioenergetics and oxidative stress. Biochim Biophys Acta 2014, 1837: 3353-3364.

Razani B, Reichardt AD, Cheng G. Non-canonical NF-κB signaling activation and regulation: principles and perspectives. Immunol Rev. 2011 Nov;244(1):44-54. doi: 10.1111/j.1600-065X.2011.01059.x. Review.

Rees J, Wen P (eds): Neuro-Oncology. Philadelphia: Saunders Elsevier, 2010

Reid MB, Moylan JS. Beyond atrophy: redox mechanisms of muscle dysfunction in chronic inflammatory disease. J. Physiol. 589: 2171-2179, 2011.

Remels AH, Gosker HR, Schrauwen P, Hommelberg PP, Sliwinski P, Polkey M, Galdiz J, Wouters EF, Langen RC, Schols AM. TNF-alpha impairs regulation of muscle oxidative phenotype: implications for cachexia? FASEB J 24: 5052–5062, 2010.

Ringholm S, Biensø RS, Kiilerich K, Guadalupe-Grau A, Aachmann-Andersen NJ, Saltin B, Plomgaard P, Lundby C, Wojtaszewski JF, Calbet JA, Pilegaard H. Bed rest reduces metabolic protein content and abolishes exercise-induced mRNA responses in human skeletal muscle. Am J Physiol Endocrinol Metab. 2011 Oct;301(4):E649-58. doi: 10.1152/ajpendo.00230.2011. Epub 2011 Jul 12.

Romanello V, Guadagnin E, Gomes L, Roder I, Sandri C, Petersen Y, Milan G, Masiero E, Del Piccolo P, Foretz M, Scorrano L, Rudolf R, Sandri M. Mitochondrial fission and remodelling contributes to muscle atrophy. EMBO J. 2010 May 19; 29(10):1774-85.

Romanello V, Sandri M. Mitochondrial biogenesis and fragmentation as regulators of muscle protein degradation. Curr Hypertens Rep. 2010 Dec;12(6):433-9. doi: 10.1007/s11906-010-0157-8.

Romanello V, Sandri M. Mitochondrial Quality Control and Muscle Mass Maintenance. Front Physiol. 2016 Jan 12;6:422. doi: 10.3389/fphys.2015.00422. eCollection 2015.

Ross JM, Olson L, Coppotelli G. Mitochondrial and ubiquitin proteasome system dysfunction in ageing and disease: two sides of the same coin? Int. J. Mol. Sci. 2015; 16, 19458–19476. 10.3390/ijms160819458

Rytinki MM, Palvimo JJ. SUMOylation attenuates the function of PGC-1alpha. J Biol Chem. 2009 Sep 18;284(38):26184-93. doi: 10.1074/jbc.M109.038943.

Salvadego D, Keramidas ME, Brocca L, Domenis R, Mavelli I, Rittweger J, Eiken O, Mekjavic IB, Grassi B. Separate and combined effects of a 10-d exposure to hypoxia and inactivity on oxidative function in vivo and mitochondrial respiration ex vivo in humans. J Appl Physiol (1985). 2016 Jul 1;121(1):154-63.

Salvadego D, Lazzer S, Marzorati M, Porcelli S, Rejc E, Simunic B, Pisot R, di Prampero PE, Grassi B. Functional impairment of skeletal muscle oxidative metabolism during knee extension exercise after bed rest. J Appl Physiol (1985). 2011 Dec;111(6):1719-26. doi: 10.1152/japplphysiol.01380.2010. Epub 2011 Sep 15.

Sameer A, Burrell KE, Wolf A, Jalali S, Hawkins C, Rutka JT, Zadeh G. Glioblastoma, a Brief Review of History, Molecular Genetics, Animal Models and Novel Therapeutic Strategies Arch. Immunol. Ther. Exp. 2013. 61:25–41.

Sánchez Cenizo LM. Función oncogénica del inhibidor de la H+-ATP Sintasa, IF1: desarrollo y caracterización de modelos Transgénicos condicionales y tejido-específicos. PhD Thesis. 2014, Madrid

Sanchez JC, Ravier F, Pasquali C, Frutiger S, Paquet N, Bjellqvist B, Hochstrasser DF, Hughes GJ. Improving the detection of proteins after transfer to polyvinylidene difluoride membranes. Electrophoresis. 1992 Sep-Oct;13(9-10):715-7.

Sánchez-Aragó M, Formentini L, Martínez-Reyes I, García-Bermudez J, Santacatterina F, Sánchez-Cenizo L, Willers IM, Aldea M, Nájera L, Juarránz A, López EC, Clofent J, Navarro C, Espinosa E, Cuezva JM. Expression, regulation and clinical relevance of the ATPase inhibitory factor 1 in human cancers. Oncogenesis. 2013;2:e46.

Sánchez-Aragó M, García-Bermúdez J, Martínez-Reyes I, Santacatterina F, Cuezva JM. Degradation of IF1 controls energy metabolism during osteogenic differentiation of stem cells. EMBO Rep 2013, 14: 638-44.

Sánchez-Cenizo L, Formentini L, Aldea M, Ortega AD, García-Huerta P, Sánchez-Aragó M, Cuezva JM. Up-regulation of the ATPase Inhibitory Factor 1 (IF1) of the Mitochondrial H+-ATP Synthase in Human Tumors

Mediates the Metabolic Shift of Cancer Cells to a Warburg Phenotype. J Biol Chem. 2010; 285(33): 25308–25313.

Sandri M. Protein breakdown in muscle wasting: Role of autophagy-lysosome and ubiquitin-proteasome. Int J Biochem Cell Biol. 2013 Oct; 45(10): 2121–2129. doi: 10.1016/j.biocel.2013.04.023

Sandri M. Signaling in muscle atrophy and hypertrophy. Physiology (Bethesda). 2008 Jun;23:160-70. doi: 10.1152/physiol.00041.2007.

Santacatterina F, Sánchez-Cenizo L, Formentini L, Mobasher MA, Casas E, Rueda CB, Martínez-Reyes I, Núñez de Arenas C, García-Bermúdez J, Zapata JM, Sánchez-Aragó M, Satrústegui J, Valverde ÁM, Cuezva JM. Down-regulation of oxidative phosphorylation in the liver by expression of the ATPase inhibitory factor 1 induces a tumor-promoter metabolic state. Oncotarget. 2016;7(1):490-508.

Scarpulla RC. Metabolic control of mitochondrial biogenesis through the PGC-1 family regulatory network. Biochim Biophys Acta. 2011 Jul;1813(7):1269-78. doi: 10.1016/j.bbamcr.2010.09.019.

Scarpulla RC. Nuclear activators and coactivators in mammalian mitochondrial biogenesis. Biochim Biophys Acta. 2002 Jun 7;1576(1-2):1-14.

Schaufelberger M, Eriksson BO, Grimby G, Held P, Swedberg K. Skeletal muscle fiber composition and capillarization in patients with chronic heart failure: relation to exercise capacity and central hemodynamics. J Card Fail. 1995;1:267–272.

Scheubel RJ, Tostlebe M, Simm A, Rohrbach S, Prondzinsky R, Gellerich FN, Silber RE, Holtz J. Dysfunction of mitochondrial respiratory chain complex I in human failing myocardium is not due to disturbed mitochondrial gene expression. J Am Coll Cardiol. 2002 Dec 18;40(12):2174-81.

Schiaffino S, Reggiani C. Fiber types in mammalian skeletal muscles. Physiol Rev. 2011 Oct;91(4):1447-531. doi: 10.1152/physrev.00031.2010.

Schröck E, Blume C, Meffert MC, du Manoir S, Bersch W, Kiessling M, et al. Recurrent gain of chromosome arm 7q in low-grade astrocytic tumors studied by comparative genomic hybridization. Genes Chromosomes Cancer. 1996; 15:199–205.

Schwab M. Encyclopedia of cancer, Springer 2011. doi 10.1007/978-3-642-16483-5

Scott JG, Basanta D, Chinnaiyan P, Canoll P, Swanson KR, Anderson ARA. Production of 2-hydroxyglutarate by isocitrate dehydrogenase 1–mutated gliomas: an evolutionary alternative to the Warburg shift?. Neuro-Oncology. 2011; 13(12):1262–1264.

Scrideli CA, Carlotti CG Jr, Okamoto OK, Andrade VS, Cortez MA, Motta FJ, et al. Gene expression profile analysis of primary glioblastomas and non-neoplastic brain tissue: identification of potential target genes by oligonucleotide microarray and real-time quantitative PCR. J Neurooncol. 2008; 88:281-91.

Shelly M, Cancedda L, Heilshorn S, Sumbre G, Poo MM. LKB1/STRAD promotes axon initiation during neuronal polarization. Cell 2007; 129: 565-577.

Sherman BT, Huang da W, Tan Q, Guo Y, Bour S, Liu D, Stephens R, Baseler MW, Lane HC, Lempicki RA. DAVID Knowledgebase: a gene-centered database integrating heterogeneous gene annotation resources to facilitate high-throughput gene functional analysis.BMC Bioinformatics. 2007 Nov 2;8:426.

Short KR, Bigelow ML, Kahl J, Singh R, Coenen-Schimke J, Raghavakaimal S, Nair KS. Decline in skeletal muscle mitochondrial function with aging in humans. Proc Natl Acad Sci U S A. 2005 Apr 12;102(15):5618-23. Epub 2005 Mar 30.

Simonini A, Long CS, Dudley GA, Yue P, McElhinny J, et al. Heart failure in rats causes changes in skeletal muscle morphology and gene expression that are not explained by reduced activity. Circ Res. 1996;79:128–136.

Skrap M, Mondani M, Tomasino B, Weis L, Budai R, Pauletto G, Eleopra R, Fadiga L, Ius T. Surgery of insular nonenhancing gliomas: volumetric analysis of tumoral resection, clinical outcome, and survival in a consecutive series of 66 cases. Neurosurgery. 2012 May;70(5):1081-93; discussion 1093-4. doi: 10.1227/NEU.0b013e31823f5be5.

Smith JS, Alderete B, Minn Y, Borell TJ, Perry A, Mohapatra G, Hosek SM, Kimmel D, O'Fallon J, Yates A, Feuerstein BG, Burger PC, Scheithauer BW, Jenkins RB. Localization of common deletion regions on 1p and 19q in human gliomas and their association with histological subtype. Oncogene. 1999 Jul 15; 18(28):4144-52.

Smith JS, Chang EF, Lamborn KR, Chang SM, Prados MD, Cha S, et al. Role of extent of resection in the long-term outcome of low-grade hemispheric gliomas. J Clin Oncol. 2008; 26:1338–1345.

Smolkova K, Plecita´-Hlavata´ L, Bellance N, Bernard G, Rossignol R, Jezek P. Waves of gene regulation suppress and then restore oxidative phosphorylation in cancer cells. Int J Biochem Cell Biol. 2010

Song R, Song H, Liang Y, Yin D, Zhang H, Zheng T, Wang J, Lu Z, Song X, Pei T, Qin Y, Li Y, Xie C, Sun B, Shi H, Li S, Meng X, Yang G, Pan S, Zhu J, Qi S, Jiang H, Zhang Z, Liu L. Reciprocal activation between ATPase inhibitory factor 1 and NF-κB drives hepatocellular carcinoma angiogenesis and metastasis. Hepatology. 2014; 60(5):1659-73.

Sperandio PA, Borghi-Silva A, Barroco A, Nery LE, Almeida DR, Neder JA. Microvascular oxygen delivery-to-utilization mismatch at the onset of heavy-intensity exercise in optimally treated patients with CHF. Am. J. Physiol. Heart Circ. Physiol. 297: H1720-H1728, 2009.

Spinazzi M, Casarin A, Pertegato V, Salviati L, Angelini C. Assessment of mitochondrial respiratory chain enzymatic activities on tissues and cultured cells. Nat Protoc. 2012 May 31;7(6):1235-46. doi: 10.1038/nprot.2012.058.

Srere PA. Citrate synthase. Methods Enzymol. 1969; 13: 3–11. doi: 10.1016/0076-6879(69)13005-0.

Stein TP, Wade CE. Metabolic consequences of muscle disuse atrophy. J Nutr. 2005 Jul;135(7):1824S-1828S.

Stock D, Gibbons C, Arechaga I, Leslie AG, Walker JE. The rotary mechanism of ATP synthase. Curr Opin Struct Biol. 2000 Dec;10(6):672-9.

Szentesi P, Bekedam MA, van Beek-Harmsen BJ, van der Laarse WJ, Zaremba R, et al. Depression of force production and ATPase activity in different types of human skeletal muscle fibers from patients with chronic heart failure. J Appl Physiol. 2005;99:2189–2195.

Takeishi Y, Bhagwat A, Ball NA, Kirkpatrick DL, Periasamy M, Walsh RA. Effect of angiotensin-converting enzyme inhibition on protein kinase C and SR proteins in heart failure. Am. J. Physiol. 1999;276:H53–H62.

Trappe TA, Raue U, Tesch PA. Human soleus muscle protein synthesis following resistance exercise. Acta Physiol Scand. 2004 Oct;182(2):189-96.

Vafai SB, Mootha VK. Mitochondrial disorders as windows into an ancient organelle. Nature. 2012 Nov 15;491(7424):374-83. doi: 10.1038/nature11707.

Vassilopoulos A, Pennington JD, Andresson T, Rees DM, Bosley AD, Fearnley IM, Ham A, Flynn CR, Hill S, Rose KL, Kim HS, Deng CX, Walker JE, Gius D. SIRT3 deacetylates ATP synthase F1 complex proteins in response to nutrient- and exercise-induced stress. Antioxid Redox Signal. 2014 Aug 1;21(4):551-64.

Ventura-Clapier R, Garnier A, Veksler V. Transcriptional control of mitochondrial biogenesis: the central role of PGC-1alpha. Cardiovasc Res. 2008 Jul 15;79(2):208-17. doi: 10.1093/cvr/cvn098.

Verhaak RG, Hoadley KA, Purdom E. Integrated genomic analysis identifies clinically relevant subtypes of glioblastoma characterized by abnormalities in PDGFRA, IDH1, EGFR, and NF1. Cancer Cell. 2010. 17:98–110.

Vina J, Sanchis-Gomar F, Martinez-Bello V, Gomez-Cabrera MC. Exercise acts as a drug; the pharmacological benefits of exercise. Br J Pharmacol. 2012 Sep; 167(1): 1–12. doi: 10.1111/j.1476-5381.2012.01970.x

Vinogradov AD, Catalytic properties of the mitochondrial NADH-ubiquinone oxidoreductase (complex I) and the pseudo-reversible active/inactive enzyme transition. Biochim Biophys Acta. 1998 May 6;1364(2):169-85.

Wagner PD. Determinants of maximal oxygen transport and utilization. Annu. Rev. Physiol. 58: 21-50, 1996.

Walker JE, Lutter R, Dupuis A, Runswick MJ. Identification of the subunits of FOF1-ATPase from bovine heart mithochondria. Biochemistry. 1991 30(22):5369-78.

Walker JE, Saraste M, Gay NJ. E. Coli F1-ATPase interacts with a membrane protein component of a proton channel". Nature. 1982 298:867-869.

Wall BT, Dirks ML, Snijders T, Senden JM, Dolmans J, van Loon LJ. Substantial skeletal muscle loss occurs during only 5 days of disuse. Acta Physiol (Oxf). 2014 Mar;210(3):600-11. doi: 10.1111/apha.12190. Epub 2013 Dec 5.

Wall BT, Dirks ML, Snijders T, Stephens FB, Senden JM, Verscheijden ML, van Loon LJ. Short-term muscle disuse atrophy is not associated with increased intramuscular lipid deposition or a decline in the maximal activity of key mitochondrial enzymes in young and older males. Exp Gerontol. 2015 Jan;61:76-83. doi: 10.1016/j.exger.2014.11.019. Epub 2014 Nov 29.

Wanagat J, Cao Z, Pathare P, Aiken JM (2001) Mitochondrial DNA deletion mutations colocalize with segmental electron transport system abnormalities, muscle fiber atrophy, fiber splitting, and oxidative damage in sarcopenia. FASEB J. 15, 322–332.

Warburg O. On respiratory impairment in cancer cells. Science. 1956 124 269–270.

Wenz T. Regulation of mitochondrial biogenesis and PGC-1α under cellular stress. Mitochondrion. 2013 Mar;13(2):134-42. doi: 10.1016/j.mito.2013.01.006. Epub 2013 Jan 22.

Wessels PH, Twijnstra A, Kessels AG, Krijne-Kubat B, Theunissen PH, Ummelen MI, et al. Gain of chromosome 7, as detected by in situ hybridization, strongly correlates with shorter survival in astrocytoma grade 2. Genes Chromosomes Cancer. 2002; 33:279–284.

Wiggs MP. Can endurance exercise preconditioning prevention disuse muscle atrophy? Front Physiol. 2015 Mar 11;6:63. doi: 10.3389/fphys.2015.00063. Review.

Willers IM, Isidoro A, Ortega AD, Fernandez PL, Cuezva JM. Selective inhibition of beta-F1-ATPase mRNA translation in human tumours. Biochem. J. 2010; 426 319–326.

Wisløff W, Støylen A, Loennechen JP, Bruvold M, Rognmo Ø, Haram PM, Tjønna AE, Helgerud J, Slørdahl SA, Lee SJ, Videm V, Bye A, Smith GL, Najjar SM, Ellingsen Ø, Skjærpe T. Superior cardiovascular effect of aerobic interval training versus moderate continuous training in heart failure patients. A randomized study. Circulation 2007; 115: 3086-3094.

Witczak CA, Sharoff CG, Goodyear LJ. AMP-activated protein kinase in skeletal muscle: from structure and localization to its role as a master regulator of cellular metabolism. Cell Mol Life Sci. 2008 Nov;65(23):3737-55. doi: 10.1007/s00018-008-8244-6.

Wittig I, Schägger H. Structural organization of mitochondrial ATP synthase. Biochim Biophys Acta. 2008 1777(7-8):592-8.

Wolf A, Agnihotri S, Guha A. Targeting metabolic remodeling in glioblastoma multiforme. Oncotarget 2010, 1: 552-562.

Woods A, Johnstone SR, Dickerson K, Leiper FC, Fryer LG, Neumann D, Schlattner U, Wallmann T, Carlson M, Carling D. LKB1 is the upstream kinase in the AMP-activated protein kinase cascade. Curr Biol 2003, 13: 2004–2008.

Wu J, Shan Q, Li P, Wu Y, Xie J, Wang X. ATPase inhibitory factor 1 is a potential prognostic marker for the migration and invasion of glioma. Oncology Letters. 2015; 10:2075-2080.

Wu YT, Lee HC, Liao CC, Wei YH. Regulation of mitochondrial F(o)F(1)ATPase activity by Sirt3-catalyzed deacetylation and its deficiency in human cells harboring 4977bp deletion of mitochondrial DNA. Biochim Biophys Acta. 2013 Jan;1832(1):216-27. doi: 10.1016/j.bbadis.2012.10.002. Epub 2012 Oct 6.

Wu Z, Puigserver P, Andersson U, Zhang C, Adelmant G, Mootha V, Troy A, Cinti S, Lowell B, Scarpulla RC, Spiegelman BM. Mechanisms controlling mitochondrial biogenesis and respiration through the thermogenic coactivator PGC-1. Cell. 1999 Jul 9;98(1):115-24.

Wüst RCI, Myers DS, Stones R, Benoist D, Robinson PA, Boyle JP, Peers C, White E, Rossiter HB. Regional skeletal muscle remodeling and mitochondrial dysfunction in right ventricular heart failure. Am. J. Physiol. Heart Circ. Physiol. 2012; 302: H402-H411.

Xie Z, Dong Y, Scholz R, Neumann D, Zou MH. Phosphorylation of LKB1 at serine 428 by protein kinase C-zeta is required for metformin-enhanced activation of the AMP-activated protein kinase in endothelial cells. Circulation. 2008 Feb 19;117(7):952-62. doi: 10.1161/CIRCULATIONAHA.107.744490. Epub 2008 Feb 4.

Xu G, Li JY. ATP5A1 and ATP5B are highly expressed in glioblastoma tumor cells and endothelial cells of microvascular proliferation. J Neurooncol. 2016 Feb;126(3):405-13. doi: 10.1007/s11060-015-1984-x.

Yan H, Parsons DW, Jin G, McLendon R, Rasheed BA, Yuan W, et al. IDH1 and IDH2 mutations in gliomas. N Engl J Med. 2009; 360:765–773

Yan S, Han X, Xue H, Zhang P, Guo X, Li T, Guo X, Yuan G, Deng L, Li G. Let-7f Inhibits Glioma Cell Proliferation, Migration, and Invasion by Targeting Periostin. J Cell Biochem. 2015 Aug;116(8):1680-92. doi: 10.1002/jcb.25128.

Zucker IH, Schultz HD, Patel KP, Wang H. Modulation of angiotensin II signaling following exercise training in heart failure. Am. J. Physiol. Heart Circ. Physiol. 2015; 308: H781-H791.

PUBLICATIONS

Paper *in extenso*

Comelli M, Domenis R, Buso A, Mavelli I. F1FO ATP Synthase Is Expressed at the Surface of Embryonic Rat Heart-Derived H9c2 Cells and Is Affected by Cardiac-Like Differentiation. J Cell Biochem. 2016 Feb;117(2):470-82. doi: 10.1002/jcb.25295.

Articles in preparation

Buso A, Correcig C, Candotti V, Comelli M, Ius T, Cesselli D, Skrap M, Mavelli I. ATPase Inhibitory Factor 1 is a prognostic factor in low-grade astrocytomas.

Buso A, Comelli M, Isola M, Picco R, Rittweger J, Salvadego D, Šimunič B, Pišot R, Grassi B, Mavelli I. Mitochondrial bioenergetics- and biogenesis-related proteins adaptations following two weeks of bed-rest and recovery in elderly and young men.

Submitted Manuscripts

Grassi B, Majerczak J, Bardi E, Buso A, Comelli M, Chlopicki S, Guzik M, Mavelli I, Nieckarz Z, Salvadego D, Tyrankiewicz U, Skórka T, Bottinelli R, Zoladz JA, Pellegrino MA. Exercise training in Tgαq*44 mice during the transition from compensated to uncompensated CHF: a functional approach to soleus muscle oxidative metabolism. *Journal of Physiology*

Abstracts

Buso A, Correcig C, Candotti V, Comelli M, Ius T, Cesselli D, Skrap M, Mavelli I, ATPase Inhibitory Factor 1 is a prognostic factor in low grade astrocytomas, (October 2016) 7th World Congress on Targeting Mitochondria, Berlin, Germany, p. 96. JWMS Vol. 2. doi:10.18143/JWMS_v2i2

Buso A, Comelli M, Isola M, Rittweger J, Salvadego D, Šimunič B, Pišot R, Grassi B, Mavelli I, Different effects of immobility and rehabilitation on PGC1α-Sirt3 axis and OXPHOS

protein expression in skeletal muscle of young and elderly men (2016). 28th "A. Castellani" Meeting of PhD Students in Biochemical Sciences, Brallo di Pregola (PV), p.15.

Buso A, Comelli M, Isola M, Grassi B, Mavelli I, Mitochondrial bioenergetics- and biogenesis-related proteins adaptation following two weeks of bed-rest and recovery in elderly and young men (2016). 10th Annual Meeting of Young Researchers in Physiology, Magnano in Riviera (UD), p. 35.

Buso A, Comelli M, Candotti V, Cesselli D, Mavelli I, ATPase-Inhibitory Factor 1 and OXPHOS complexes in human gliomas (2015). Annual Meeting of the Italian Group of Biomembranes and Bioenergetics (GIBB), Udine (UD), p. 21

ARTICLE
Journal of Cellular Biochemistry 117:470–482 (2016)

Journal of Cellular Biochemistry

F_1F_O ATP Synthase Is Expressed at the Surface of Embryonic Rat Heart-Derived H9c2 Cells and Is Affected by Cardiac-Like Differentiation

Marina Comelli,[1,2] Rossana Domenis,[1] Alessia Buso,[1] and Irene Mavelli[1,2]*

[1]*Department of Medical and Biological Sciences and MATI Centre of Excellence, University of Udine, p.le Kolbe 4, Udine 33100, Italy*

[2]*INBB Istituto Nazionale Biostrutture e Biosistemi, Viale Medaglie d'oro, Rome 00136, Italy*

ABSTRACT

Taking advantage from the peculiar features of the embryonic rat heart-derived myoblast cell line H9c2, the present study is the first to provide evidence for the expression of F_1F_O ATP synthase and of ATPase Inhibitory Factor 1 (IF_1) on the surface of cells of cardiac origin, together documenting that they were affected through cardiac-like differentiation. Subunits of both the catalytic F_1 sector of the complex (ATP synthase-β) and of the peripheral stalk, responsible for the correct F_1-F_O assembly/coupling, (OSCP, *b*, F6) were detected by immunofluorescence, together with IF_1. The expression of ATP synthase-β, ATP synthase-*b* and *F6* were similar for parental and differentiated H9c2, while the levels of OSCP increased noticeably in differentiated cells, where the results of *in situ* Proximity Ligation Assay were consistent with OSCP interaction within ecto-F_1F_O complexes. An opposite trend was shown by IF_1 whose ectopic expression appeared greater in the parental H9c2. Here, evidence for the IF_1 interaction with ecto-F_1F_O complexes was provided. Functional analyses corroborate both sets of data. i) An F_1F_O ATP synthase contribution to the exATP production by differentiated cells suggests an augmented expression of holo-F_1F_O ATP synthase on plasma membrane, in line with the increase of OSCP expression and interaction considered as a requirement for favoring the F_1-F_O coupling. ii) The absence of exATP generation by the enzyme, and the finding that exATP hydrolysis was largely oligomycin-insensitive, are in line in parental cells with the deficit of OSCP and suggest the occurrence of sub-assemblies together evoking more regulation by IF_1. J. Cell. Biochem. 117: 470–482, 2016.

KEY WORDS: ecto-F_1F_O ATP SYNTHASE; IF_1; OSCP; PLASMA MEMBRANE; CARDIAC-LIKE DIFFERENTIATION

For a long time F_1F_O ATP synthase was thought to exclusively locate in the inner mitochondrial membrane, generating energy by coupling the transmembrane delivery of protons to the synthesis of ATP [Stock et al., 1999]. However, many reports from several laboratories in recent years reported the location and function of the F_1F_O ATP synthase complex, or its component subunits, on the external surface of the plasma membrane. Various mammalian cell types have been investigated, including vascular endothelial cells, hepatocytes, adipocytes, myotubes, and tumor cells [Vantourout et al., 2010], as well as neural cells [Xing et al., 2012] and developing muscle cells [Garcia, 2011]. Plasma membrane F_1F_O-components, most usually β subunit, have been identified as receptors for multiple ligands, which combined with ecto-cellular ATP hydrolysis or ATP synthesis are involved in numerous biological processes. The most consolidated of these are control of intracellular pH, cholesterol homeostasis, and HDL endocytosis, regulation of endothelial cells proliferation/differentiation and angiogenesis, recognition of immune responses of tumor cells [Chi et al., 2006]. It has been also documented a role of the enzyme in regulation of calcium release especially during early development of myotubes [Garcia, 2011]. More recent evidence indicated that the cell surface ATP synthase is a binding protein for amyloid-β peptide (Aβ) on neural cells and suggested that the surface ATP synthase may be involved in oligomeric Aβ neurotoxic effects and neuro-degeneration [Xing et al., 2013]. Thus, the ectopic expression of F_1F_O ATP synthase (ecto-F_1F_O ATP synthase) is now widely recognized, but nothing has been reported so far about cells of cardiac origin. The idea that its subunit organization is the same as the mitochondrial enzyme is accepted based on several suggestions [Wang et al., 2006; Ma et al., 2010; Rai et al., 2013]. Of note, a characterization of the

Conflict of interest: None.
Grant sponsor: University of Udine.
*Correspondence to: Prof. Irene Mavelli, Department of Medical and Biological Sciences, University of Udine, p.le Kolbe 4, 33100 Udine, Italy. E-mail: irene.mavelli@uniud.it
Manuscript Received: 22 January 2015; Manuscript Accepted: 29 July 2015
Accepted manuscript online in Wiley Online Library (wileyonlinelibrary.com): 30 July 2015
DOI 10.1002/jcb.25295 • © 2015 Wiley Periodicals, Inc.

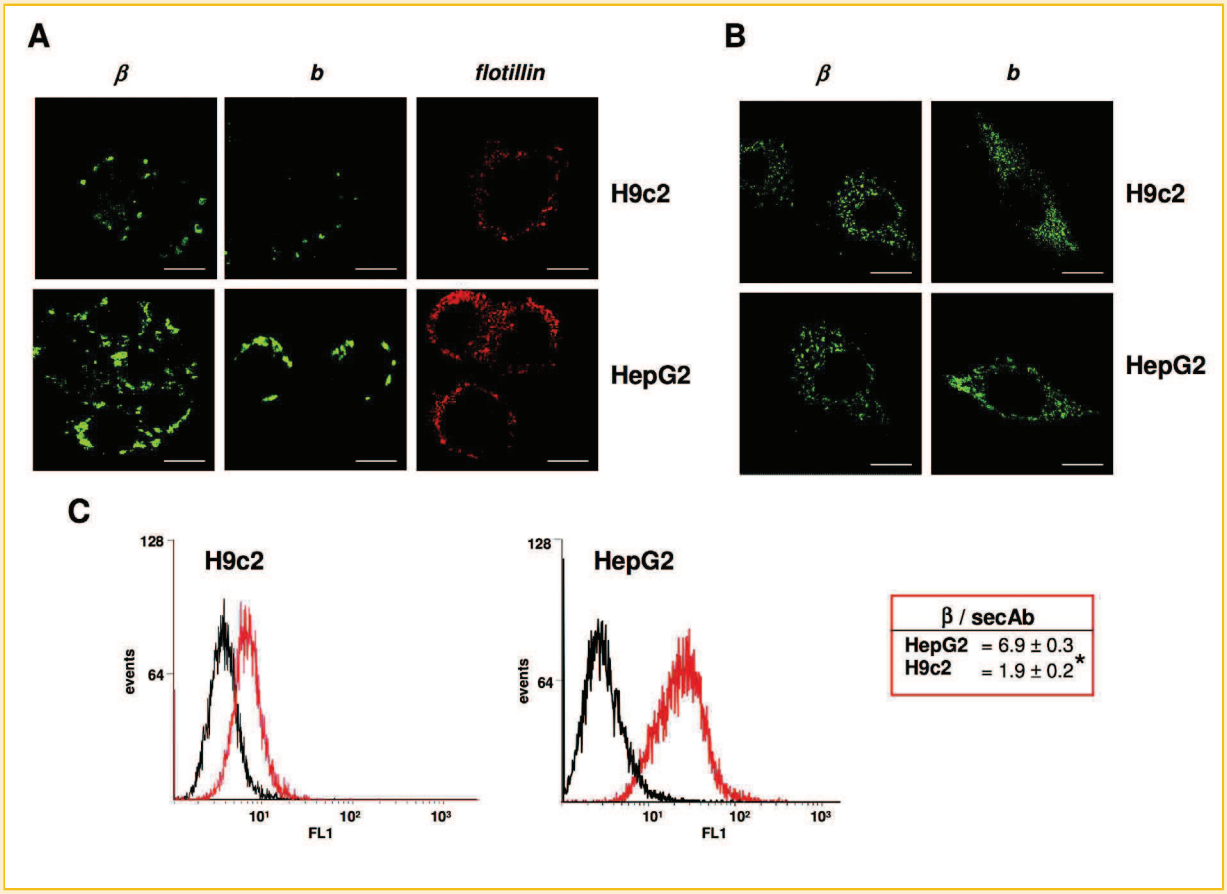

Fig. 1. Ectopic expression of β and *b* subunits of F_1F_O ATP synthase in H9c2 cells *vs* HepG2 cells. (A, B) Confocal microscopy analysis of intact (A) and permeabilized (B) cells for ATP synthase-β and ATP synthase-b. Profiles of intact cells were stained with polyclonal antibody anti-flotillin. Representative images of three separate experiments were reported. Bars = 30 μm. (C) Histogram plot of flow cytometry for ATP synthase-β. Black traces (left histograms) show cells incubated with only the secondary antibody and red traces (right histograms) cells labelled with monoclonal anti−β antibody. One experiment representative of three is shown. The mean fluorescence values relative to their own negative controls are reported in the insert (mean ± SD; n = 3; $^*P < 0.001$). Experimental procedures are in Methods.

complex of plasma membranes from rat liver was recently provided, documenting that it has a similar molecular weight to the monomeric form of the mitochondrial complex and contains not only nuclear but also mitochondrially-encoded subunits [Rai et al., 2013]. The authors concluded that this finding makes it unlikely that the enzyme assembles on the plasma membranes, but suggests it to be transported from mitochondria by still unknown pathways, in accordance with previous reports [Wang et al., 2006; Ma et al., 2010].

The mitochondrial F_1F_O ATP synthase presents a hydrophobic membrane domain, F_O, containing a H^+ channel in proximity of the interface between the *c*-ring and the associated *a*-subunit, and a hydrophilic domain, F_1 ($\alpha_3\beta_3$ subunits), bearing the adenine nucleotide processing sites. F_O and F_1 domains are connected by the so-called central (γ, δ, ε subunits) and peripheral stalks [Baker et al., 2012]. The peripheral stator stalk consists of single copies of oligomycin-sensitivity conferral protein (OSCP), *b*,*d* and *F6* subunits. It associates with the apex of the F_1 domain through OSCP and extends along the periphery of the F_1, running along an α/β-interface, into the membrane domain of the enzyme. Thus, the peripheral stator stalk enters the lipid bilayer throughout the membrane-bound portion of subunit *b*, that is the only subunit observed to span the soluble and membrane-embedded parts of the stalk. The mitochondrial enzyme contains also the ATPase Inhibitory Factor 1 (IF_1), which is a basic protein that reversibly binds to one of the three β subunits thereby inhibiting the enzyme [Green and Grover, 2000; Bason et al., 2011]. IF_1 functions in mitochondrial membrane as a regulatory protein and binds in response to decrease in pH and/or under conditions favoring the ATPase mode of the enzyme functioning, for example at low transmembrane potential as occurs under cardiac ischemia or after preconditioning [Green and Grover, 2000; Di Pancrazio et al., 2004]. IF1 also binds when the enzyme complex is partially uncoupled or sub-assemblies are present in mitochondrial membranes [Carrozzo et al., 2006; Mourier et al., 2014]. IF_1 is expressed even on the external surface of endothelial [Cortes-Hernandez et al., 2005; Martinez et al., 2015] and hepatic cells [Contessi et al., 2007; Mangiullo et al., 2008; Giorgio et al., 2010; Martinez et al., 2015], as well as in myelin vesicles [Ravera et al., 2011]. On the cell surface IF_1 function might be not

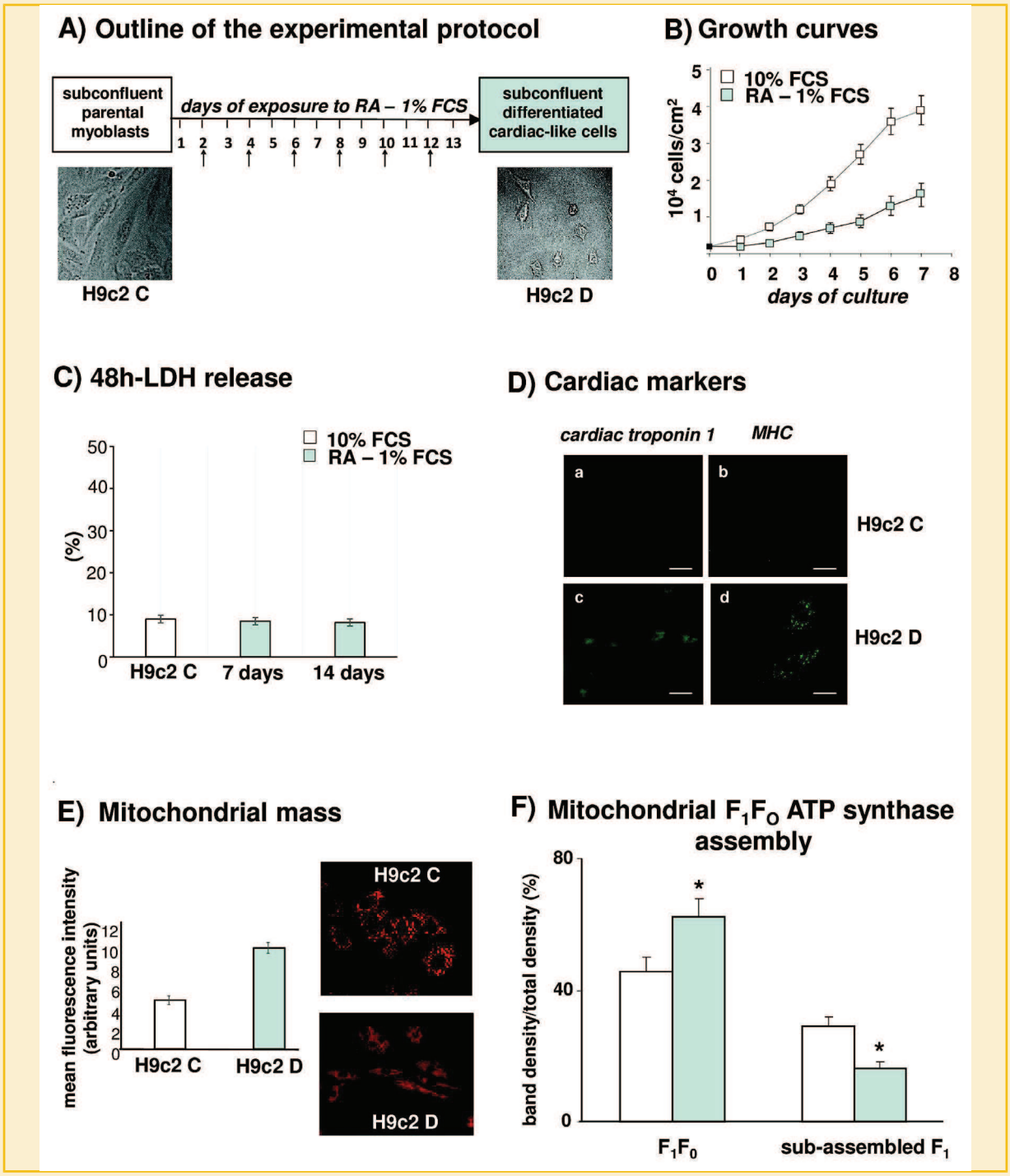

Fig. 2. Overall description of H9c2 cardiac-like differentiation protocol and some relevant changes occurring alongside. (A) Outline of the experimental protocol. RA = *all-trans*-retinoic acid; FCS = fetal calf serum; the arrows indicate the days of the medium replacement during cell culturing under differentiating conditions. (B) Growth curves. Data (cells/cm^2) were from Trypan Blue dye exclusion tests and represent means ± SD of four different experiments. Cells were followed until seven days of culture in normal (10% FCS) or in differentiating (RA-1% FCS) conditions. (C) 48 h-LDH release. 48 h-LDH release indicates the release of LDH in the growth medium during 48 h of culture, before the medium replacement. The values are expressed as a percentage of the total LDH activity of the cells: that is extracellular LDH/(extracellular LDH + intracellular LDH). Data represent means ± SD of three different experiments. (D) Cardiac markers analyzed by confocal microscopy. Images of parental myoblasts (H9c2 C) and differentiated cardiac-like cells (H9c2 D) were selected from three different experiments (Bar = 30 μm). MHC = myosin heavy chain. (E) Changes in mitochondrial mass by flow cytometry and confocal microscopy analyses. Parental myoblasts (H9c2 C) and differentiated cardiac-like cells (H9c2 D) were probed with mitotracker red. The histograms represent the mean fluorescence intensity of three different experiments (means ± SD). Pictures are confocal images selected from three different experiments. (F) Changes in assembly of mitochondrial F_1F_O ATP synthase in membrane. BN-PAGE (4–11%) analysis of n-dodecylmaltoside (DDM) mitochondrial extracts for the fully assembled enzyme complex F_1-F_O and the sub-assembled F_1 in H9c2 C (white columns) and in H9c2 D cells (light blue/gray columns). Data are from Comelli et al., 2011.

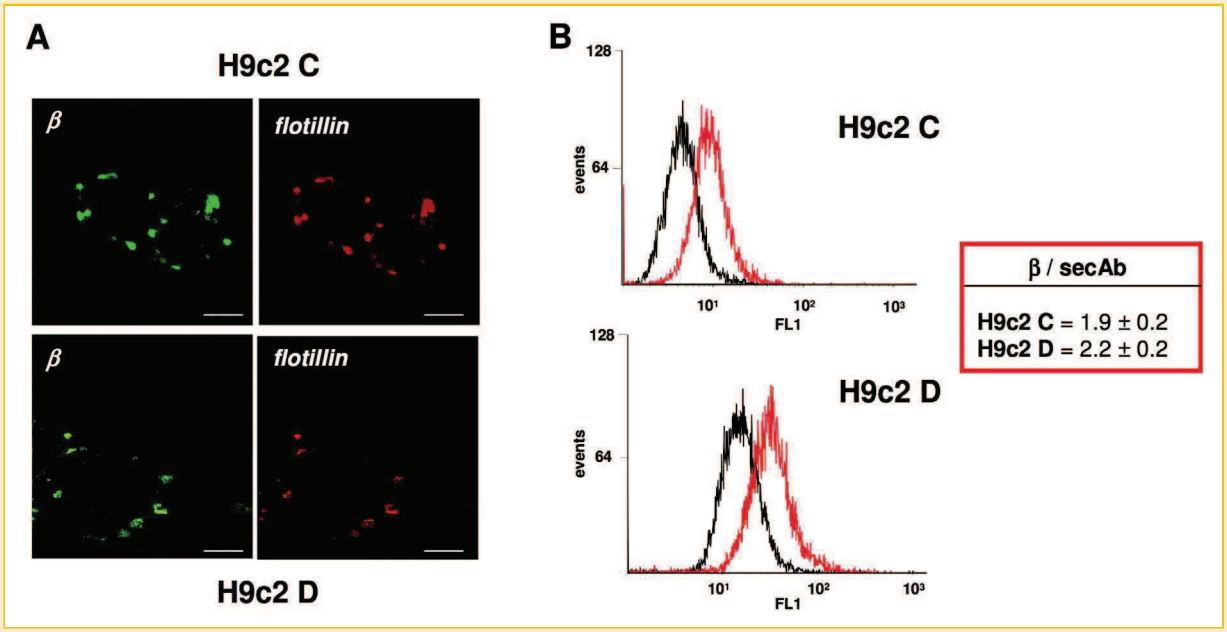

Fig. 3. Expression of F_1F_O ATP synthase-β on the surface of H9c2 cells induced to cardiac-like differentiation. (A) Parental (H9c2 C) and differentiated (H9c2 D) intact cells were treated with monoclonal anti-β or polyclonal anti-flotillin antibody and analyzed by confocal microscopy. Representative images of three separate experiments were reported. Bars = 30 μm. (B) Histogram plot of flow cytometry for H9c2 C and H9c2 D cells labelled with only the secondary antibody (black traces/left histograms), or with anti−β antibody (red traces/right histograms). One experiment representative of three is shown. The relative mean fluorescence values are reported in the insert (mean ± SD). Experimental procedures are in Methods.

limited to regulation of F_1F_O ATP synthase [Cortes-Hernandez et al., 2005] and it might interact with different target proteins such as calmodulin [Contessi et al., 2007].

A main goal of the present study was to investigate whether ecto-F_1F_O ATP synthase is expressed on H9c2 myoblasts, considering the extensive application of this cell line as a model for cardiac cells in a multiplicity of studies [Pereira et al., 2011 and references therein; Kuznetsov et al., 2015]. Indeed, H9c2 myoblasts are derived from the ventricular part of embryonic rat heart and, although are not true cardiac cells, they possess similar morphological, electrophysiological, and biochemical properties, for example energy metabolism, to primary cardiomyocytes [Hescheler et al., 1991, Kuznetsov et al., 2015], while maintain characteristics of immature embryonic cells [Kageyama et al., 2002].

We used immunofluorescence approaches and enzymatic activity measurements allowing us to get evidence on intact and viable cells. Our findings are consistent with the expression on the external surface of H9c2 cells of F_1F_O ATP synthase subunits that are part of the F_1 domain or of the peripheral stator stalk, including β, OSCP, *b*, and *F6*, as well as of the regulatory protein IF_1.

It is worth mentioning that proliferating H9c2 myoblasts can be differentiated towards a more cardiomyocyte-like phenotype by culturing cells in reduced serum medium containing *all-trans*-retinoic acid. We recently reported that these conditions induce the appearance of cardiomyocyte-like ultrastructural features and enhance the assembly of mitochondrial F_1F_O ATP synthase along with mitochondria biogenesis and remodelling [Comelli et al., 2011; Bisetto et al., 2013]. Thus, a primary aim of this study was also to compare proliferating and differentiating H9c2 cells focusing on ecto-F_1F_O ATP synthase. Overall, the results provide evidence for an increase of catalytically competent and well assembled/coupled F_1F_O complexes on cell surface of H9c2 along with the acquisition of the more cardiomyocyte-like phenotype.

MATERIALS AND METHODS

CELL CULTURES AND MATERIALS

H9c2 embryonic rat heart-derived myoblasts (ATCC CRL-1446), purchased from the American Type Culture Collection, were grown as in [Comelli et al., 2011]. Sub-confluent cells (70–80%) were sub-cultured to prevent low serum-culturing and loss of myoblastic cells. In fact, H9c2 myoblasts can rapidly lose their characteristics and undergo spontaneous trans-differentiation, becoming multi-nucleated myotubes, under conditions of decreased serum concentration and of achieved confluence [Menard et al., 1999].

H9c2 cells were also cultured in reduced serum medium containing *all-trans*-retinoic acid (RA) as in [Comelli et al., 2011], to induce differentiation of the parental line toward cardiac-like phenotype, with the medium being replaced every 2 days. Cytotoxicity was monitored by a sensitive LDH release assay following manufacturer's instructions (Cytotox 96 non-radioactive assay kit, Promega, Medison, WI).

Human hepatocarcinoma HepG2 cells (ATCC HB8065) were grown as in [Contessi et al., 2007].

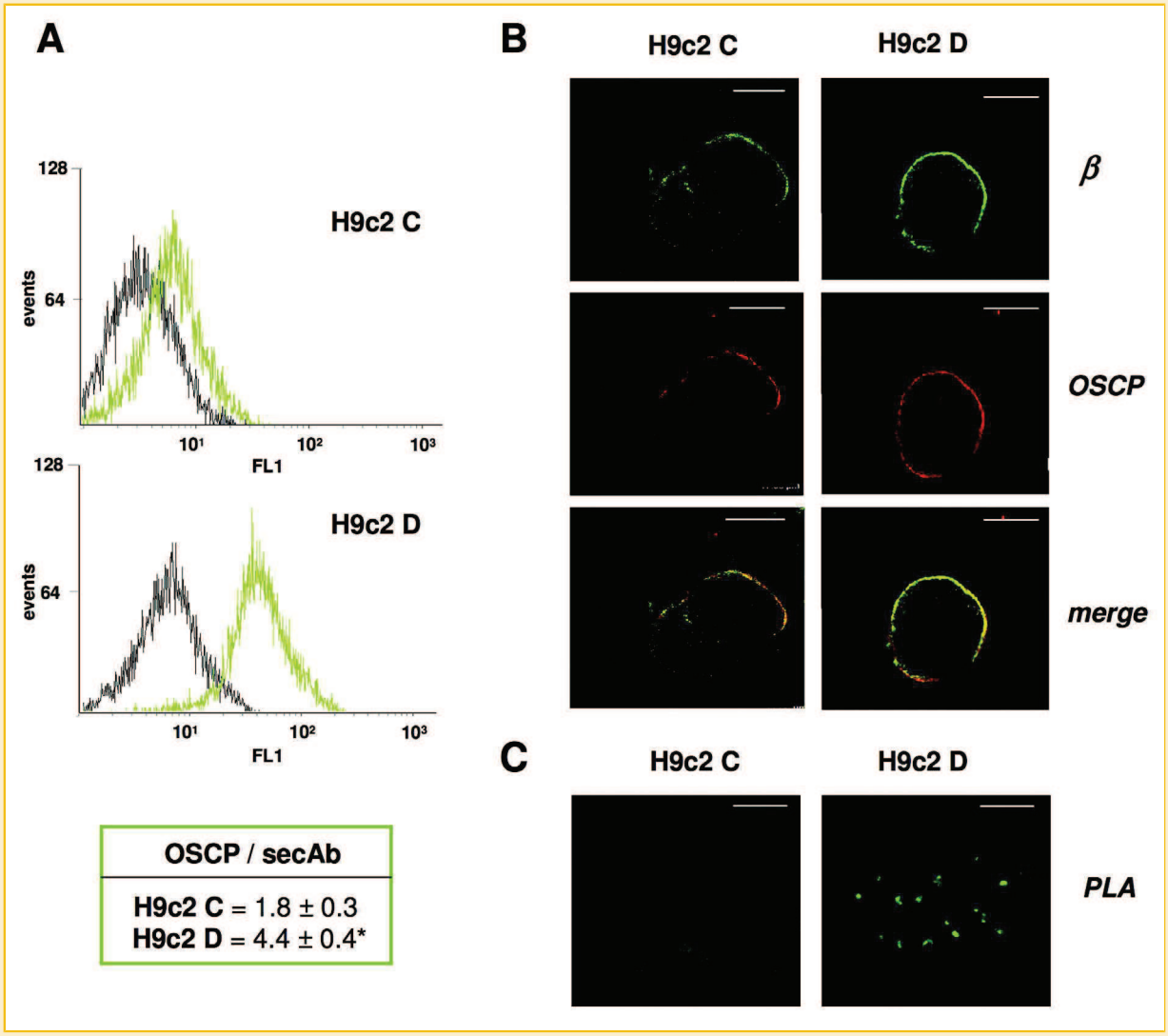

Fig. 4. Effect of H9c2 cardiac-like differentiation on the ectopic expression of F_1F_O ATP synthase OSCP subunit. Parental (H9c2 C) and differentiated (H9c2 D) cells were treated and analyzed by cytofluorimetry and confocal microscopy (cell surface immunostaining and in situ PLA assay) as described in Methods. (A) Cytofluorimetry histogram plots: black traces (left histograms) indicate cells incubated in the presence of only the secondary antibody and green traces (right histograms) cells incubated with anti-OSCP antibody. One experiment representative of three is shown. The mean fluorescence values relative to their own negative controls are reported in the insert (mean ± SD; n = 3; $^*P < 0.001$). (B) Confocal microscopy analysis of live cells doubly labelled with monoclonal anti-β and polyclonal anti-OSCP antibody. The merged image indicates colocalization of the two fluorophores. Representative images of three separate experiments were reported. Bars=30 μm. (C) Images from in situ PLA assay used to demonstrate β-OSCP interaction. Distinct fluorescent dots (PLA signals), indicating the occurrence of interaction, are evident in H9c2 D. Representative images of three separate experiments were reported. Bars =30 μm.

All the experiments were done with cells not approaching confluence.

All chemicals and reagents were purchased from Sigma (St. Louis, MO), unless specifically indicated.

IMMUNO-BASED ASSAYS

The primary antibodies were: rabbit polyclonal and mouse monoclonal antibody anti-β (Abcam, Cambridge, UK); rabbit polyclonal anti-α/β kindly provided by dr. F. Dabbeni-Sala, Department of Pharmacology, University of Padua, Italy); mouse monoclonal anti-IF_1 (Santa Cruz Biotecnology, Inc., CA); mouse monoclonal anti-OSCP (Abcam, Cambridge, UK); mouse monoclonal anti-*F6* (Abcam, Cambridge, UK); rabbit polyclonal anti-*b* (Proteintech Europe, Manchester, UK); rabbit polyclonal anti-flotillin 1 (Abcam, Cambridge, UK).

FITC-conjugated rabbit anti-mouse IgG or TRIC-conjugated goat anti-rabbit IgG (Chemicon International, Temecule, CA) were used as secondary antibodies.

Parental and differentiated cells were tested together in order to avoid possible differences in efficacy of the antisera. Cells treated with only secondary antibody served as negative controls.

CONFOCAL MICROSCOPY

5×10^4 cells were plated in complete growth medium on glass coverslips, grown overnight, and treated as in [Contessi et al., 2007].

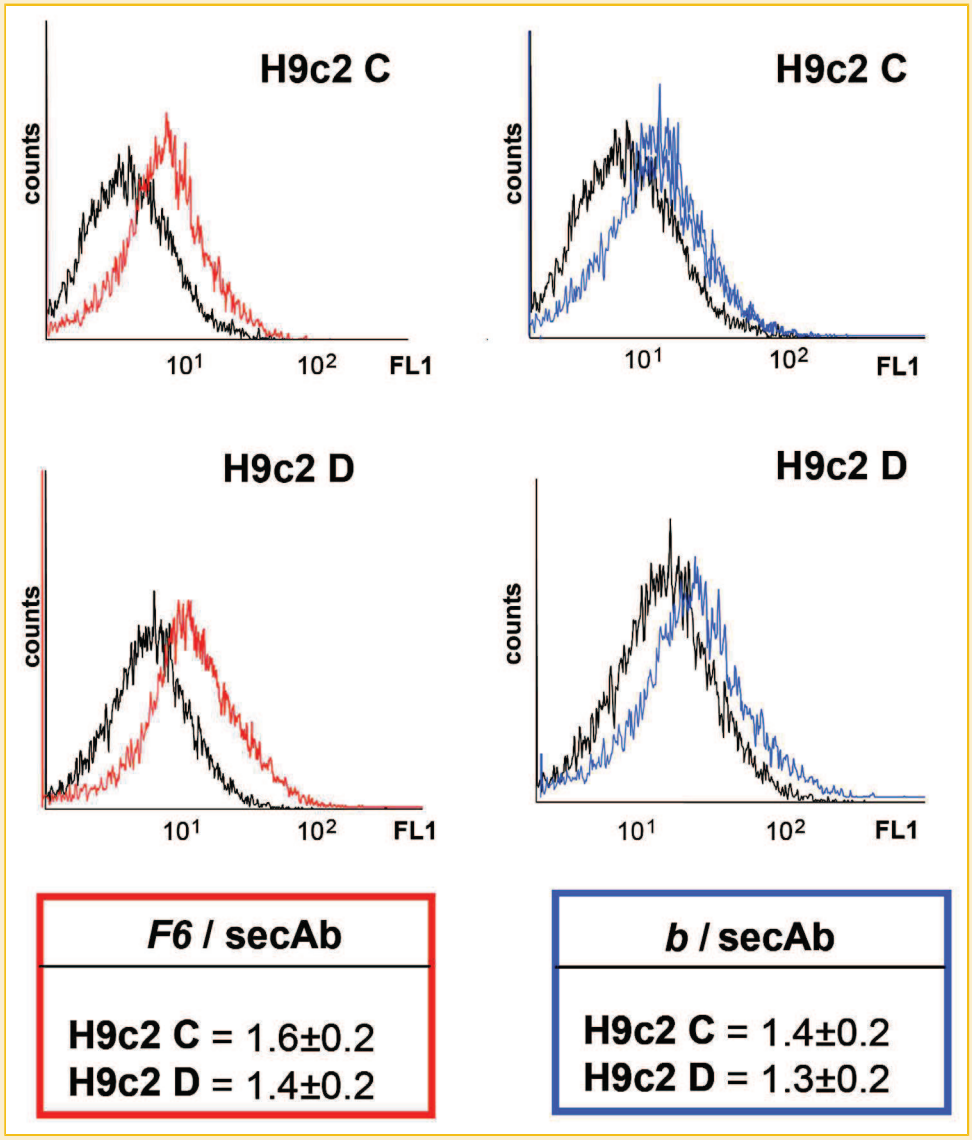

Fig. 5. Flow cytometry analysis of the ectopic expression of ATP synthase F_6- and *b*-subunits in parental and cardiac-like differentiated H9c2. Parental (H9c2 C) and differentiated (H9c2 D) cells were treated and analyzed by cytofluorimetry as described in Methods. Histogram plots: black (left) traces indicate cells incubated in the presence of only the secondary antibody, red or blue (right) traces cells incubated with anti-*F6* or anti-*b* antibody. One experiment representative of three is shown. The mean fluorescence values relative to their own negative controls are reported in the inserts (mean ± SD; n = 3; $^*P < 0.001$).

Briefly, cells fixed with 3.7% paraformaldehyde in phosphate-buffered saline pH 7.4 (PBS) were washed three times with PBS and treated with (permeabilized cells) or without (intact, non-permeabilized cells) 0.2% Triton X-100 for 5 min. Cells were then incubated for 3 h in blocking solution (1% bovine serum albumin in PBS) at room temperature with primary antibodies. After three washings with PBS, cells were stained for 2 h at room temperature with FITC-conjugated or TRIC-conjugated IgG. After washings, the coverslips were mounted in glycerol-based mounting fluid (Chemicon International), and examined with a laser scanning microscope equipped with a 488–534 nm Ar laser and a 633 nm He-Ne laser (Leica TCS NT, Leica Mycrosystems, Wetzlar, Germany) by confocal optical sections taken through the z-axis. Five microscope fields per slide (at least two slides) were viewed for each group analysed. The cells showed a staining pattern symptomatic of homogeneous populations. An accurate setting of the instrument allowing to minimize spectral overlap was made in order to evaluate the merged images correctly. The specificity of the immunostaining pattern was confirmed by verifying that no staining was observed in control cells treated with only secondary antibodies.

IN SITU PROXIMITY LIGATION ASSAY (PLA)

To analyse the protein–protein interaction, we used the in situ PLA technology Olink Bioscience (Uppsala, Sweden) following manufacturer's instructions. Briefly, this method utilizes dual target recognition of two proteins that putatively interact, and consists of a pair of primary antibodies raised in different species and two

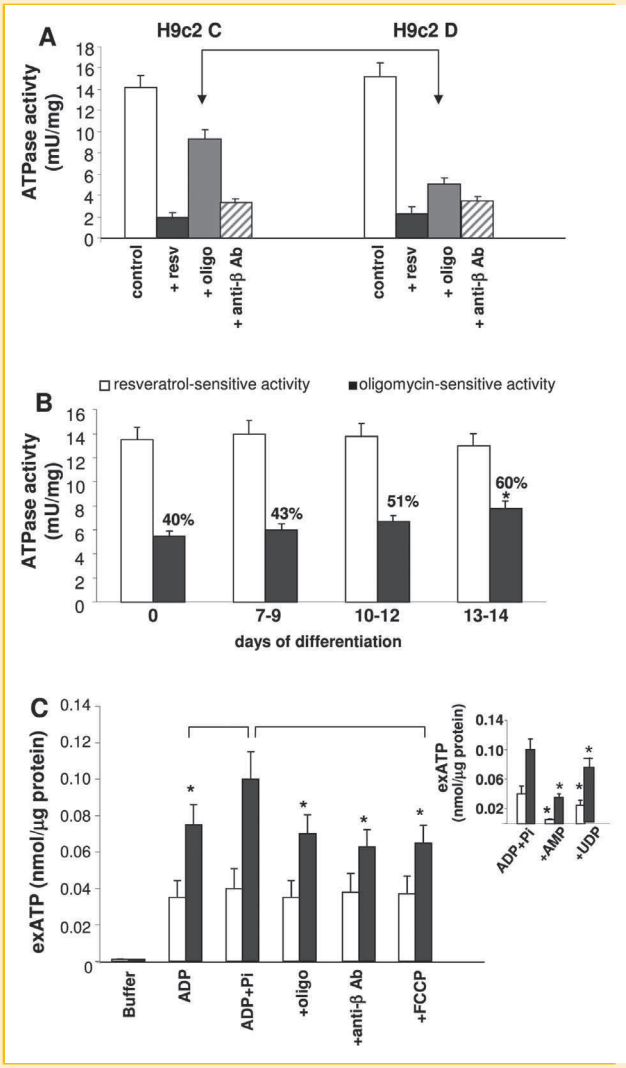

Fig. 6. exATP hydrolysis rate and exATP production by ecto-F_1F_O ATP synthase on cell surface of H9c2 and effect of cardiac-like differentiation. (A) Maximal exATP hydrolysis rate by intact parental (H9c2 C) and differentiated (H9c2 D) cells was analyzed by a spectrophotometric coupled pyruvate kinase/lactate dehydrogenase assay, in the absence or in the presence of the indicated inhibitors (20 μM resveratrol, 10 μM oligomycin, 1:100 anti-β Ab). Values represent means ± SD of three different experiments. The arrows mark the only significant difference observed ($P < 0.01$) in H9c2 D *vs* H9c2 C. (B) Ecto-ATPase activity (resveratrol-sensitive) and ATPase activity of holo-F_OF_1 ATP synthase (oligomycin-sensitive) by intact cells were analyzed during the differentiation protocol. Values represent means ± SD of three different experiments. (C) Ex-ATP production was measured in parental (white columns) and differentiated H9c2 (black columns), incubated with buffer alone (buffer), or with buffer plus ADP (ADP), or with buffer plus ADP and Pi (ADP+Pi). After 30 s the medium samples were collected and ATP measured by luciferin-luciferase assay. Measurements in the presence of (ADP+Pi) were also made after 15 min pretreatment with specific inhibitors: 10 μM oligomycin (oligo), AMP (11 mM) (in the insert), UDP (2 mM) (in the insert), FCCP (25 μM) and anti-β antibody (1:100). Basal ex-ATP levels in the absence of ADP (buffer) produced bioluminescence signals <3% of the uninhibited levels in the presence of ADP+Pi. Three separate experiments were performed in triplicate. Data shown are means ± S.D., n = 3, $^*P < 0.01$ vs. ADP+Pi. Experimental procedures are in Methods and *Supporting Information*.

different secondary antibodies conjugated with oligonucleotides (PLA probes). If the two antibodies bind epitopes that are in close proximity on interacting proteins, the oligonucleotides will also be brought into proximity and form a DNA circle that will be replicated using rolling circle amplification (RCA). The RCA product, made of fluorophore-labeled oligonucleotides, can be easily detected by confocal microscopy as a brightly fluorescent, submicrometer-sized spot (PLA signal) [Leuchowius et al., 2010]. Technical controls, represented by the omission of primary antibodies, resulted in the complete loss of PLA signal. Cells were visualized through a Leica TCS SP laser-scanning confocal microscope (Leica Microsystems, Wetzlar, Germany).

FLOW CYTOMETRY

Sub-confluent cells were washed twice in PBS, and treated as in [Contessi et al., 2007]. Briefly, cells detached with trypsin-EDTA were fixed with 3.7% paraformaldehyde in PBS for 15 min, and washed twice in blocking solution (PBS containing 1% BSA). Fixed cells were incubated in blocking solution with primary antibodies at 20°C for 1 h. The cells were then washed in PBS and incubated with FITC-conjugated IgG at 20°C for 30 min. After washings in PBS, cells were suspended at a concentration of 2×10^6 cell/ml in PBS and analyzed with a FACScan flow cytometer (Becton–Dickinson, New York) equipped with a single argon laser at 488 nm (excitation wavelength). The emission was monitored at 530 nm (FL-1 green fluorescence). The scatter plot showed a homogeneous cell population with no dead cells or debris for all the analyzed conditions. Data were acquired in list mode and analyzed with CellQuest Software (Becton–Dickinson, New York). 10,000 cells were analyzed per group.

EXTRACELLULAR ATP HYDROLYSIS ASSAY

The rate of extracellular ATP (exATP) hydrolysis by intact cells was measured by an enzyme-coupled assay with ATP-regenerating system according to [Comelli et al., 2011], using an UV plate reader equipped with a 340 nm filter (EL 808, Bio-Tek Instruments Inc., Winooski, VT). Cell suspensions were pre-incubated 15 min at room temperature with or without inhibitors. For details, see *Supporting Material*.

EXTRACELLULAR ATP PRODUCTION

Adherent cells were pre-incubated 15 min at 37°C with or without inhibitors, 50 μM ADP alone or plus 5 mM Pi was added and exATP generated after 30 s was measured using the ATP bioluminescence kit ATPlite (Perkim Elmer, Groningen, The Netherlands), following manufacturer's instructions. Luminescence was measured in a microplate luminometer (Modulus II-Turner Biosystems). After the assay, viability was monitored in each microplate well by Trypan blue test. For details, see *Supporting Material*.

STATISTICAL ANALYSIS

Data are reported as means ± S.D. Intergroup comparison were made using unpaired two-tailed Student's *t*-test. Values of $P > 0.05$ were considered as not statistically significant and were not indicated.

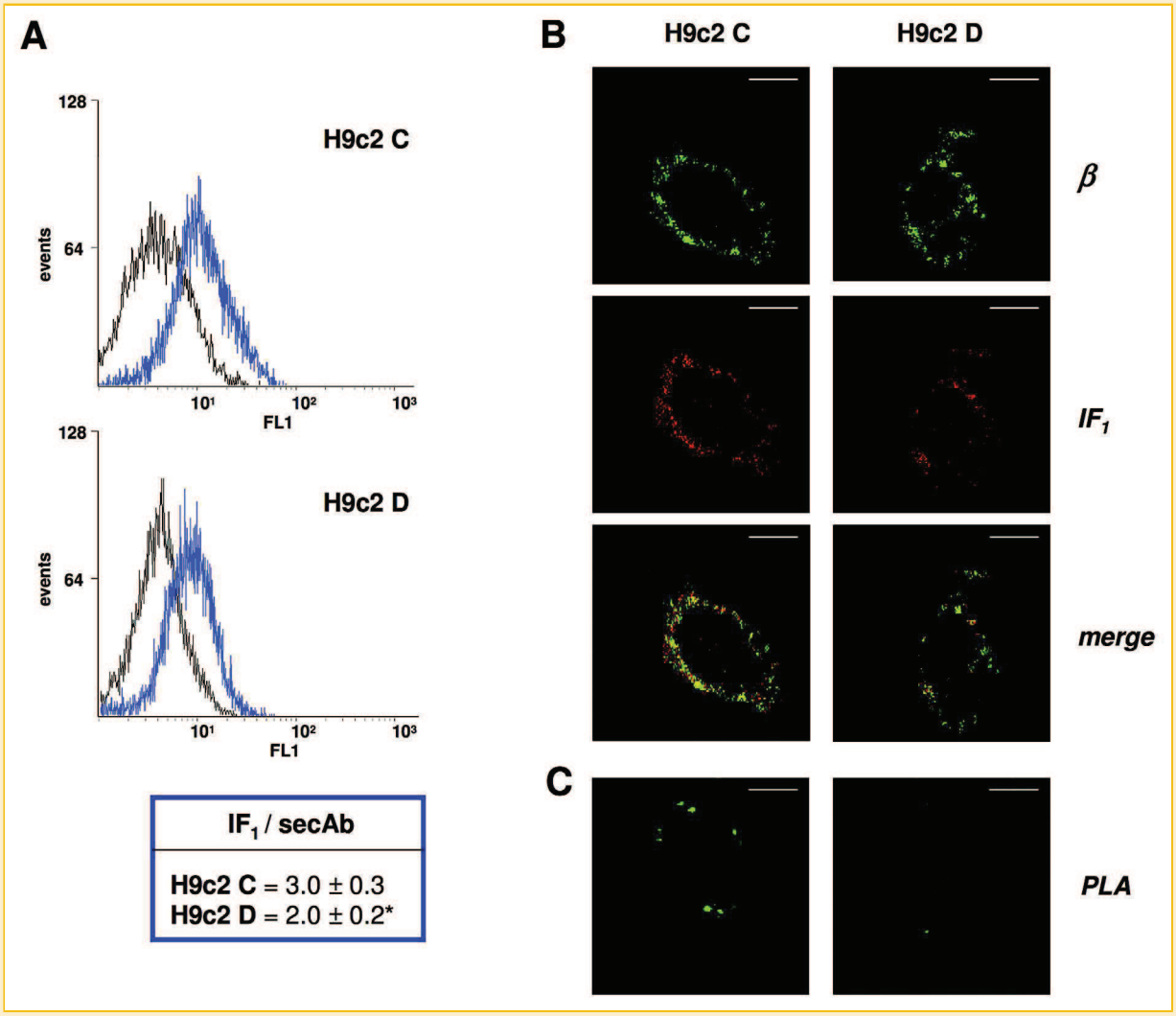

Fig. 7. IF_1 expression on the surface of H9c2 cells and interaction with ecto-F_1F_O ATP synthase are affected by cardiac-like differentiation. Parental (H9c2 C) and differentiated (H9c2 D) cells were treated and analyzed by cytofluorimetry and confocal microscopy (cell surface immunostaining and *in situ* PLA assay) as described in Methods. (A) Citofluorimetry histogram plots: black traces (left histograms) indicate cells incubated in the presence of only the secondary antibody and blue traces (right histograms) cells incubated with anti-IF_1 antibody. One experiment representative of three is shown. The mean fluorescence values relative to their own negative controls are reported in the insert (mean ± SD; n = 3; $^*P < 0.01$). (B) Confocal microscopy analysis of live cells doubly labelled with monoclonal anti-β and polyclonal anti-IF_1 antibody. The merged image indicates colocalization of the two fluorophores. Representative images of three separate experiments were reported. Bars=30 μm. (C) Images from *in situ* PLA assay used to demonstrate the IF_1-β interaction. Distinct fluorescent dots (PLA signals), indicating the occurrence of interaction, are evident in H9c2 C. Representative images of three separate experiments were reported. Bars =30 μm.

RESULTS AND DISCUSSION

F_1F_O ATP SYNTHASE ON THE SURFACE OF EMBRYONIC RAT HEART-DERIVED H9C2 CELLS

We tested for the presence of ecto-F_1F_O ATP synthase embryonic rat heart-derived H9c2 cells using immunofluorescence. We compared the data with hepatic HepG2 cells where an abundant ecto-cellular expression of the enzyme was well documented, and its subunit composition was thoroughly investigated [Bae et al., 2004; Contessi et al., 2007; Kim et al., 2010]. Analyses were carried out for two subunits with different properties, that is the hydrophilic ATP synthase-β, that is part of the catalytic F_1 sector, and the partially hydrophobic ATP synthase-*b*, assigned to the peripheral stator stalk. Subunits of F_O domain were not investigated taking into account the challenging immunostaining of such subunits, which are largely hydrophobic and membrane-embedded. In H9c2 cells the ectopic expression was well detectable for ATP synthase-β and hardly visible but not negligible for ATP synthase-*b* (Fig. 1A, upper pictures), compared to HepG2 where they were both well detectable (Fig. 1A, lower pictures). The focus of the analysis in Figure 1 was to demonstrate the localization on the cell surface of the two ATP synthase subunits by the accessibility of externally added

antibodies, while flotillin served to label cell profile (Fig. 1A). Non-permeabilized cells showed a patchy and punctuate staining pattern resembling cell profile and suggesting that ATP synthase-β and ATP synthase-*b* localize to plasma membrane in H9c2, as for HepG2 cells [Contessi et al., 2007]. Immunostaining of flotillin, a marker of lipid rafts, showed an analogous patchy and punctuate pattern (Fig. 1A). This was in accordance with the localization of ecto-F_1F_O ATP synthase in lipid rafts from plasma membranes reported for several cell types [Bae et al., 2004; Wang et al., 2006; Kim et al., 2010; Raj et al., 2013]. Absence of immunofluorescence signal in cells treated with only secondary antibody (*Supplementary Fig. 1 and 2*) indicated that the staining pattern was specific for ATP synthase-β or ATP synthase-*b*. Indeed, no cross-reactions were expected due to the high specificity of the primary antibodies, as verified by immunoblotting analyses of detergent-extracts of the cells (not shown). When cells were doubly labelled with anti-β and anti-*b* antibodies, even if the staining for ATP synthase-*b* was little appreciable, the merged image displayed a yellowish-orange punctuate staining, mainly matching ATP synthase-*b* brighter spots, and recalling co-localization of the two subunits (*Supplementary Fig. 3)*. Of note, parallel experiments run on permeabilized cells showed for both β and *b* subunits a very different pattern, typical of mitochondrial staining with a characteristically tubular/reticular appearance (Fig. 1B).

In conclusion, we are confident that both ATP synthase-β and ATP synthase-*b* localize on the cell surface of H9c2, though ATP synthase-*b* is only just observable if compared to ATP synthase-β. As the subunit organization of the ecto-F_1F_O complex should reflect that of the mitochondrial complex [Yonally et al., 2006; Wang et al., 2006; Ma et al., 2010; Rai et al., 2013], the low immunostaining of ATP synthase-*b* may be ascribed to its low accessibility. Indeed, based on the known structure of the peripheral stator stalk of the mitochondrial enzyme [Rees et al., 2009; Baker et al., 2012], a very extensive area of the membrane extrinsic region of subunit *b* is buried from its interactions with subunits *d* and *F6*. Nevertheless, considering the well detectable immunofluorescence staining observed in mitochondria (Fig. 1B), as well as on HepG2 cell surface (Fig. 1A), which is in line with a high expression of F_1F_O ATP synthase, we can state that the hardly visible ATP synthase-*b* signal is consistent with low levels of F_1F_O ATP synthase.

We validated confocal microscopy data by cytofluorimetric analyses and quantified the expression of ATP synthase-β on the cell surface of H9c2 with reference to HepG2 cells (Fig. 1C). For both cell types data showed a noticeable increase in the mean fluorescence intensity when cells were labelled with anti-β antibody, relative to that observed omitting the primary antibody. The values for H9c2 were 3.6-fold lower than HepG2, in line with a lower ectopic expression of F_1F_O ATP synthase for non-tumoral cells [Bae et al., 2004; Yonally et al., 2006; Mangiullo et al., 2008; Rai et al., 2013; Wang et al., 2013].

EFFECTS OF CARDIAC-LIKE DIFFERENTIATION ON THE ECTO-F_1F_O ATP SYNTHASE EXPRESSION

Proliferating H9c2 myoblasts are not fully differentiated cardiac cells and can be differentiated towards a more cardiomyocyte-like phenotype by culturing cells in reduced serum medium containing *all-trans* retinoic acid. These conditions promote the expression of L-type Ca^{2+} channel and troponin 1 and induce the appearance of cardiomyocyte-like ultrastructural features [Menard et al., 1999; Comelli et al., 2011]. Cells induced to differentiate towards the more cardiomyocyte-like phenotype were recently validated as a good model to investigate the cardioprotective and cardiotoxic actions of quercetin and its in vivo metabolites [Daubney et al., 2015].

We decided to verify the hypothesis that in differentiated H9c2 cells well assembled/coupled F_1F_O ATP synthase complexes would be present in greater amount at cell surface, as already observed in mitochondria [Comelli et al., 2011; Bisetto et al., 2013]. With this aim, we induced H9c2 cells to differentiate towards the cardiac lineage and monitored by immunofluorescence the effects on ecto-F_1F_O ATP synthase. The overall description of the differentiating treatments was outlined in Figure 2, together with some characteristics acquired by the cells and relevant for the discussion of the results (i.e., growth rate, cardiac markers, mitochondrial mass, and mitochondrial F_1F_O ATP synthase assembly). During the treatment, cytotoxicity was verified by a sensitive LDH-release assay, as widely reported for several cell systems [Jurisic, 2003; Jurisic et al., 2004]. Very low treatment cytotoxicity was observed (Fig. 2C) after either 7 ($8.5 \pm 0.1\%$) or 14 days ($8.2 \pm 0.2\%$), similar to that of proliferating parental cells ($9.0 \pm 0.1\%$). We focused on the catalytic subunit ATP synthase-β together with three subunits composing the peripheral stator stalk, which is responsible for the correct F_1-F_O assembly/coupling, specifically OSCP, *b*, and *F6*. Confocal microscopy analysis for ATP synthase-β (Fig. 3A) showed a patchy and punctuate staining pattern, resembling flotillin, in both parental (upper pictures) and cardiac-like differentiated (lower pictures) cells. Quantification by cytofluorimetric analysis showed very similar values for ATP synthase-β on the cell surface of parental and differentiated cells (Fig. 3B).

For OSCP, flow cytometry indicated a significantly more marked ectopic expression in differentiated H9c2 with respect to control cells (Fig. 4A). Confocal microscopy showed a well-defined fluorescent signal symptomatic of plasma membrane localization both in control and in differentiated cells and, when cells were doubly labelled with anti-β and anti-OSCP antibodies, the merged images displayed a yellowish-orange punctuate staining recalling co-localization of the two subunits, that appears to be enhanced in cardiac-like differentiated cells (Fig. 4B). Then we decided to verify the actual assembly of OSCP within the ecto-F_1F_O ATP synthase, and we carried out a protein–protein interaction analysis by *in situ* PLA to get evidence on intact cells. PLA assay is a highly selective and sensitive method for detecting protein–protein interaction and it has been applied to a range of different biological systems [Leuchowius et al., 2010]. Based on the mitochondrial F_1F_O ATP synthase structural data documenting that OSCP interacts at the top of F_1 domain with the subunit α and to a less extent with β [Rees et al., 2009], we probed OSCP interaction with the enzyme using a polyclonal antibody able to recognize α/β subunits. A clear PLA signal visible as distinct florescent green dots was exhibited by only cardiac-like differentiated cells (Fig. 4C), where ecto-OSCP was expressed more than twofold of the parental cells. Thus, taking advantage from the high sensitivity of the method, we can state that such signal is consistent with increased levels

induced by the differentiation of the amount of OSCP really interacting within the enzyme complex. Nevertheless, we cannot rule out improved detection of signal resulting from conformational changes in the enzyme as a possible explanation. Contrary to OSCP, cytofluorimetric analyses for subunits *F6* and *b* showed low immunofluorescence at the surface of H9c2 cells and no increase during differentiation (Fig. 5). The low immunostaining of *F6*, as stated above for ATP synthase-*b*, might be in line with the buried surface area in *b*-*F6* interface, based on the known structure of the peripheral stator stalk of mitochondrial enzyme [Rees et al., 2009; Baker et al., 2012]. Indeed, subunits *F6* and *b* are partially masked by each other, differently from OSCP that sits on top of the F_1 domain.

It is worth mentioning that the F_1F_O ATP synthase mitochondrial biogenesis is reported to involve an assembly from modular sub-assemblies [Fox, 2012], with the two main sub-assemblies expected in membrane being F_1-c ring (containing subunits β) and *a*-*A6L* linked to incomplete stator stalk (containing subunit *b* but not OSCP). On these bases, it may be inferred that the immuno-detection of subunits β and *b*, cannot discriminate between sub-assemblies and assembled enzyme complexes. Conversely, OSCP can be immuno-detected only in the assembled enzyme complex, as the final assembly appears to involve the binding of OSCP, completing the stator stalk, along with the joining of the two sub-assemblies [Fox, 2012]. Based on these considerations, our data might account for the existence of sub-assemblies on the surface of parental H9c2 cells, together with properly assembled F_1Fo complexes, which seem to augment along with the cardiac-like differentiation.

EFFECTS OF THE CARDIAC-LIKE DIFFERENTIATION ON EXATP HYDROLYSIS AND EXATP PRODUCTION BY ECTO-F_1F_O ATP SYNTHASE

As its name implies, OSCP is necessary for F_1F_O ATP synthase to display sensitivity to oligomycin, a well-known inhibitor of the enzyme activity able to prevent the catalytic rotation through its binding to F_O sector, at the interface between the *c*-ring and subunit *a* [Devenish et al., 2000]. The requirement of OSCP probably reflects its important protein–protein interactions made within the assembled complex and transmitted down the peripheral stator stalk, influencing proton channel function and favoring the F_1-F_O coupling. Thus, oligomycin inhibits the ATPase/synthase activity only of the correctly assembled and well coupled F_1F_O complex (holo-F_1F_O ATP synthase). Based on these considerations, we further investigated the possible effect of cardiac-like differentiation of H9c2 on the exATP hydrolysis rate and exATP production by the enzyme at cell surface, focusing in particular on the oligomycin effects.

When we studied the exATP hydrolysis rate, we also used the F_1–targeting inhibitor resveratrol, able to suppress the contribution of uncoupled F_1-F_O complexes and/or sub-assemblies, if there are any, together with that of holo-F_1F_O ATP synthase. Moreover, using resveratrol allowed us to ignore possible intracellular interferences, considering that it was shown to not promptly cross cell membranes [Arakaki et al., 2003]. The results reported in Fig. 6A show that the exATP hydrolysis rate was reduced by more than 75% by 20 μM resveratrol in both parental and cardiac-like differentiated H9c2. Such a marked reduction was elicited also by the antibody for the F_1 catalytic subunit ATP synthase-β, thereby demonstrating low contributions by interferences on cell surface. As the reduction by the antibody resembled the effect of resveratrol, this result validated a good selectivity of resveratrol for the enzyme under our conditions. Thus, the value of exATP hydrolysis rate suppressed by resveratrol was considered as a measure of the enzyme activity at cell surface (ecto-ATPase activity), which resulted to be not significantly different for parental and cardiac-like differentiated cells (13.5 ± 1.5 vs. 12.7 ± 1.4 mU/mg). Conversely, the exATP hydrolysis rate suppressed by oligomycin, estimated as a measure of the ATPase activity of holo-F_1F_O ATP synthase only, was low in parental cells (i.e., 40%) and increased significantly ($P < 0.01$) during the differentiation up to 60% (ecto-ATPase activity taken as 100%) (Fig. 6B). These results indicate that holo-F_1F_O ATP synthase was present at the cell surface of H9c2, it was catalytically competent and augmented in cardiomyocyte-like differentiated cells. Moreover, the finding that a significant portion of the ecto-ATPase activity was insensitive to oligomycin, mainly in the parental cells, suggests that uncoupled complexes and/or sub-assemblies have to be present on the plasma membrane, thus supporting our assumption explaining the immunofluorescence data (see above).

If ecto-F_1F_O ATP synthase is homologous to the mitochondrial enzyme, the holo-enzyme at the cell surface might be able not only to hydrolyse but also to synthesize exATP [Stock et al., 1999], although this aspect is largely debated based on energetic considerations [Mangiullo et al., 2008; Moser et al., 2011; Panfoli et al., 2011; Harris and Attwel, 2012]. Therefore, we thoroughly analyzed exATP production by H9c2 cells, and investigated the effect of the cardiac-likedifferentiating treatment. There are three known enzymes by which exADP may be converted to exATP at the cell surface, specifically adenylate kinase (AK), nucleoside diphosphokinase (NDPK), and F_1F_O ATP synthase; among these AK is recognized to have a prevalent role despite some differences depending on the cell characteristics [Vantourout et al., 2010]. Contrasting with AK and NDPK, F_1F_O ATP synthase requires inorganic phosphate (Pi) to catalyse the ATP synthesis from ADP. Thus, we evaluated the relative contributions of these enzymes based on such substrate specificity, and using a pharmacologic approach with inhibitors. We monitored the exATP production after exposure of intact cells to ADP, or ADP plus Pi, in the absence, or in the presence of oligomycin, or AMP, or UDP, to inhibit the single enzymes selectively (specifically oligomycin to inhibit F_1F_O ATP synthase, AMP to inhibit AK and UDP to inhibit NDPK). For each inhibitor conditions were settled based on inhibitor-titrations experiments (*Supplementary Fig. 4)*, in the range of inhibitory concentrations reported for other cell types [Yegutkin et al., 2001; Fabre et al., 2006; Vantourout et al., 2010]. ATP release from intracellular pool was avoided by accurately monitoring the cell viability for each microplate well (Trypan blue exclusion test, data not shown). In accordance, the level of ATP measured in the absence of exADP was very low (Fig 6C). The exATP generation after adding ADP greatly increased in both parental and differentiated cells (Fig. 6C), indicating that AK represented a major contribution as expected. The addition of ADP+Pi significantly increased (+25%)

the exATP production with respect to ADP alone by cardiac-like differentiated cells only (Fig. 6C, black bars). Based on the Pi substrate specificity, this suggests a role of ectopic holo-F_1F_O ATP synthase in such cells but not in the parental counterpart. In accordance, AMP reduced markedly the exATP production (Fig. 6C inset), confirming a great contribution of AK, which however was not exclusive in cardiac-like differentiated cells, as AMP-inhibition was significantly less (i.e., −65% *vs* −87% in parental cells). Although searching for an explanation for such decrease of AK activity is not the purpose of our work, it may enhance the relative contribution of ectopic holo-F_1F_O ATP synthase in cardiac-like differentiated H9c2 cells. UDP had a less, but still significant effect (Fig. 6C inset), which was not affected by differentiation under our conditions (-22% *vs* −25% in parental cells). Of note, treatment with oligomycin prevented the generation of ADP+Pi-stimulated exATP and reduced (−30%) the conversion of exADP to exATP to the level observed with ADP alone. A similar preventive effect was observed also in the presence of anti-β antibody (−37%), confirming that ADP+Pi-stimulated exATP generation was by ectopic holo-F_1F_O ATP synthase and pointing to a high specificity of oligomycin under our conditions. No effects were elicited on the parental cells either by oligomycin or anti-β antibody. Thus we ascribed to ectopic holo-F_1F_O ATP synthase a different part in the exATP production by the two cell types, that is considerable for cardiac-like differentiated H9c2 cells (black bars), but negligible for parental cells (empty bars). Addition of the protonophore FCCP, known as a mitochondrial uncoupler, suppressed the generation of ADP+Pi-stimulated exATP by differentiated cells and, similarly to oligomycin or anti-β antibody, reduced exATP production (−35%) to a level near to that of ADP alone. In accordance with various reports about different cell types [Arakaki et al., 2003; Mangiullo et al., 2008; Moser et al., 2011; Panfoli et al., 2011; Wang et al., 2012], we consider this clear effect of the protonophore as an evidence for the assumption that the plasma membrane might employ an electrochemical gradient of protons (may be established locally by still unknown pathways) and ectopic holo-F_1F_O ATP synthase to generate exATP. Whether this occurs in heart is unknown, and further investigation is needed to assess the plausibility of this hypothesis.

In summary, the contribution of ectopic holo-F_1F_O ATP synthase to exATP production appears to be significant in cardiac-like differentiated H9c2 only, although to a less extent with respect to AK. Interestingly, although no direct evidence is provided for F_1F_O assembly on the cell surface, the ADP+Pi-stimulated exATP production by ectopic holo-F_1F_O ATP synthase, becomes detectable in concomitance with the increase in OSCP expression and its interaction with α/β subunits. This analysis corroborates in situ PLA results and suggests more well assembled F_1-F_O complexes at the cell surface. Thus, based on the evidence provided by others [Yonally et al., 2006; Wang et al., 2006; Ma et al., 2010; Rai et al., 2013] that makes it unlikely that the enzyme assembles on the plasma membranes, we postulate that sub-assemblies may be transported as holo-F_1F_O ATP synthase from mitochondria to the plasma membranes. Then we may infer that the biogenesis of F_1F_O complexes, that was shown to take place in mitochondria concomitant with the H9c2 cardiac-like differentiation, was able to reduce the presence of sub-assemblies vs. assembled F_1F_O complexes also on plasma membrane, as occurred in mitochondria.

Accordingly, in the parental cells the absence of contribution to exATP production by the holo-enzyme is consistent with the prevalence of sub-assembled/uncoupled complexes; nevertheless, we cannot exclude the involvement of factors reducing exATP generation by the holo-enzyme in such cells.

EFFECTS OF THE CARDIAC-LIKE DIFFERENTIATION ON THE ECTO-F_1F_O ATP SYNTHASE REGULATORY PROTEIN IF_1

Another point that deserves consideration is the possibility that the cardiac-like differentiation may affect the ectopic expression of the regulatory protein ATPase Inhibitory Factor 1 (IF_1), if there is any in embryonic rat heart-derived myoblasts as in endothelial and hepatic cells [Burwick et al., 2005; Cortes-Hernandez et al., 2005; Contessi et al., 2007; Mangiullo et al., 2008]. In order to investigate this aspect, we evaluated by immunofluorescence the ecto-IF_1 expression in parental H9c2 and in differentiated cells. As shown in Fig. 7, IF_1 is actually present on the surface of these cells and differentiation shows a peculiar effect. Cytofluorimetry demonstrated that the IF_1 ectopic expression level was higher in parental than in differentiated cells (Fig. 7A). A greater IF_1/ATP synthase-β ratio was inferred for parental cells with respect to cardiac-like differentiated cells, due to the significant difference of IF_1 expression compared to the equal levels of its natural target ATP synthase-β at the cell surface. Confocal microscopy showed a good co-localization of IF_1 with ATP synthase-β (merged images), which appeared to be more intense in parental cells (Fig. 7B). The analysis by in situ PLA documented that a signal, visible as distinct florescent green dots, was exhibited only by parental cells (Fig. 7C), suggesting that in this case IF_1 really interacts with ATP synthase-β at the cell surface.

These data are consistent with a higher binding of the regulatory protein IF_1 to its target subunit β within the enzyme complexes on the surface of parental proliferating H9c2, thereby evoking a more strictly regulatory role in these cells with respect to cardiac-like differentiated cells. Based on the known properties of IF_1 binding to mitochondrial F_1F_O ATP synthase [Green and Grover, 2000; Bason et al., 2011] and considering our data about the enzyme activity on the surface of the parental cells (i.e., low sensitivity to oligomycin and undetectable generation of ex-ATP), we postulate that more regulation by IF_1 might be required by the presence on the surface of the parental cells of smaller quantity of holo-F_1F_O ATP synthase and greater quantity of sub-assemblies. Of note, in agreement with our hypothesis are the previous reports revealing in different models of genetic disorders a great IF_1 quantity associated to F_1F_O ATP synthase sub-assemblies in mitochondrial membrane [Carrozzo et al., 2006; Mourier et al., 2014]. To reinforce our evidence we exposed the parental myoblasts to lower pH, considering that decrease of pH favors IF_1 binding to ATP synthase. Under conditions mimicking acidosis without affecting cell viability (i.e., pH 7.0), the ATPase activity of the enzyme at the cell surface was 20% lower than at pH 7.4 (results not show), supporting our hypothesis that endogenous IF_1 is able to regulate the enzyme at the cell surface of myoblasts.

The relevance of our study is in the fact that few reports provided evidence for an inhibitory effect elicited by endogenous IF_1 on the enzyme on the cell surface [Cortes-Hernandez et al., 2005; Contessi et al., 2007; Mangiullo et al., 2008; Giorgio et al., 2010; Ravera et al., 2011; Martinez et al., 2015], and none was in the context of cardiac-like differentiation.

CONCLUDING REMARKS

The present study is the first to demonstrate that holo-F_1F_O ATP synthase was expressed on the plasma membranes of embryonic rat heart-derived myoblasts, also showing that it increased along with cardiac-like differentiation, as occurs in mitochondria. As a matter of fact, the results of the functional measurements together with the *in situ* PLA data for OSCP corroborate the hypothesis of a higher expression of ecto-F_1F_O complexes that were properly assembled/coupled on the surface of cardiac-like differentiated cells. Of note, a contribution of F_1F_O ATP synthase to the exATP production (specifically ADP+Pi-stimulated exATP generation) was observed in differentiated cells. Conversely, in the parental counterpart the finding that exATP hydrolysis ascribed to the enzyme was largely oligomycin-insensitive is in line with the deficit of OSCP and suggests the occurrence of sub-assemblies. Overall, our results are consistent with the hypothesis that plasma membrane can reflect the forms resident inside mitochondrial membrane and the modifications occurring during cardiac-like differentiation and enzyme complex biogenesis. It is difficult to exclude based on our data that the plasma membrane localization of the enzyme complex is just an aberration of cell trafficking in a cultured cell line. Nevertheless, one may infer that it is not the case based on evidence from different laboratories on i) rat liver plasma membranes [Giorgio et al., 2010; Raj et al., 2013], ii) rat liver *ex vivo* [Martinez et al., 2003], iii) mice liver in vivo [Song et al., 2014]. Further investigations on heart are needed. Notably, the expression of ecto-IF_1 was reduced by differentiation opposed to OSCP, and the interaction of IF_1 with ATP synthase-β observed at the cell surface suggests that it might regulate the prevailing exATP hydrolysis by the enzyme in parental cells (at least partially due to sub-assemblies).

Defining the role of the enzyme on the plasma membrane of H9c2 cells is out of the purpose of our work. Several laboratories largely investigated the role of the enzyme on endothelial and tumoral cells, hepatocytes, adipocytes, myotubes [Vantourout et al., 2010 and references therein], as well as in developing muscle cells [Garcia al., 2011] and neural cells [Xing et al., 2012]. Hence, it is now accepted that cell surface ATP synthase likely functions as a cell surface receptor for a number of ligands triggering hydrolysis or synthesis of ATP in the extracellular milieu. In that way, it regulates H^+ concentration across the membrane and affects purinergic signaling [Chi et al., 2006; Vantourout et al., 2010]. The more studied ligands are: angiostatin [Moser et al., 2011], coupling factor 6 [Osanai et al., 2012], apoliporotein A–I (ApoA–I) [Martinez et al., 2015], oligomeric amyloid-β peptide (Aβ) and the amyloid precursor protein [Xing et al., 2012], α2/δ1 subunit of calcium channels [Garcia al., 2011]. Consequently, cell surface ATP synthase seems to be involved in processes as angiogenesis, vascular tone, cholesterol, and lipoprotein metabolism [Chi et al., 2006; Kim et al., 2010], calcium release regulation especially during early development of myotubes [Garcia al., 2011], oligomeric Aβ neurotoxic effects and neurodegeneration [Xing et al., 2013]. Thus, the emerging idea is that cell surface ATP synthase may be an intervening target of pathogenesis of several diseases (e.g., cancer, atherosclerosis, hypertension, and lipid disorders, Alzheimer disease). In this scenario, it is tempting to postulate two of the roles mentioned above as more likely to be played by the enzyme in H9c2 cells, considering that i) the regulation of Ca^{2+} homeostasis in cardiomyocytes is crucial as in myotubes, α2/δ1 subunits are the same in both cardiac and muscle calcium channels [Kamp and Hell, 2000] and the expression of L-type Ca^{2+} channel was shown to be promoted in H9c2 by the cardiomyocyte-like differentiation [Menard et al., 1999], ii) cardiac amyloidosis is a rare but known cause of cardiomyopathies, and mainly disorders of the conduction system and valves [Falk andDubrney, 2010].

ACKNOWLEDGMENT

We are thankful to Dr. Guy Waley for proofreading the English language of the manuscript. This work was supported by University of Udine.

REFERENCES

Arakaki N, Nagao T, Niki R, Toyofuku A, Tanaka H, Kuramoto Y, Emoto Y, Shibata H, Magota K, Higuti T. 2003. Possible role of cell surface H^+-ATP synthase in the extracellular ATP synthesis and proliferation of human umbilical vein endothelial cells. Mol Cancer Res 1:931–993.

Bae TJ, Kim MS, Kim JW, Kim BW, Choo HJ, Lee JW, Kim KB, Lee CS, Kim JH, Chang SY, Kang CY, Lee SW, Ko YG. 2004. Lipid rafts proteome reveals ATP synthase complex in the cell surface. Proteomics 4:3536–3548.

Baker LA, Watt IN, Runswick MJ, Walker JE, Rubinstein JL. 2012. Arrangement of subunits in intact mammalian mitochondrial ATP synthase determined by cryo-EM. PNAS 10:11675–11680.

Bason JV, Runswick MJ, Fearnley IM, Walker JE. 2011. Binding of the Inhibitor Protein IF_1 to Bovine F_1-ATPase. J Mol Biol 406:443–453.

Bisetto E, Comelli M, Salzano AM, Picotti P, Scaloni A, Lippe G, Mavelli I. 2013. Proteomic analysis of F_1F_O-ATP synthase super-assembly in mitochondria of cardiomyoblasts undergoing differentiation to the cardiac lineage. Biochim Biophys Acta 1827:807–816.

Carrozzo R, Wittig I, Santorelli FM, Bertini E, Hofmann S, Brandt U, Schagger H. 2006. Subcomplexes of human ATP synthase mark mitochondrial biosinthesis disorders. Ann Neurol 59:265–275.

Chi SL, Pizzo SV. 2006. Cell surface F_1F_O ATP synthase: A new paradigm?. Ann Med 38:429–438.

Comelli M, Domenis R, Bisetto E, Contin M, Marchini M, Ortolani F, Tomasetig L, Mavelli I. 2011. Cardiac differentiation promotes mitochondria development and ameliorates oxidative capacity in H9c2 cardiomyoblasts. Mitochondrion 11:315–326.

Comelli M, Metelli G, Mavelli I. 2007. Downmodulation of mitochondrial F0F1 ATP synthase by diazoxide in cardiac myoblasts: A dual effect of the drug. Am J Physiol Heart Circ Physiol 292:H820–H829.

Contessi S, Comelli M, Cmet S, Lippe G, Mavelli I. 2007. IF(1) distribution in HepG2 cells in relation to ecto-F(0)F(1)ATPsynthase and calmodulin. J Bioenerg Biomembr 39:291–300.

Cortes-Hernandez P, Dominiguez-Ramirez L, Estrada-Berna A, Montez-Sanchez DG, Zentella-Dehesa A, deGomez-Puyou MT, Gomez-Puyou A, Garcia JH. 2005. The inhibitor protein of the F_1F_O-ATP synthase is associated to the external surface of endothelial cells. Biochim Biophys Res Commun 330:844–849.

Daubney J, Bonner PL, Hatgreaves AJ, Dickenson JM. 2015. Cardioprotective and cardiotoxic effects of quercetin and two of its in vivo metabolites on differentiated H9c2 cardiomyocytes. Bas Clin Pharmacol Toxicol 116:96–109.

Devenish RJ, Prescott M, Boyle GM, Nagley GM. 2000. The oligomycin axis of mitochondrial ATP synthase: OSCP and the proton channel. J Bioenerg Biomembr 32:507–515.

Fabre ACS, Vantourout P, Champagne E, Tercè F, Rolland C, Perret B, Collet X, Barbaras R, Martinez LO. 2006. Cell surface adenylate kinase activity regulates the F1-ATPase/P2Y/13)-mediated HDL endocytosis pathway on human hepatocytes. Cell Mol Life Sci 63:2829–2283.

Falk RH, Dubrey SW. 2010. Amyloid heart disease. Prog Cardiovasc Dis 52:347–361.

Fox TD. 2012. Mitochondrial protein synthesis, import, and assembly. Genetics 192 1203–1234.

Garcia J. 2011. The calcium channel a2/≏1 subunit interacts with ATP5b in the plasma membrane of developing muscle cells. Am J Physiol Cell Physiol 301:C44–C52.

Giorgio V, Bisetto E, Franca R, Harris DA, Passamonti S, Lippe G. 2010. The ectopic F(0)F(1) ATP synthase of rat liver is modulated in acute cholestasis by the inhibitor protein IF1. J Bioenerg Biomembr 42:117–123.

Green DW, Grover GJ. 2000. The IF(1) inhibitor protein of the mitochondrial F (1)F(0)-ATPase. Biochim Biophys Acta 1458:343–355.

Harris JJ, Attwel D. 2012. Is myelin a mitochondrion?. J Cerebral Blood Flow Metab 1–4.

Hescheler J, Meyer R, Plant S. 1991. Morphological, biochemical, and electrophysiological characterization of a clonal cell (H9c2) line from rat heart. Circulation Res 69:1476–1486.

Jurisic V. 2003. Estimation of cell membrane alteration after drug treatment by LDH release. Blood 101:2894.

Jurisic V, Bumbasirevic V, Konjevic G, Djuricic B, Spuzic I. 2004. TNF-alpha induces changes in LDH isotype profile following triggering of apoptosis in PBL of non-Hodgkin′s lymphomas. Ann Hematol 83:84–91.

Kamp TJ, Hell JW. 2000. Regulation of cardiac L-type calcium channels by protein kinase A and protein kinase C. Circ Res 87:1095–1102.

Kim BW, Lee CS, Yi JS, Lee JH, Lee JW, Choo HJ, Yung SY, Kim MS, Lee SW, Lee MS, Yoon G, Ko Y. 2010. Lipid raft proteome reveals that oxidative phosphorylation system is associated with the plasma membrane. Expert Rev Proteomics 7:849–866.

Kuznetsov AV, Javadovb S, Sickinger S, Frotschnig s, Grimm M. 2015. H9c2 and HL-1 cells demonstrate distinct features of energy metabolism, mitochondrial function and sensitivity to hypoxiareoxygenation. Biochim Biophys Acta 1853:276–284.

Leuchowius KJ, Jarvius M, Wickstrom M, Rickardson L, Landegren U, Larsson R, Soderberg O, Fryknas M, Jarvius J. 2010. High content screening for inhibitors of protein interaction and post-translational modifications in primary cells by proximity ligation. Mol Cell Proteomics 9:78–183.

Ma Z, Cao M, Liu Y, He Y, Wang Y, Yang C, Wang W, Zhou YDM, Gao F. 2010. Mitochondrial F_1F_O-ATP synthase translocates to cell surface in hepatocytes and has high activity in tumor-like acidic and hypoxic environment. Acta Bioch Biophys Sin 242:530–537.

Mangiullo R, Gnoni A, Leone A, Gnoni GV, Papa S, Zanotti F. 2008. Structural and functional characterization of F_OF_1-ATP synthase on the extracellular surface of rat hepatocytes. Biochim Biophys Acta 1777:1326–1335.

Martinez LO, Jacquet S, Esteve JP, Rolland C, Cabezón E, Champagne E, Pineau T, Georgeaud V, Walker JE, Tercé F, Collet X, Bertrand Perret B, Barbara R. 2003. Ectopic β-chain of ATP synthase is an apolipoprotein A-I receptor in hepatic HDL endocytosis. Nature 421:75–79.

Martinez LO, Najib S, Perret B, Cabou C, Lichtenstein L. 2015. Ecto-F1-ATPase/P2Y pathways in metabolic and vascular functions of high density lipoproteins. Atherosclerosis 238:89–100.

Menard C, Pupier S, Mornet D, Kitzmann M, Nargeot J, Lory P. 1999. Modulation of L-type calcium channel expression during Retinoic acid-induced differentiation of H9C2 cardiac cells. J Biol Chem 274:29063–29070.

Moser TL, Kenan DJ, Ashley TA, Roy JA, Goodman MD, Misra UK, Cheek DJ, Pizzo SV. 2011. Endothelial cell surface F_1-F_O ATP synthase is active in ATP synthesis and is inhibited by angiostatin. Proc Natl Acad Sci USA 98:6656–6661.

Mourier A, Ruzzenente B, Brandt T, Kühlbrandt W, Larsson N. 2014. Loss of LRPPRC causes ATP synthase deficiency. Hum Mol Genet 23:2580–2592.

Osanai T, Tanaka M, Magota K, Tomita H, Okumura K. 2012. Coupling factor 6-induced activation of ecto-F1F(o) complex induces insulin resistance, mild glucose intolerance and elevated blood pressure in mice. Diabetologia 55:520–529.

Panfoli I, Ravera S, Bruschi M, Candiano G, Morelli A. 2011. Proteomics unravels the exportability of mitochondrial respiratory chain. Exp Rev Proteomics 8:231–239.

Pereira SL, Ramalho-Santos J, Branco AF, Sardao VA, Oliveira PJ, Rui AC. 2011. Metabolic remodeling during H9c2 myoblast differentiation: Relevance for in vitro toxicity studies. Cardiovasc Toxicol 11:180–190.

Rai AK, Spolaore B, Harris DA, Dabbeni-Sala F, Lippe G. 2013. Ectopic F_OF_1 ATP synthase contains both nuclear and mitochondrially-encoded subunits. J Bioenerg Biomembr 45::569–579.

Ravera S, Panfoli I, Aluigi MG, Calzia D, Morelli A. 2010. Characterization of myelin sheath F(o)F(1)-ATP synthase and its regulation by IF (1). Cell Biochem Biophys 59:63–70.

Rees DM, Leslie AG. 2009. The structure of the membrane extrinsic region of bovine ATP synthase. Proc Natl Acad Sci USA 106:21597–21601.

Song K, Han Y, Zhang L, Liu G, Yang P, Cheng Y, Bu L, Sheng H, Qu S. 2014. ATP synthase β-Chain overexpression in SR-BI knockout mice increases HDL uptake and reduces plasma HDL level. Int J Endocrinol 356432:1–12.

Stock D, Leslie AG, Walker JE. 1999. Molecular architecture of the rotary motor in ATP synthase. Science 286:1700–1705.

Vantourout P, Radojkovic C, Lichtenstein L, Pons V, Champagne E, Martinez LO. 2010. Ecto-F_1-ATPase: A moonlighting protein complex and an unexpected apoA-I receptor. World J Gastroenterol 16:5925–5935.

Wang T, Chen Z, Wang X, Shyy JY, Zhu Y. 2006. Colesterol loading increases the translocation of ATP synthase b chain into membrane caveole in vascular endothelial cells. Biochim Biophys Acta 1761:1182–1190.

Wang WJ, Ma Z, Liu YW, He YQ, Wang YZ, Yang CX, Du Y, Zhou MQ, Gao F. 2012. A monoclonal antibody (Mc178-Ab) targeted to the ecto-ATP synthase β-subunit-induced cell apoptosis via a mechanism involving the MAPKase and Akt pathways. Clin Exp Med 12:3–12.

Wang WJ, Shi XX, Liu YW, He YQ, Wang YZ, Yang CX, Gao F. 2013. The mechanism underlying the effects of the cell surface ATP synthase on the regulation of intracellular acidification during acidosis. J Cell Biochem 114:1695–1703.

Xing SL, Chen B, Shen DZ, Zhu CQ. 2012. β-amyloid peptide binds and regulates ectopic ATP synthase α-chain on neural surface. Int J Neurosci 122:290–297.

Xing S, Shen D, Chen C, Wang J, Liu T, Yu Z. 2013. Regulation of neuronal toxicity of β-amyloid oligomers by surface ATP synthase. Mol Med Rep 8:1689–1694.

Yegutkin G, Henttinen T, Jalkanen S. 2001. Extracellular ATP formation on vascular endothelial cells is mediated by ecto-nucleotide kinase activities via phosphotransfer reactions. FASEB J 15:251–260.

Yonally SK, Capaldi RA. 2006. The F_1F_O ATP synthase and mitochondrial respiratory chain complexes are present on the plasma membrane of an osteosarcoma cell line: An immnocytochemical study. Mitochondrion 6:305–314.

SUPPORTING INFORMATION

Additional supporting information may be found in the online version of this article at the publisher′s web-site.

JOURNAL

WORLD MITOCHONDRIA SOCIETY

JWMS ARCHIVES

ARCHIVES

Abstracts of 7th World Congress on TARGETING MITOCHONDRIA

October 24-25-26, 2016
Maritim ProArte, Berlin, Germany

October 2016 | JWMS Vol. 2 | DOI: 10.18143/JWMS_v2i2

ATPase-INHIBITORY FACTOR 1 IS A PROGNOSTIC FACTOR IN LOW GRADE ASTROCYTOMAS

BUSO, Alessia (1); CORRECIG, Cecilia (2); CANDOTTI, Veronica (2); IUS, Tamara (3); COMELLI, Marina (1); CESSELLI, Daniela (2); SKRAP, Miran (3); MAVELLI, Irene (1)

1: University of Udine, Italy 2: "Santa Maria della Misericordia" University Hospital, University of Udine, Italy 3: "Santa Maria della Misericordia" University Hospital, Italy

buso.alessia@spes.uniud.it

The purpose of the study was to investigate the expression levels and the prognostic value of ATPase-Inhibitory Factor 1 (IF1), the regulatory protein of mitochondrial ATPsynthase, in human WHO grade II gliomas, which still need to be categorized as high or low risk. Surgical specimens of astrocytomas (LGA), from patients well characterized by state-of-the-art clinical, histological and molecular parameters, were analysed for IF1. Evaluation of the tumor border zone from 19 specimens showed significantly greater IF1 values in the tumoral zone. Immunohistochemistry analyses of 71 specimens by Tissue-MicroArrays proved a positive correlation of IF1 with NFkB p65-subunit expression. Kaplan–Meier estimation of patients overall survival indicated that IF1 may serve as a prognostic marker. Intriguingly, IF1 expression significantly increased in lesions with first signs of anaplastic transformation (LGA*) as showed, in accordance, by immunofluorescence (12 specimens), immunohistochemistry (49) and immunoblot (9) analyses. Finally, immunoblot analyses provided a picture of mitochondrial and glycolytic markers, delineating metabolic phenotype changes in LGA* and suggesting no improvement of glycolysis.

In conclusion, IF1 might be considered as a new sensitive predictor of poor prognosis for LGA/LGA*, in analogy with carcinomas and high grade gliomas [1-5], and a non-canonical IF1 role in LGA progression might emerge.

References:

1. Sánchez-Aragó M. et al., Oncogenesis. 2, doi: 10.1038/oncsis.2013.9 (2013)

2. Tao Yin et al., Biomedicine; Pharmacotherapy. 70, 90-96 (2015)

3. Gao Y.X. et al., Am J Cancer Res. 6(5):1141-8. eCollection (2016)

4. Song R. et al., Hepatology. 60(5):1659-73. (2014)

5. Wu J. et al., Oncology Letters. 10:2075-2080. (2015)

Acknowledgments

I would like to express my thanks my two supervisor professor Irene Mavelli and professor Bruno Grassi, who gave me the opportunity to work on several different and interesting projects and to expand my expertise and scientific knowledge.

I would also like to thank Dr. Marina Comelli, not just a tutor or a colleague but also a friend.

A thanks is owed to dr. Miriam Isola for the help given with the statistical analyses used in this Thesis.

A special thanks to professor Jerzy A. Zoladz for serving as my external reviewer in these 3 years, for giving me the opportunity to work in his lab for such an interesting project as Harmonia was and for the interest and help showed in my other projects.

A thanks to Dr. Daniela Cesseli for the opportunity to develop an *ex vivo* model for the study of IF1 in glioma.

The greater acknowledgement goes to my parents who always believed in me and supported me in these 3 years.

I would like to thank also the fellow colleagues met during these 4 years at University of Udine: Davide, Ivan, Stefano, Marco, Eleonora, Joanna, Magda, Jessica and Benedetta.

A special thanks to my closest friends Luca, Alessia, Giulia, Adriana, Ivan, Mattia and Andrea, who supported and support me in the good and bad times.

I cannot forget to thank Silvia for her technical help in the lab and her friendship.

I would also like thank Luigi, Sandro and Rolando for our morning coffees and chats.